A unique form of locomotion in Swartkrans hominins: An analysis of the trabecular structure of the first metatarsal.

Klara Komza

MSc Dissertation

The University of Kent

Supervisors:

Dr. Matthew Skinner

Dr. Tracy Kivell

Abstract

Changes in foot bone morphology within the hominin clade are crucial for reconstructing the evolution of bipedalism and a modern human-like gait. Studies of the external morphology of the first metatarsal in humans, non-human apes and fossil hominins, have documented changes in its robusticity, epiphyseal shape and its articulation with the medial cuneiform. Trabecular bone structure has been shown to reflect habitual joint positioning, and as a result offers a promising method of interpreting first metatarsal loading in extant and fossil apes. In this study, microtomography is used to quantify the trabecular structure throughout the head and base of the first metatarsal, of a comparative sample of *Homo sapiens* (n=11), *Pan troglodytes* (n=10), *Gorilla gorilla* (n=10), and *Pongo pygmaeus* (n=6). Results from these analyses are then applied to two fossil hominin first metatarsals (SKX 5017 and SK 1813), the former being attributed to *Paranthropus robustus*, and the latter being of unassigned taxonomic status. Results show that within the comparative sample, bone volume fraction (BV/TV) and degree of anisotropy (DA) effectively separate bipedalism from all other forms of locomotion. Specific patterns in anisotropy and trabecular bone density distribution support the hypothesis that higher BV/TV in the dorsal regions of the bone and overall higher DA are reflective of a foot adapted for bipedalism. SKX 5017 shows patterns that are different from all modern taxa, indicating a unique form of bipedalism characterized by a habitually hyperdorsiflexing metatarsophalangeal joint and retained arboreal adaptations. SK 1813 shows a trabecular distribution in the head that is different from SKX 5017 and intermediate between modern human and non-human primates, indicating habitual but less frequent bipedalism than modern *Homo sapiens* and greater arboreal adaptations than SKX 5017. These results suggest that Swartkrans hominins employed habitual bipedalism, but also displayed a wider range of locomotor behaviour than modern humans.

Acknowledgements

I would like to thank my supervisor, Dr. Matthew Skinner, for all his guidance throughout the year. I would also like to thank Dr. Tracy Kivell for her invaluable input in my project. I am grateful for being able to participate in their research group, and take part in an exciting field of palaeoanthropology.

For access to specimens, I thank the Max Plank Institute for Evolutionary Anthropology (Christoph Boesch and Uta Schwarz), the Powell-Cotton Museum (Inbal Livine), the Johann-Freidrich-Blumenbach-Institutfür Zoologie und Anthropologie der Georg-August-Universität Göttingen (Birgit Großkopf), and the Zoologische Staatsammlung Munich (Anneke van Heteren).

For scanning, I thank David Plotzki (Max Plank Institute for Evolutionary Anthropology) and Keturah Smith (Cambridge University).

For technical assistance, I thank Dieter Pahr (University of Vienna).

I would also like to thank my colleagues, Christopher Dunmore, Leoni Georgiou, and Tom Davies for their assistance in various aspects of my project, as well for providing moral support and an enjoyable work atmosphere each day.

Table of contents

List of Tables

List of Figures

Chapter 1. Introduction

1.1 Objectives

The goal of this study is to quantify trabecular bone properties within the first metatarsal (MT1) of a range of non-human great apes and modern humans. By analyzing various trabecular parameters, I will determine if they correspond to known modes of locomotion within each taxon. Furthermore, I will compare these results to two fossil hominin MT1s from Swartkrans to draw inferences about *Paranthropus robusts* and/or early *Homo* locomotor behaviour. The objectives of the study are as follows:

1. Analyze trabecular parameters within the head and base of the MT1 to see if they correspond to known differences in habitual joint positioning at the metatarsophalangeal and tarsometatarsal joints.
2. Compare these results to fossil hominin MT1s with the ultimate goal of inferring their locomotor repertoire.

1.2 Thesis outline

This thesis is presented as a two-part work: a literature review of relevant research, and the original research, presented as a manuscript.

Chapter 2 – Outlines current literature and research into forefoot structure and positioning in the study sample during locomotion, and the application of trabecular bone morphology in inferring locomotion. It also details research on Plio-Pleistocene hominin locomotor adaptations.

Chapter 3 – This chapter presents a manuscript that includes the methods, results, and the discussion of the project.

Chapter 4 – Conclusion: Summarizes the study’s findings.

Chapter 2. Literature Review

2.1 Introduction

The following chapter will detail relevant literature regarding the locomotor behaviour of the taxa within the research sample, and describe the corresponding morphology of their feet with an emphasis on the first metatarsal. Because the emphasis of this dissertation is on the locomotor behaviour of extinct hominin taxa, a broad description of the evolution of bipedalism is also covered. This dissertation focuses on trabecular structure as a method of interpreting locomotor behaviour, and for this reason this chapter will also review what is known about trabecular bone functional adaptation.

2.2 Descriptive morphology

2.2.1 *Homo sapiens*

The human foot is a rigid structure that reflects adaptations for a strictly bipedal mode of locomotion. The forefoot in particular highlights its specialization for bipedality. Features that emphasize this adaptation include an adducted first metatarsal that is larger and more robust relative to the laterals metatarsals, metatarsal heads that are oriented perpendicular to the ground to allow greater metatarsophalangeal joint excursion in the dorsoplantar plane, and relatively short and stout phalanges (Morton, 1964; Susman, 1983; Rolian, 2009). Beyond the forefoot, the orientation and shape of the human tarsals within the midfoot contributes towards the presence of a longitudinal arch. The longitudinal arch is maintained by the plantar aponeurosis, a ligamentous band that originates from the calcaneal tuberosity and inserts distally on the proximal phalangeal bases. Together, the two act as a stable push-off lever during bipedal walking (Elftman and Manter, 1935; Hicks, 1954; Bojsen-Møller, 1979;

Bojsen-Moller and Lamoreaux, 1979; Susman, 1983; Alexander et al. 1987; Alexander 1991; Caravaggi et al., 2009; DeSilva, 2010), but see (Holowka et al. 2017).

Forefoot kinematics have long been studied from clinical perspectives (Bojsen-Møller and Lamoreux, 1979; Kidder et al., 1996; Leardini et al., 2007; Nawoczenski et al., 1999; MacWilliams et al., 2003; Halstead et al., 2005; Simon et al., 2006; Scott et al., 2007; Caravaggi et al., 2009). In order to understand which parts of the foot experience the highest strain during locomotion, ground reactions forces have been studied (Hutton and Dhanendran, 1981; Katoh et al., 1983; Soames, 1985; Munro, 1987; Lee and Farley, 1998; Hunt et al., 2001; Vereecke et al., 2003; Nester et al., 2007; Griffin et al., 2010a). The latter show the magnitude and direction of loading applied to the foot and measure the pressure path throughout the entire gait cycle. It is thought that bone remodels most strongly to dynamic elevated loads (Rubin and Lanyon, 1982; Griffin and Richmond, 2005), therefore knowing where the foot experiences the highest loads would help explain internal bone morphology.

The gait cycle is comprised of two major phases: the swing and the stance phase. The stance phase begins when the heel makes contact with the substrate, and ends with toe-off when the foot is no longer in contact with the ground, marking the beginning of the swing phase (Novachek, 1998; Perry et al., 1992; Vaughan et al., 1999). During heel strike, when the stance phase begins, peak plantar pressure is located under the posterior lateral aspect of the foot, under the calcaneus. As the midfoot reaches the ground, the longitudinal arch of the foot maintains a pressure distribution under the lateral side of the foot, under the cuboid and proximal ends of the lateral metatarsals. Weight is then transferred to the metatarsal heads, and to the medial side of the foot. The heel then rises, placing all of the body weight on the forefoot, and forcing the metatarsal heads into dorsiflexion during which each proximal phalanx moves onto the dorsum of its respective MT head (Soames, 1985; Vereecke et al., 2003; DeSilva, 2010; Griffin et al., 2015; Fernandez et al. 2016). Dorsiflexion, which occurs towards the end of the stance phase, causes tightening of the

plantar aponeurosis. It stabilizes the foot during the stance phase and elevates the longitudinal arch, changing its conformation to a stiff propulsive lever for propulsion and ultimately toe-off (Hicks, 1954; Bojsen-Moller, 1979; Susman, 1983; Griffin and Richmond, 2010; Caravaggi et al. 2010; Griffin et al., 2015). As shown by *in vivo* studies of plantar pressure distribution within the human foot, it is during dorsiflexion that the medial forefoot shows a spike in loading (Hutton and Dhanendran, 1981; Katoh et al., 1983; Soames, 1985; Munro, 1987; Lee and Farley, 1998; Hunt et al., 2001; Nester et al., 2007; Griffin et al., 2010). The phalanges are the last elements to leave the ground, at which point the centre of pressure lies under the first and second toes. (Veerecke et al., 2003; Griffin et al. 2010a).

In terms of which metatarsals incur the most pressure, there is general agreement that the medial ones are more active in propulsion, and by default incur the highest peak pressures (Rodgers, 1995; Veerecke et al., 2003; Griffin et al., 2010a) (see Figure 1). The first metatarsal (MT1) bears a large portion of this compressive load, which is evident in its external morphology. However, based on methodology and forefoot proportions, there are variable loading patterns between the first and second digits. This can be caused by relative protrusion of the metatarsal segments and the length of the metatarsals in relation to each other (Cavanagh and Rodgers, 1985; Rodgers, 1995; Rodgers and Cavanagh, 1989), as well as variables like speed, shod vs. unshod walking, and structural characteristics of the foot (high vs. low arch) (Rodgers, 1995).

It is also largely related to the method used in measuring plantar pressure distribution. Most of these methods separate the foot into discrete segments, mainly to reduce the complexity of the foot for experimental (Hunt et al., 2001; Simon et al., 2006; Leardini et al., 2006; Kitaoka et al., 2006) and clinical studies (Woodburn et al., 2004; Khazzam et al., 2006; Tome et al., 2006). The ways in which these segments are determined usually vary, and for this reason, studies often yield mixed results in regards to specific details about foot kinematics. Additionally, the method used to record pressure affects the results (bone-mounted marker, skin markers, floor mounted transducers) (Hutton and Dhanendran, 1981;

Soames, 1985; Nester et al., 2007). Despite the variability of the data obtained using these methods, peak pressure values are often found to be highest in the medial metatarsals and lowest in the fifth (Donahue and Sharkey, 1999).

Figure 1. Example of footscan image, showing maximal pressures under a left human foot during ground contact in a bipedal walking sequence. Dotted line in foot illustrates displacement of center of pressure (dot interspace, 4 msec).

Nonetheless, the external structure of the MT1 is reflective of the high compressive forces it incurs and of its active role in propulsion. The proximal articular surface of the MT1 is mediolaterally wide, likely related to the bending stresses experienced near the base. Because the plantar ligaments are exposed to high tensile forces, and the basal joint surfaces to high compressive forces, the bone within the metatarsal responds by increasing in cross-sectional area proximally, thus providing greater moments of resistance in the proximal section of the shaft (Stokes et al., 1979a; Griffin and Richmond, 2005). The MT1 head is generally larger than that of other great apes, and the superior aspect of the articular surface of the head expands to the dorsum of the bone, resulting in a raised appearance in relation to its shaft, which is thought to increase the range of dorsiflexion at the metatarsophalangeal joint (MTPJ) (Stokes et al., 1979; Susman and Brain, 1988; Susman and de Ruiter, 2004; Griffin and Richmond, 2005; Griffin et al., 2010). The human MT1 head

is also unique in its wide medio-lateral breadth on the dorsal aspect. This shape enhances joint stability during push-off and facilitates close-packing of the MTPJ by tightening the collateral MTP ligaments when the joints are in dorsiflexed position. Furthermore, this tightening limits joint motion outside the sagittal plane and increases joint stability when maximum joint congruency is achieved (Susman and Brain, 1988; Hetherington et al., 1989; Susman and de Ruiter, 2004; Pontzer et al., 2010). The MT head possesses a large metatarsophalangeal articular surface, sesamoid bones that give the flexor tendons a good mechanical advantage to minimize joint forces, a large inclination to the horizontal to minimize its shear and bending forces, and low axial torsion at the head relative to the base because it is loaded mainly in the sagittal plane. (Morton, 1922; Elftman and Manter, 1935; Aiello and Dean, 1990; Berillon, 1999; Susman and de Ruiter 2004; Drapeau and Harmon, 2013).

The other four metatarsals (especially the second and third) are generally longer and less robust, and tend to be loaded out of proportion to their sizes (Stokes et al. 1979; Christensen and Jennings 2009). When gait is accelerated, the centre of pressure in the foot follows an even more medial trajectory, at which point the MT1 plays an even more significant role in propulsion and balance (Bojsen-Moller, 1979). Its short, straight, and stout shaft is considered more efficient for bipedalism because it reduces the torque of the ground reaction force and the required balancing contraction of the toe flexors. This shortness also decreases the work required by the digital flexor muscle during the stance phase, and in theory decreases the amount of energy needed to swing the leg forward (Preuschoft, 1971; Rolian et al., 2009; Myers and Steudel, 1985).

The structure of the tarsometatarsal joint of the first ray (MT1-first cuneiform) reflects the range of motion, in particular prehension and hallucal abduction that would be possible in the foot. The proximal end of the human MT1 is characterized by a relatively flat articular surface when compared to other non-human primates, with a saddle or crescent-shaped profile. This articular shape corresponds with a stable tarso-metatarsal joint complex that reduces

mediolateral mobility of the hallux, and keeps it in line with the other metatarsals. (Morton, 1924; Susman and Brain, 1988; Proctor et al. 2008; Gill et al. 2015).

2.2.2 Non-human primates

Analyzing foot kinematics in extant non-human apes is less straight-forward compared to modern humans because they employ a wider range of locomotion, from terrestrial to arboreal quadrupedalism, vertical climbing, suspension, and occasional terrestrial bipedalism. Kinematic information about non-human primate locomotion is also less abundant mainly because of ethical concerns. Classically, foot structure in non-human primates is associated with a more mobile overall foot, capable of a wide range of grasping for both climbing and dorsiflexion during quadrupedalism. This increased mobility is partially attributed to the mid-tarsal break, an area of great mid-foot joint mobility that presumably reflects greater conformity of the foot to arboreal substrates *(*Elftman and Manter, 1935; Susman, 1983; D'Aout et al., 2002; DeSilva, 2010), but see Holowka (2017). It is likely attributed to the articular surface features between the calcaneus and cuboid (Susman, 1983), the rounded cuboid-metatarsal joints (DeSilva 2010; Proctor 2013), and the lack of a well-developed plantar aponeurosis (Susman, 1983). Combined with a lack of arching in the sagittal plane of the foot, the result is an overall different footfall pattern within all non-human primates (Elftman and Manter 1935; Hicks, 1954; Susman 1983; Crompton et al. 2008; DeSilva 2010).

Knuckle-walkers

Gorillas (*Gorilla gorilla*) and chimpanzees (*Pan troglodytes*) can both be broadly considered knuckle-walkers, though they vary in frequency of arboreal vs. terrestrial locomotion. Though both gorillas and chimpanzees exhibit arboreal behaviour, gorillas spend more time using terrestrial locomotion. Amongst *Pan, Gorilla,* and *Pongo*, adult gorillas (*Gorilla gorilla*) exhibit the least climbing behaviour, with <1% of total locomotor behaviour in mountain gorillas (*Gorilla gorilla beringei*) and 8% in lowland gorillas (*Gorilla gorilla gorilla*) (Remis, 1998). Adult chimpanzees exhibit an intermediate and variable level of climbing that is influenced both by body size and seasonality, with their proportion of arboreal locomotion ranging from 7.5% during the dry season and 62.9% during the wet season, when not foraging (Wrangham, 1977; Gebo 1996; Takemoto 2004). Interspecific differences also occur due to their disparate sizes, and partly due to different overall body morphology (Jungers, 1984; Cant, 1992; Doran, 1993a,b; Hunt, 1992, 1994).

Gorillas and chimpanzees of similar sizes but differing ontogenetic stages overlap considerably in locomotor behaviour, despite the fact that throughout ontogeny, gorillas have relatively shorter and straighter phalanges and metacarpals than chimpanzees (Susman, 1979; Shea, 1981; Inouye, 1992; Doran 1997). Differences in pedal structure are amplified in later stages of life, with ontogenetically decreasing phalangeal curvature among *Pan* (Congdon, 2012) and *Gorilla* (Richmond, 1998), reflecting a decrease in climbing frequency. Relatively long and curved digits are associated with gripping during arboreal climbing, and shorter, straight digits are associated with less suspensory or climbing behaviour (Tuttle 1969; Marzke 1971; Susman 1979; Gebo 1985; Hunt 1991; Stern et al. 1995; Richmond 1998; Richmond 2007; Congdon 2012). However, between the two taxa, *Pan* retains more curved digits than *Gorilla*, reflective of its more frequent arboreal locomotion (Stern and Susman 1983; Richmond 1998; Congdon 2012). Although gorillas can locomote arborearly, their size restricts them to supports of larger diameters, and they typically do not use their

feet for suspension. Their feet are instead used for vertical climbing or walking, and because the supports they use for climbing are usually large relative to their foot size, there is little flexion of the metatarsophalangeal and interphalangeal joints (Sarmiento, 1994; Remis, 1995).

Hallmark forefoot features for both chimpanzees and gorillas include a highly abducted and everted MT1 and an inverted MT2, causing the plantar surfaces of the heads to face each other (Morton, 1922; Elftman and Manter, 1935; Susman, 1983; Drapeau and Harmon, 2008). The orientation of the MT heads in relation to their bases reflects the positioning of the phalanges and their range of motion (Wunderlich,1999). In this regard, *Pan* and *Gorilla* are very similar, with statistically indistinguishable metatarsal torsion values (Pontzer et al. 2010; Drapeau and Harmon, 2008, 2013). This pattern of inversion and eversion has been shown to be a strong signal of prehensile capabilities (Harcourt-Smith and Aiello, 2004; Pontzer et al., 2010; Drapeau and Harmon, 2013). The metatarso-cuneiform joint also reflects the potential range of hallucal mobility. Both *Pan* and *Gorilla* possess a concave MT1 proximal articular surface and a convex distal articular surface of the medial cuneiform, allowing for multiaxial movement of the hallux. This allows for more effective grasping abilities and a more flexible forefoot during climbing (Berillon, 1999; Latimer and Lovejoy, 1990; McHenry and Jones, 2006; Tocheri et al., 2011; Drapeau and Harmon, 2013). Despite this similarity in tarsometatarsal joint structure, the gorilla foot nonetheless reflects more terrestrial behaviour. Interspecific analysis of this joint's morphology in *Gorilla* and *Pan* has shown that gorillas have a relatively flatter facet, reflective of lessened hallucal mobility and a more stable joint (Gebo 1992; Tocheri et al., 2011; Gill et al. 2015). Gorillas also possess broader and flatter calcaneocuboid and subtalar joints, a flattened talar body, and a proximally wider calcaneus, all features indicative of more plantigrade foot positioning (Gebo, 1992). In contrast, *Pan* has a rounder and more medially oriented facet for the MT1 (Latimer and Lovejoy 1990, McHenry and Jones, 2006), indicative of a more abducted hallux.

Locomotion in chimpanzees and gorillas varies from modern humans in that it is less stereotyped in the dorsoplantar direction, and there is variation in hallucal position and centre of pressure during the stance phase (Veerecke et al., 2003). The cortical bone of the MT1 diaphysis reflects this difference in loading; human MT1s are reinforced in the distal midshaft region to resist bending in a dorsoplantar orientation. They also vary less in orientation of high stiffness, suggesting relatively stereotyped dorsoplantar load orientations. Chimpanzee and gorilla MT1s exhibit greater obliquely-oriented stiffness, likely related to the wider range of motion involved within their locomotor regimes (Jashashvili et al. 2015).

Recent studies on plantar pressure distribution within *Pan paniscus* (Aerts et al., 2000; D'Aout et al., 2004; Vereecke et al., 2003) have shown that the centre of pressure remains more laterally positioned throughout the stance phase, and that it tends to fluctuate more in the mediolateral direction than what is observed in humans (De Cock et al., 2008; Nagel et al., 2008). The heel and lateral midfoot touch down simultaneously at the beginning of the stance phase, followed by a shift in pressure to the anterior portion of the foot, and a medial pressure transfer across the metatarsal heads during heel-off (see Figure 2). However, the hallux occasionally makes contact with the substrate before the lateral toes (Veerecke et al., 2003). There is also variation during midstance, at which point the first ray may be adducted or abducted, and the lateral rays may be plantigrade or curled (Elftman and Manter, 1935; Susman, 1983). The lateral and medial toes vary in terms of which ones leave the ground last, with the highest pressure being located under the lateral midfoot, near the fifth metatarsal (Veerecke et al., 2003; Griffin et al., 2010a). Susman (1983) observed that toe-off in *P. troglodytes* occurs at the second or third digits, while Wunderlich (1999) found that it occurs most often between the first and second digits and less frequently at the first or third ones.

During bipedal walking, the impact on the heel is lower than in terrestrial quadrupedalism (D'Aout et al., 2004) and there is a more variable course of the centre of pressure,

characterized by shorter contact time attributed to smaller steps at higher frequencies (Aerts et al., 2000). This plantar pressure distribution is further shifted during climbing. Wunderlich and Ischinger (2017) examined the plantar pressure distribution within the feet of *P. troglodytes* during vertical climbing, and found that during vertical climbing, chimpanzees exhibit the highest peak pressures on metatarsals 2/3 and the lowest pressures on the metatarsals 4/5. This corresponds with the external morphology of their metatarsals, with the medial ones being more robust and strongly inverted (Marchi, 2005). This pattern of inversion allows for the plantar surface of the toes to make better contact with the substrate, which increases the propulsive capacity of the foot on vertical supports (Drapeau and Harmon, 2013). Furthermore, these peak pressures are relatively higher than during ground locomotion or locomotion on a horizontal pole, meaning the medial metatarsals play the most active role during vertical climbing (Wunderlich and Ischinger, 2017). The importance of the medial digits for climbing is further displayed in the physiological cross-sectional area (PCSA) of the digital extensor muscles in the feet. The muscles within the medial digits, and particularly within the hallux, show a higher PCSA than the lateral digits, indicating hallux-assisted power gripping in arboreal locomotion (Oishi et al., 2012).

It is important to note that there are considerable differences in locomotion and morphology between bonobos and chimpanzees: chimpanzees are generally larger and possess different limb to body proportions (Shea, 1981; Doran 1993). Data on plantar pressure distribution within gorillas is scarce, but limited available data displays a directly-forwards path of centre of pressure (Crompton et al., 2008). In contrast to chimpanzees and bonobos, gorillas possess a flatter, more plantigrade foot. Specifically, they lack the curled under toe postures characteristic of chimpanzees, lack a longitudinal arch, and show little dorsiflexion at the distal tarsal joints or at the tarsometatarsal joints (Sarmiento, 1994). Consequently, it is very likely that the gorilla foot incurs pressure under different areas than chimpanzees. In

general, the structure of chimpanzee MT1s reflects a more arboreal locomotor mode, and gorilla MT1s reflect a more terrestrial locomotor mode.

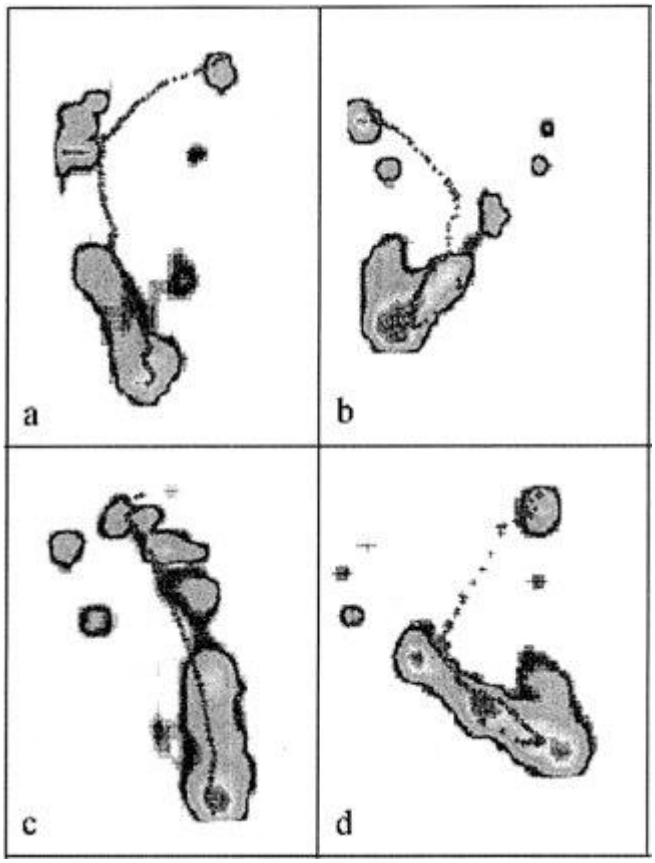

Figure 2. Examples of footscan images during quadrupedal (a–c) and bipedal walking (d) of bonobos. Plantar pressure profiles in a and d are from a left bonobo foot, those in b and c from a right bonobo foot. During quadrupedal locomotion (a–c), initial contact is made by the heel. Then the center of pressure moves anteriorly towards the metatarsal heads and lateral toes, and eventually bends towards the hallux. During bipedalism (d), initial contact is made by the lateral midfoot and the center of pressure moves eventually towards the hallux. Note the variability in plantar pressure distributions, with a V-curved pattern in b and an almost straight course of center of pressure (indicated by dotted line) in c, in contrast with the general pattern with a curved course of center of pressure, shown in a. From Vereecke et al., 2003.

Suspension

Though orangutans (*Pongo pygmaeus*) are capable of a wide range of locomotion including terrestrial quadrupedalism, they differ from African apes in that they exhibit the highest frequency of climbing behaviour. Brachiation can be attributed to 11% of locomotion, quadrupedalism for 12%, vertical climbing for 18%, tree-swaying for 7%, and clambering for 51% (Cant, 1987; Gebo, 1996; Thorpe and Crompton, 2006). Differences in phalangeal and metatarsal length and proportions reflect adaptations to suspension from a horizontal or oblique support, through power and hook grasping **(**Morton, 1924; Tuttle, 1970, Cant, 1987). Their feet are more inverted than the African apes, and the lateral digits are elongated whereas the hallux is relatively shortened (Gebo, 1992). The curvature of the metatarsals and phalanges is thought to be related to highly arboreal locomotion (Jouffroy and Lessertisseur, 1960; Preuschoft, 1970; Marzke, 1971; Susman, 1979; Rose, 1988; Hunt, 1991; Stern et al., 1995; Richmond, 1998). According to Preuschoft (1970, 2004), curved digits experience lower bending moments than straight digits, and are thus adaptations to large bending stresses. Oxnard (1973) argued that orangutan digits are “more efficient” than chimpanzee digits in suspension by using photoelastic stress models to show that a more curved phalanx experienced lower stress during suspensory grasping. Theoretical models by Preuschoft (1970) and Oxnard (1973) are further validated by biomechanical studies of phalangeal curvature in siamangs and gibbons (Richmond, 2007; Nguyen et al., 2014). Though the lateral metatarsals are elongated and curved, the hallux is relatively short and reflects different habitual positioning of the foot during locomotion from African apes (Morton, 1924; Gebo, 1992). As mentioned earlier, chimpanzees locomote arboreally through the use of the hallux for gripping. The same authors (Oishi et al. 2012) also analysed the PCSA values within orangutans and found a higher value within the lateral digits, indicating a specialization for hook-like gripping without the involvement of the hallux in arboreal locomotion. This relatively low degree of movement and compressive load upon the MT1

head during locomotion is also reflected within its smaller proportions when compared to chimpanzees and gorillas (Rose, 1988; Marchi, 2010). However, just as in chimpanzees and gorillas, the plantar aspect of the orangutan MT1 head is mediolaterally expanded to allow for close-packing during dorsiflexion. (Stern and Susman, 1983; Susman, 1983; Latimer and Lovejoy, 1990; Griffin and Richmond, 2010; Marchi 2010; Fernandez et al., 2016). As well, torsion patterns within the metatarsals of orangutan MT1s shows a similar, but more pronounced condition to African apes wherein the MT1 is strongly everted and the MT2 is strongly inverted (Drapeau and Harmon 2013). This difference in torsion is partially attributed to the shape of the metatarsal shaft, and to the more medial orientation of the hallucal tarsometatarsal joint (Gomberg, 1981; Gill et al., 2015).

Overall, the subtalar, transverse tarsal, and MTP joints, and the ligaments of the corresponding joints in orangutans are specialized for inversion-eversion movements for locomotion in arboreal substrates (Kanamoto et al., 2011), which results in a much more inverted foot position on the ground when compared to the flattened foot of African apes (Tuttle, 1970; Tuttle & Beck, 1972; Susman, 1983; D'Aout et al., 2002; Griffin et al., 2010a). According to Oxnard (1980), orangutan feet have a high transverse arch, similar to modern humans, in contrast to gorillas and chimpanzees, which possess flatter transverse arches, related to the positioning of the intermediate and lateral cuneiforms and the cuboid. On account of this difference in foot positioning, orangutans distribute weight differently from African apes, and should not be viewed as equivalent to the plantigrade foot positions utilized by chimps and gorillas. When locomoting terrestrially, orangutans place the entire lateral side of their feet in contact with the ground, similar to bonobos (Tuttle, 1970, 1972; Vereecke et al., 2003; Crompton et al., 2008; 2012). However, because plantar pressure distribution data within orangutans is lacking, subtle differences in their locomotion compared to other great apes using this method are not known.

Much of this data is relative in that it looks at the entire foot; the medial metatarsals of chimpanzees are only loaded more highly in relation to the lateral ones. Because this research focuses on the first metatarsal alone, much of this information simply serves to understand the general biomechanics of each locomotor type. Therefore, this research will not be able to confirm or deny if in fact known pressure distributions are reflected within the trabecular bone of the entire foot. However, knowing that the dorsal aspect of the human first metatarsal experiences relatively higher peak pressures than other non-human apes remains useful in interpreting potential relative differences in bone volume distribution across taxa.

2.3 Biomechanical adaptations of bone

Gathering accurate information about locomotor behaviour based on external morphology alone can be challenging. Bone is influenced by genetic and nongenetic factors, which are differentially reflective of functional adaptations, and highly difficult to isolate (Lieberman, 1997). Additionally, *in vivo* studies that have been used to measure foot kinematics in humans and non-human apes cannot be applied to fossil hominins. Furthermore, while articular surfaces indicate the joint positions an individual was able to adopt, internal bone is more likely to show how the joint was actually loaded (Ruff and Runestad, 1992; Kivell, 2016). Cortical bone has been shown to respond to mechanical stress (Ruff, 1982; Cowin et al., 1985; Doden, 1993; Ruff et al., 2006), and is known to respond to tension and compression in the shaft (Ruff, 1983; Cowin et al., 1985; Doden, 1993; Carlson, 2005; Ruff et al., 2006). It is less effective in inferring joint positioning at the epiphyses, which is where analysis of trabecular bone can become more useful. Trabecular bone remodels at a faster rate than cortical bone (Eriksen, 2010), and can therefore provide evidence of *in vivo* loading that is not seen in the cortical structure (Rubin et al., 2002; Pontzer et al., 2006; Barak et al., 2011; but see Bertram and Swartz, 1991).

2.3.1 Trabecular bone

The idea that bone adapts to its mechanical environment has been first credited to Julius Wolff (Wolff, 1892). What is today called Wolff's law has been modified throughout the 19th century, and incorporates three central tenets (Martin et al., 2015: pg. 276):

1. Optimization of strength with respect to weight
2. Alignment of trabeculae with principal stress directions
3. Self-regulation of bone structure by cells responding to a mechanical stimulus.

Wolff's law is fairly vague, and much what is currently considered part of it was not initially postulated by Wolff himself (Martin et al., 2015). Martin et al. (1998) instead proposed an alternative name for bone's adaptability to mechanical loading: the mechanical adaptability hypothesis. It states that, "bone structure is regulated to find the optimum solution to minimize both fracture risk and bone mass for the loadings that the bone experiences." (Martin et al., 1998: pg. 302).

Trabecular bone is quantified through two main parameters: bone volume fraction (BV/TV), which is affected by both trabecular thickness and spacing, and degree of anisotropy (DA), which measures the degree to which the trabecular struts are oriented in the same direction. A high DA value would be reflective of stereotypically oriented trabeculae (along the same axis), whereas a low DA value would reflect less stereotypically oriented struts. Anisotropy is obtained by factoring in mean intercept length (average distance from one trabecular surface to another through the marrow), and the measurement direction. This produces a three-dimensional ellipse, the eccentricity of which is a measure of anisotropy (Whitehouse, 1974; Odgaard, 1997). Combined, BV/TV and DA account for 70-80% of variation in Young's modulus of elasticity, which is a measure of material properties calculated as the ratio of stress strain which represents the stiffness of a material (Turner, 1992; Biewener, 1996;

Stauber et al., 2006; Macquer et al., 2015). Though BV/TV and DA are the most quantified parameters within trabecular bone studies, there is a wide range of additional structural properties that affect overall trabecular architecture. These include trabecular thickness, spacing, and number (Tb.Th, Tb.Sp, Tb.N), as well as the interconnectedness and structure of the trabeculae (plate-like vs. rod-like). The number of trabeculae is thought to not have a significant effect on the overall mechanical properties of the bone (Gibson, 1985), whereas the interconnectedness and structure do (Hodgskinson & Currey, 1990; Liu et al. 2008; Maquer et al. 2015). Liu et al., (2008) have shown a heterogeneity in the function of plate-like and rod-like trabeculae: the majority of trabecular plates are oriented in line with the principal direction of loading, whereas the rods serve as transverse connections between longitudinal plates. Additionally, their structure changes over time, with rod-like trabecular bone being associated with older age (Ding and Hvid, 2000; Wehril, 2007; Shi et al., 2010). Mittra et al. (2005, 2008) used a sheep sample to show that there are strong relationships between BV/TV and trabecular connectivity, spacing, and structure model index (SMI), a measure of the relative proportion of plate-like and rod-like trabeculae. Cotter et al. (2009) studied the vertebral bodies of apes and humans and found similar results, with the exception of trabecular thickness and DA, neither of which were significantly correlated to BV/TV within their sample. These studies suggest that as BV/TV increases, so does trabecular number; trabeculae become more plate-like, less widely-spaced, and more interconnected (Ryan & Shaw 2012). Whereas BV/TV is influenced by both trabecular thickness and spacing, the optimization of anisotropy has been hypothesized to be caused by the reduction of trabecular number by preferentially removing unnecessary trabeculae (Saparin et al. 2011; Skedros et al. 2012).

Some of the first experiments on trabecular orientation adaptability were conducted on sheep calcanei (Lanyon, 1973,1974; Skerry and Lanyon, 1995), which showed a correlation between the principal orientations of trabeculae and the principal compressive and tensile strain directions. Since then, a multitude of studies on trabecular bone structure have

emphasized its adaptability to biomechanical stressors (Biewener et al., 1996; Rubin et al., 2002; Mittra et al., 2005; Pontzer et al., 2006; Barak et al. 2011). Many studies have also shown that there is a difference in how trabecular bone models vs. remodels (Cunningham & Black 2009a,b; Partiff et al. 2000; Tanck et al. 2001; Raichlen et al. 2015). There is evidence that trabecular bone modelling follows an initial template, which has been demonstrated using human neonatal ilia (non-weight bearing bones). Trabecular bone within these elements has shown values of BV/TV, thickness, spacing, and number similar to adult ilia, meaning there is a strong genetic component to its structure (Cunningham & Black, 2009a,b). Support for a genetic blueprint which controls trabecular architecture is further supported by Skedros et al. (2004), based on evidence that the characteristic structure of trabecular bone within deer calcanei is already present in foetal deer. Parfitt et al. (2000) investigated the ontogeny of trabecular bone within the human ilium, and showed that between the ages of 1.5 and 23 years, there was an increase in BV/TV and trabecular thickness, but that the trabecular number stayed the same. In an ontogenetic study of trabecular bone in pigs, Tanck et al. (2001) found that BV/TV and trabecular thickness increased first, corresponding with a rapid increase in body size during growth. DA was shown to adapt later in their development (Tanck et al., 2001). Raichlen et al. (2015) confirm this with a human sample, showing that the degree of anisotropy within the distal tibia converges on higher values and becomes less variable at a later age. This result has also been repeated in the investigation of trabecular bone structure within the proximal femur (Ryan & Krovitz 2006). There is general agreement that the same ontogenetic pattern is present across elements, and that only once the adult trabecular bone architecture is finalized, does it begin to optimize based on biomechanical stressors. Later in life, trabecular architecture adapts in a more variable way; some studies show an increase in thickness in response to increased loading, and some show a reduction in trabecular number in areas of lower loading (Saparin et al. 2011). Despite these studies that show a specific ontogenetic pattern in trabecular bone modelling, and by extension a significant genetic component to the architecture of trabeculae, [genetics in baboons (Havill et al. 2010) and rodents (Alam et

al. 2005)] there is still substantial evidence that external loads cause remodelling that results in a trabecular architecture that differs from its original template (Rubin et al., 2002; Pontzer et al., 2006; Barak et al., 2011; but see Bertram and Swartz, 1991).

Biewener et al. (1996) studied the trabecular bone within the calcaneus of potoroos (small marsupials) to specifically see how it would adapt to principal strains, and how it changes during disuse. Their results supported predictions that trabeculae would be oriented with the principal strain direction in the cortical surface. After eight weeks of disuse, BV/TV was lower as a result of reduced trabecular thickness and increased spacing, but the orientation of the bone remained the same. They inferred that trabeculae may be formed and aligned in response to principal strain magnitudes and directions during growth, and that the resulting trabecular alignment prevents the realignment of trabecular bone during different loading once a specific trabecular architecture has been laid out (Biewener et al. 1996).

Several *in vivo* studies have been performed which show that trabecular bone structure and orientation can be changed based on changes in habitual positional behaviour and mechanical loading (Barak et al. 2011, Biewener et al., 1996; Guldberg et al., 1997; Mittra et al., 2005; Pontzer et al., 2006; Chang et al. 2008). Barak et al. (2011) measured the trabecular reorientation in the ankle joints of a sample of sheep after subjecting them to daily exercise on inclined treadmills. After one month, they found that the trabeculae within the distal tibia were reoriented to match the angle of the external load applied at the ankle (Barak et al. 2011). This is further supported by computational models (Huiskes et al., 2000), which show that the rotation of an applied load changes the orientation of trabeculae to a corresponding degree. When mechanical loading remains stable, remodelling continues without affecting the architecture of the overall bone (Huiskes et al. 2000).

Despite many studies proving the adaptability of trabecular bone to biomechanical stressors, it is still difficult to measure how it might vary differentially to frequency or magnitude of the external load (Kivell, 2016). Is trabecular bone more likely to adapt to low-frequency but high-magnitude forces, or vice versa? Frost's (1987) 'mechanostat' hypothesis addresses this question by presenting the strain thresholds required to elicit a remodelling in bone: strains below 100-300 με trigger a response in trabecular bone, whereas much higher levels are needed to trigger a response in cortical bone mass (1500-3000 με) (Frost, 1987). The effect of frequency on trabecular remodelling has been investigated by Skerry & Lanyon (1995) and Barak et al. (2011). Both used sheep to study the effect of stress frequency on trabecular bone architecture, and found that brief periods of loading were not sufficient to elicit a noticeable response in trabecular remodelling, and that the individuals that did show trabecular reorientation were those that were constantly subjected to the loading pressures. Lambers et al. (2013) investigated the trabecular structure within the vertebrae of mice, and found that it required 10 weeks for any noticeable change to appear within the trabeculae, when inflicted with a high frequency external load for 5 minutes, 3 times a week. This would suggest that trabecular bone requires a minimum duration of loading to show any true difference, and that the sheeps' trabecular bone would have simply required more time to remodel. Rubin et al. (2001, 2002) exposed sheep to low-level, high-magnitude stress via oscillation plates, and found that after a year, the sheep showed a 34.2% increase in trabecular bone density, suggesting a low level external load can contribute to trabecular architecture. Other studies have shown that dramatic but brief changes in external loading can also contribute to changes in trabecular structure (Simkin et al. 1989; Bassey & Ramsdale, 1994; Pontzer et al. 2006; Barak et al. 2011; Lambers et al. 2013). In general, the minimum duration is likely variable across species, and it is difficult to assess how much time and how much magnitude would be required for species of different body sizes to reach an equivalent level of trabecular remodelling (Lambers et al. 2013).

Studies using non-primates usually involve sheep and mice, animals which are on opposite ends of the size spectrum, and which could potentially affect interpretations. A relationship has been found between larger body size and trabecular architecture: larger mammals have absolutely thicker and wider spaced trabeculae, but relative to their body mass, the struts are thinner and more closely-packed (Swartz et al. 1998; Doube et al. 2011; Barak et al. 2013; Ryan and Shaw, 2013). This could in turn affect how trabecular bone responds to external forces. This pattern is also not taxon specific; it is consistent among primates and mammals. Anisotropy, on the other hand, does not appear to scale with body mass. Specific trabecular parameters vary depending on the element and taxonomic group (Cotter et al. 2009; Fajardo et al. 2013; Ryan & Shaw, 2013). The reason for this negative allometry could be attributed to metabolic and biomechanical factors than govern trabecular architecture. Kerschnitzki et al. (2013) suggested that this pattern may be caused by requirements to maintain an adequate surface area for the release and deposition of calcium. Additionally, trabecular thickness can be affected by the size of the lacunae, which are about 30-60 μ in depth (Kivell et al., 2016). Christen et al. (2015) emphasized the role of osteocyte constraints on trabecular structure – namely osteocyte density and the distance an osteocyte signal can travel towards osteoblasts at the bone surface. There are other ways in which large animals respond to higher external forces than smaller animals: different locomotor kinematics, and adaptation of the cortical bone (Kivell et al. 2016). For this reason, in order to gain complete understanding of an animal's biomechanical adaptations, a holistic method of analysing cortical, trabecular, and external morphology would be most effective.

2.3.2 Cortical bone

As mentioned earlier, cortical bone has been shown to adapt in response to external forces (Ruff, 1982; Cowin et al., 1985; Doden, 1993; Ruff et al., 2006). Ideally, a comprehensive interpretation of trabecular structure should combine an analysis of the cortical bone. Studies

of cortical cross-sectional geometry of the long bones have consistently shown that cortical bone responds to principal directions of stress by aligning its orientation to corresponding directions, and adding more bone to areas that experience higher strain (Goodship et al., 1979; Ruff, 1983; Cowin et al., 1985; Demes, 1993; Carter et al., 1996; Sumner and Andriacchi, 1996; Lieberman et al., 2004). Interpretations based on cortical bone are not always straight forward though, since it has been shown to display systemic (as opposed to localized) patterns within the skeleton in response to biomechanical differences. Lieberman (1996) exercised young pigs on a treadmill, and compared their cortical structure with a control group that had not undergone strenuous exercise. The exercised pigs displayed a higher cortical thickness in their limb bones. However, other, non-weight bearing elements also showed a corresponding increase in cortical thickness (cranial vault bones, caudal vertebrae, and penultimate ribs). Systemic changes in cortical bone were also recorded in rats in zero-gravity conditions, showing lower cortical bone volume in the mandible, an element which does not bear loads regardless of environment (Simmons et al., 1983).

Trabecular bone has been shown to be more functionally adaptive, and more localized to the elements that experience external forces (Lanyon, 1974; Hodgskinson and Currey, 1990; Biewener et al., 1996; Rubin et al., 2001, 2002; Mittra et al., 2005; Pontzer et al., 2006; Barak et al. 2011). The sheep that were studied by Rubin et al. (2001, 2002) and Barak et al. (2001) showed an increase in the trabecular bone mass in the hindlimbs but not in the radii (which were not exposed to the same external loads), and a change in anisotropy in the elements that were exposed to changes in direction. Some examples from primate studies, however, show that despite its more localized nature compared to cortical bone, there are still examples in which trabecular bone shows systematic, possibly genetic patterns (Alam et al., 2005; Havill et al., 2010), including overall higher BV/TV within non human primates than modern humans (Tsegai et al. 2013; Maga et al. 2006; Cotter et al. 2009; Ryan & Shaw 2012; Scherf et al. 2013). When trying to quantify the relationship between activity patterns

and trabecular and cortical bone shape and size, both genetic and behavioural factors must be considered. Both structures are undoubtedly influenced by a genetic blueprint, but a vast swath of literature also clearly demonstrates how they adapt in response to behavioural differences.

2.4 Trabecular bone studies in hominoids

Trabecular bone studies on human samples have most often been applied to clinical contexts, investigating osteopenia and osteoporosis (Eriksen, 1986; Simkin et al. 1987; Smith et al. 1989; Dempster, 2000), and sports related contexts, often focusing on differences caused by highly different joint loading (Harrison et al. 2011; Modlesky et al. 2008; Chang et al. 2008a). Applications on live primates pose ethical concerns, and for this reason are fairly sparse.

Before 3D analyses of trabecular bone became technologically possible, most analyses were done by 2D analyses which provide a single image within an entire bone or epiphysis. Some of these first applications of 2D analysis on anthropoids included studies on the femur and vertebrae of a rhesus macaque (Beddoe, 1978), and the talus and calcaneus of two sympatric species of lemur (Ward & Susman, 1979). These studies were fairly limited in scope, and it was only until the 90s that the first extensive 2D trabecular analyses of the humerus and femur in prosimians and anthropoids were conducted (Rafferty & Ruff, 1994). The most precise technology now available for the analysis of trabecular bone is 3D high resolution µ-CT (voxel size of approximately 30 µm). Fajardo and Muller (2001) conducted one of the first analyses of non-human anthropoid trabecular bone using 3D µ-CT. They examined the proximal humerus and femur, with the goal of linking structure to type of locomotion (terrestrial vs. arboreal) (Fajardo and Muller, 2001), and found that suspensory

taxa (more prone to loading in multiple directions) had more isotropic bone, whereas terrestrial taxa had more stereotypical trabecular orientation. However, Fajardo et al. (2007) later contradicted these findings when they expanded their sample size and found a large degree of overlap between suspensory and terrestrial species within the proximal femur, and that there was no clear correlation between trabecular structure and locomotor behaviour (Fajardo et al. 2007). They suggested that the hip joint in general might show higher degrees of similarity across taxa, or that current methods may be too simplistic (Fajardo et al. 2007). Similar studies have been conducted on the proximal femur, supporting the Fajardo et al. (2007) conclusions. Ryan and Walker (2010) investigated the trabecular bone of the proximal femur and humerus across five anthropoid taxa with the same purpose as the above study. Contrary to their predictions, they found that all taxa had significantly higher BV/TV in the femur and greater isotropy in the humerus. Many additional studies which have focused on the proximal femur and humerus have reached similar conclusions (Rafferty & Ruff, 1994; MacLatchy & Muller, 2002; Ryan & Ketcham, 2002).

Several other studies on extant primates have supported the lack of clear relationship between trabecular bone structure and locomotor type (Maga et al., 2006; Cotter et al. 2009; Ryan et al. 2010; Ryan and Walker, 2010; DeSilva and Devlin, 2012; Shaw and Ryan, 2012; Schilling et al. 2014). Instead, there seems to be support for certain similarities across many anthropoid taxa. Ryan and Walker (2010) found that despite their variable locomotor types, suspensory primates, climbing primates, and quadrupedal terrestrial ones showed a similar pattern of BV/TV distribution between the humeral heads and proximal femurs (Ryan and Walker, 2010). On the other hand, strepsirrhines have shown much clearer functional signals within their trabecular bone structure than hominoids and anthropoids. Leaping taxa (galagines, indriids, and tarsiers) have more anistropic trabeculae than non-leaping taxa (*Cheirogaleus, Loris, Perodictius, Otolemur*) (Ryan & Ketcham, 2002; 2005). These

conclusions have been repeated numerous times in extant and fossil strepsirrhines (MacLatchy & Muller, 2002; Ryan & Ketcham, 2002).

Given the fact that trabecular bone has undoubtedly been shown to adapt to biomechanical loading (Barak et al. 2011; Rubin et al. 2002), the fact that these studies show such equivocal results could be attributed to a multitude of factors. Even among taxa that are grouped in the same general locomotor category (knuckle-walker, suspensory, and bipedal) there is still variation in locomotor behaviour among individuals of the same group. Within chimpanzees (broadly considered terrestrial knuckle-walkers), there is variation in the degree of arboreal locomotion between males and females (potentially related to body size), with females consistently displaying more arboreal behaviour than males (Doran 1993). Matters are further complicated when social rank is added to the equation. Hunt (1992) found that chimpanzee positional behaviour within males was largely affected by social rank; social rank more consistently predicted branch diameter choice than body size (Hunt, 1992). A comparative study of the ontogeny of positional behaviour of gorillas and chimpanzees found that when the two taxa are at similar sizes (although widely disparate ages), they perform similar locomotor activities, with the exception of less suspensory behaviour in gorillas (Doran 1997). Given that we still don't know for sure what kind of external forces trabecular bone most likely responds to (frequent low magnitude, infrequent high magnitude), it is possible that certain dynamic forces (suspension, brachiation), which vary considerably, may affect the trabecular bone structure, hide the habitual locomotor patterns, and create a wider range of variability within taxa (Kivell, 2016).

Additionally, many of the studies that have reached equivocal results about the inefficiency about trabecular bone in locomotor reconstructions have focused on the proximal humerus and femur (Rafferty & Ruff, 1994; MacLatchy & Muller, 2002; Ryan & Ketcham, 2002).

These are both located within complex joints loaded in multiple directions and affected by soft tissues in addition to reaction forces. This makes understanding their kinematics much more complicated than studying simpler, uniaxial elements. For this reason, studying a relatively simple element like the first metatarsal, which experiences relatively consistent compressive loads, would make interpretations more secure.

Another reason why trabecular bone studies have yielded such mixed results could be because of the relatively simplistic biomechanical models that are relied upon to draw conclusions. According to Ryan and Shaw (2012), many studies tend to isolate individual trabecular parameters, and by doing so, fail to show clear functional differences across locomotor modes. By combining multiple trabecular bone variables, they found that a locomotor signal may be detectable in the anthropoid femoral head, and less obviously in the humeral head. Based on their analysis, they found unique trabecular bone characteristics. Within bipeds (*Homo sapiens*), trabecular architecture included a low number of thin, concave plate-like trabeculae that are highly anisotropic. Terrestrial quadruped-climbers (*Pan*) showed relatively numerous, thick, highly concave trabeculae that formed a dense isotropic structure. The other locomotor groups fell between these two ends of the spectrum, with *Pongo* showing fewer, relatively isotropic trabeculae (Ryan and Shaw, 2012). Studies that have combined comparative with experimental methods have also shown some more optimistic results. Barak et al. (2013) used data on kinematic and ground reaction forces from chimpanzees during terrestrial knuckle-walking and human bipedalism. They combined this information with the data they obtained from the trabecular bone structure within the distal tibia, and found that the trabeculae in chimpanzees were more obliquely oriented than in humans. This was interpreted as being reflective of a more dorsiflexed tibio-talar joint during midstance as opposed to an extended ankle human during human bipedal walking.

Recently, research has been released on the trabecular bone structure within the hand bones of modern humans, and a wide range of non-human primate taxa (Tsegai et al. 2013; Skinner et al. 2015), using a novel whole-epiphysis approach. Research by Tsegai (2013) on the third metacarpal has shown that the regions of greatest BV/TV and trabecular stiffness fit predictions based on the habitual behaviour displayed by the taxa within the study. *Pan* and *Gorilla* show a more dorsal concentration of trabecular bone on the metacarpal head, which is consistent with the joint's position during knuckle-walking. *Pongo* show a more palmar concentration, which is consistent with the power grasping associated during suspension. Though this new methodology has not yet been applied to the foot bones, there already exists research on the trabecular bone structure within the foot bones, notably the first metatarsal of human and non-human apes. Griffin et al. (2010b), demonstrated a correlation between trabecular bone structure within the first two metatarsals, and the locomotor behaviour of a sample of humans and non-human primates. They examined BV/TV and DA, and hypothesized that the dorsal regions of the human metatarsals would display higher BV/TV and DA values. This was based upon kinematic data on the metatarsals, which emphasize pronounced stress on the dorsal aspect of the metatarsophalangeal joints during dorsiflexion, and a more uniaxial direction of the human MT1s. While they found no significant difference in the BV/TV values between humans and non-human apes, human metatarsal heads showed more anisotropic trabecular bone organization in the dorsal regions compared to the corresponding areas of the great ape metatarsal heads. Functionally, this is important, because a higher degree of anisotropy is reflective of stereotypical loading along a specific axis (Ryan and Ketcham, 2002), and could indicate a rigid foot, built for unidirectional movement. According to Griffin et al. (2010b), these differences suggest that within trabecular bone properties, the degree of anisotropy is the most indicative feature of a forefoot habitually used for propulsion during gait (Griffin et al. 2010b). These findings support the idea that trabecular bone within the metatarsals is in fact responsive to biomechanical stressors, and that this method could be applied to fossil hominins to reconstruct locomotor behaviour in the past.

2.5 Evolution of bipedalism

Ultimately, the reason why we're interested in studying trabecular bone morphology is because of its potential utility in palaeoanthropology. If trabecular bone structure can be correlated to locomotor behaviour, this can then be used to reconstruct fossil hominin behaviour. As will be shown in this section, based on the analysis of external bony morphology of fossil hominins, there is a vast array of interpretations regarding the locomotor adaptations of fossil hominins. Among more recent hominin taxa (*Homo antecessor, Homo heidelbergensis, Homo neanderthalensis*), there is general agreement that they were fully adapted to obligate bipedalism (Trinkaus 1983; Lorenzo et al. 1999). Despite known differences in lower limb proportion in these taxa, most of the debate revolves around earlier specimens, including pre-Australopiths, Australopiths, and early *Homo*.

There are two main theories for how obligate bipedalism evolved. One major theory is of a knuckle-walking ancestor similar to modern African apes, originally proposed by Washburn (1967) which has been supported by others (Richmond & Strait, 2000; Richmond et al. 2001; Orr, 2005) based on the wrist morphology of *Australopithecus afarensis*. Many key adaptations to knuckle walking are observed in the distal radius, carpals, tarsals, and phalanges of African apes as well as *Australopithecus* and *Homo sapiens,* although others argue that these features are not unique to knuckle walking and are not observed in early hominins (Tuttle and Basmajian, 1974)**.** Instead, it has been proposed that the locomotor behaviour immediately antecedent to the evolution of bipedalism involved vertical climbing and orthograde clambering, but no significant terrestrial locomotion (Fleagle et al., 1981). This ancestor is described as a small-bodied climber and arboreal biped by some (Tuttle and Basmajian, 1974; Tuttle, 1975, 1981), and as a larger-bodied ancestor that used all four limbs for grasping during vertical climbing and suspension by others (Stern, 1975; Prost,

1980; Hunt, 1996). It has also been proposed that the antecedent locomotor type would have been similar to pronograde clambering as seen in orangutans (Crompton et al., 2003; Thorpe and Crompton, 2005).

The earliest evidence of bipedalism comes from early hominins such as *Sahelanthropus* (Brunet et al., 2002; Guy et al., 2005), *Orrorin* (Pickford et al., 2002), and *Ardipithecus* (Haile-Selassie, 2001). Though these individuals all display adaptations to a bipedal mode of locomotion, there has been disagreement over the extent and importance of continued arboreality that they display (Ward, 2002). This is largely due to the problematic interpretation of symplesiomorphic and synapomorphic character statues within their postcrania (Ward, 2002). With the large fossil record in Eastern Africa, research has largely focused on *A. afarensis* remains from Hadar. Ethiopia, dated between 3.0 and 3.6 Ma, as well as footprints from Laetoli, Tanzania (c. 3.6-3.7 Ma). Additional postcranial remains have contributed to discussion about early bipedalism, including *Homo habilis* remains (e.g. OH 62 and OH 8) (Leakey, 1960; Johanson et al., 1987), *Aaustralopithecus garhi* (Asfaw et al., 1999), and *Australopithecus anamensis* (Leakey et al., 1995, 1998).

Australopith remains attributed to *A. afarensis* have been the subject of many debates because of the mosaic nature of the postcranial remains and attract two opposing interpretations of their locomotor behaviour. On one hand, they are said to be fully compliant with bipedal locomotion (Latimer & Lovejoy, 1989, 1990; Latimer et al. 1987). Others emphasize that they display a mosaic of terrestrial and arboreal locomotion (Susman & Stern 1982; Stern & Susman 1983; Susman 1983; Duncan et al. 1994; Berillon, 1999). The former perspective would argue for an erect, modern human-like posture, whereas the latter would argue for a “bent-hip, bent-knee” posture seen in the bipedal gait of chimpanzees. The mosaic nature of *Australopithecus* morphological features can be clearly seen in the ‘Lucy’

skeleton (AI288-1, c. 3.2 Ma), which shows adaptations for bipedalism (human-like pelvis with a short iliac blade and wide sacrum, a human-like bicondylar angle of the femora, and a human-like talo-crural joint) (Stern & Susman, 1983). It also shows adaptations for arboreal locomotion (cranially-oriented glenoid, a funnel-shaped thorax, and long and curved pedal and manual phalanges) (Stern, 2000; Ward, 2002). The functional interpretations of these features can be placed in two camps. Stern, Susman, and Jungers (Junger 1982; Jungers and Stern, 1983; Stern & Susman, 1983; Rose, 1984; Susman et al. 1984; Stern, 1999) emphasize that the primitive, ape-like features within the skeleton are indicative of habitual arboreal locomotion. Latimer, Lovejoy, and Ohman (Latimer et al. 1987; Latimer & Lovejoy 1989; Latimer, 1991) argue that *A. afarensis* was an obligate biped based on the fact that certain features that are essential for arboreal locomotion were not preserved (a grasping foot and long and curved toe and finger bones). They argue that the anatomical features associated with arboreal locomotion are merely evolutionary remnants, and that *A. afarensis* was a committed biped (Lovejoy, 1988). Combined with the rest of the *A. afarensis* postcranial collection, it has been suggested that there is more than one form of locomotor behaviour represented within the species (Senut, 1981; 1983; Stern and Susman, 1983; Senut and Tardieu, 1985). It has been shown that *A. afarensis* is highly sexually size-dimorphic (Richmond & Jungers, 1995; Johanson & White, 1979; Kimbel & White, 1988; McHenry, 1991; Lockwood et al., 1996), and the smaller individuals retained features that would allow for more efficient climbing, whereas the larger individuals showed features more efficient in bipedal walking. Recently discovered footprints at Laetoli (Masao et al. 2016) corroborate the original (Johanson et al., 1979) description of the species as highly dimorphic in size. This dimorphism could indicate multiple locomotor patterns within a single taxon, and emphasize intraspecies variability.

This variation in locomotor repertoire has alternatively been interpreted as there being two separate species of hominins with two different sets of behaviour (Deloison, 1999). It has

been proposed that postcranial features could be clear phylogenetic indicators, and that the differences seen in the *A. afarensis* material represent a deep dichotomy in their locomotion (Senut, 1996; Senut et al., 2001). The smaller *A. afarensis,* along with *Paranthropus aethiopicus, Paranthripus robustus,* and *Paranthropus boisei* specimens comprise a lineage of climbers/bipeds, whereas the larger *A. afarensis*, *A. anamensis*, *Orrorin tugenensis*, and early *Homo* comprise obligate bipeds (Senut, 1996; Senut et al., 2001). Discounting which theory is more plausible, most evidence points to a scenario in which more than one locomotor repertoire was present at the same time. There was *A. africanus* with inferred ape-like intermembral proportions, overlapping with the Bouri skeleton with human-like intermembral proportions, *H. habilis* with ape-like intermembral proportions overlapping with *Homo ergaster* with human-like intermembral proportions (Richmond et al. 2001).

Of particular relevance to this study are the postcranial remains of South African robust australopiths attributed to *P. robustus*. This taxon is mainly represented by cranial remains (Grine, 1993; Constantino and Wood, 2007), and postcranial remains are sparse. Until 1988, very little postcrania had been attributed to *Paranthropus*, making inferences about their body size and proportions very difficult. Based on the material found up until 1988, which included 57 specimens from various postcranial elements, McHenry (1991) concluded that *Paranthropus* had a very small body in relation to modern humans, and that it may have displayed as high level of sexual dimorphism. Some research has been done to define the type of locomotion they exhibited (Napier, 1964; Robinson, 1974; Grine et al., 1991; McHenry et al., 2007). Two notable works can be attributed to Napier (1964), and Robinson (1974), who compared *Paranthropus* to *A. africanus* postcrania. Both agreed that *P. robustus* and *A. africanus* had considerable adaptations to bipedalism, but that there were nonetheless differences in postcranial morphology between them. Napier (1964) argued based on the pelves and proximal femora of the two taxa, that *P. robustus* had a less efficient form of bipedalism than *A. africanus*, with a ‘waddling gait’ and an inability to

transfer body weight from one foot to the other during walking. He attributed this difference to different ecological preferences of the two taxa. *P. robustus* was said to have spent more time in woodland savannah settings, whereas *A. africanus* spent more time in open savannah settings. However, any substantial interpretations of their behaviour are hindered by a paucity of material and by overt generalizations of simplistic ecological models.

The most recent large-scale discovery of postcrania attributed to *Paranthropus* from Swartkrans comes from a mixed assemblage that also includes early *Homo* remains, bringing the total number of hominin postcranial remains from Swartkrans to about 70 (Susman et al., 2001). Recent research has shed light on *Paranthropus* gait through the inner structural morphology of pedal elements from Swartkrans (Su and Carlson, 2017; Dowdeswell et al., 2017). Trabecular analysis of the talus (Su and Carlson, 2017) and diaphyseal cortical bone properties within the fifth metatarsal (Dowdeswell et al., 2017) indicate a medial weight transfer of the foot during push-off, and loading of the lateral column in a human-like way.

2.5.1 Feet in the fossil record

The fossil record is already fairly scarce in terms of complete foot remains from Plio-Pleistocene taxa, and it is even further reduced if taking into consideration complete, or partially complete feet. The most complete hominin pedal remains from the Plio-Pleistocene are attributed to *Ar. ramidus* (White et al., 1994; Lovejoy et al., 2009), *A. afarensis* (Johanson et al., 1989), *A. africanus* (Clarke and Tobias, 1995), and *H. habilis* (Leakey et al., 1964), all of which possess complete or partial MT1s.

The earliest of the aforementioned species, *Ar. ramidus* (~4.5 mya) possessed a foot with a range of primitive and derived features, likely capable of hallucal grasping due to its abducted MT1 and a lateral foot that potentially acted as an effective lever for toe-off during bipedalism (Lovejoy et al., 2009; White et al., 2015). Later australopiths show clearer adaptations for habitual bipedalism. Most of what we know about *A. afarensis* foot morphology comes from fossils recovered from Hadar, in particular the A.L.333 collection, which is composed of tarsals, metatarsals, and phalanges (Latimer et al., 1982). Cumulatively, these elements suggest that the foot was close in morphology and function to modern great apes (Stern and Susman, 1983; Susman et al., 1984, McHenry and Coffing, 2000). The first metatarsal from this collection (A.L.333-54) preserves only the proximal portion, consequently most interpretations centred around this specimen have focused on the proximal articular surface (Latimer et al., 1982; Proctor et al., 2008; Proctor, 2010). It is described as more similar to non-human primates because it lacks the facet which would indicate contact with the second metatarsal, and because of the relatively curved proximal articular surface that is more similar to extant apes (Proctor et al., 2008; Proctor et al., 2010). The remaining pedal elements have shown adaptations for bipedality and arboreal locomotion, including longer and ventrally curved phalanges and well-developed insertions for the flexor sheaths, but also human-like expansion of the dorsal articular surface of the head of the proximal phalanges that indicates an enhanced range of dorsiflexion at the joints (Tuttle, 1981; Stern and Susman, 1983; Susman et al., 1984). A limited amount of information can also be drawn about locomotor behaviour in fossil hominins based on footprint patterns. Based on footprint patterns from Laetoli, dated to 3.66 Ma and attributed to *A. afarensis* (Bennett et al. 2009; Raichlen et al. 2010; White & Suwa 1987; Leakey & Hay, 1979), it has been argued that *A afarensis* lacked a medial weight transfer and retained an ability to abduct the hallux. However, Stern and Susman (1983) emphasize a marked adduction of the hallux, a deep impression of the ball of the foot, as well as a uniformity of the toes, features that are seen in obligate bipeds.

Little Foot (Stw 573), which was found at Sterkfontein, South Africa, is currently attributed to *A. africanus*, and has preserved the talus, navicular, medial cuneiform, and first metatarsal (Clarke and Tobias, 1995; Clarke, 2008). Interpretations of the first metatarsal have been fairly varied, with some authors suggesting it was divergent (Clarke and Tobias, 1995). This was based largely on the medial orientation of distal articular surface of the medial cuneiform. However, more recently, studies have observed the degree of divergence of the hallux within the great apes and fossils by examining the relationship between the medial cuneiform and the first metatarsal (Berillon, 1999; McHenry and Jones, 2006). By examining the corresponding articular facets of the MT1 and the medial cuneiform, they concluded that the specimen did not have an abducted hallux, and falls within the range of modern *Homo sapiens* (McHenry and Jones, 2006; Proctor et al., 2008; Proctor, 2010). Additionally, multivariate analyses of the Stw 573 tarsal bones using geometric morphometrics have demonstrated that the foot shows a more ape-like talus, an 'intermediate' navicular, and a human-like medial cuneiform that suggests a lack of abduction (Harcourt-Smith, 2002).

Locomotor diversity within Plio-Pleistocene hominins is further emphasized by pedal remains from Ethiopia dated to 3.4 mya. The Burtele foot (Haile-Selassie et al., 2012) is described as similar to Ar. ramidus in its abducted hallux, and degree of MT2 torsion, with a lateral foot that was capable of bipedalism. Despite the fact that it is contemporaneous to A. afarensis, the two taxa do not share many similarities, and they are interpreted as having highly different modes of locomotion. This has been suggested as indicating the presence of more than one hominin species during the Late Pliocene of eastern Africa, and of the persistence of species with a similar mode of locomotion to *Ar. ramidus*.

Of the pedal elements attributed to early *Homo*, the Olduvai foot (OH 8), attributed to *Homo habilis*, has been crucial in our understanding of hominin foot evolution (Leakey, Tobias, and

Napier, 1964). It consists of a talus, metatarsals lacking their heads, and a damaged calcaneus (Day and Napier, 1965). It possesses features which have been said to resemble a talus assigned to *Paranthropus robustus* (Susman and Stern, 1982), and features more similar to modern *Homo*. These include bases of the MT1 and MT2 that indicate no hallucial abduction, a short MT1, and a strong longitudinal arch. However, the overall morphology of the metatarsals indicates a more robust overall structure than *Homo sapiens.* (Day and Napier, 1964; Day and Wood, 1968; Susman and Stern, 1982; Wood, 1992). Wood (1973, 1974) compared the OH8 talus to a talus from Koobi Fora (KNM-ER 813), which is similar in age to OH 8, and was interpreted as have a more human-like morphology.

2.5.2 SKX 5017 and SK 1813

The fossils used for this study (SKX 5017 and SK 1813) were both found in isolation, meaning they cannot be attributed to a specific taxon, however they have been most closely aligned to *Paranthropus robustus* (Brain, 1984; Susman and Brain, 1988).

Specimen SKX 5017 is an isolated left MT1 recovered from the lower layer of Swartkrans Member 1, which is dated to approximately 1.5-1.8 Ma (Susman and Brain, 1988; Susman and de Ruiter, 2004). Along with the other fossils found within this level, SKX 5017 is attributed to *Paranthropus robustus*. If this dating is accurate, the specimen could be contemporaneous to OH 8 (1.8 Ma), and potentially Stw573 from Sterkfontain (Zipfel & Kidd 2006). The specimen is described as short, and closely resembling OH 8 in overall size, and similar in length to female bonobos (Susman and Brain, 1988). The base of the metatarsal resembles human morphology in that it is relatively flat, as opposed to the concave surface characteristic of great ape basal metatarsal shape (Berillon, 1999; Latimer and Lovejoy, 1990; McHenry and Jones, 2006; Tocheri et al., 2011; Drapeau and Harmon, 2013). This would indicate a limited range of motion within the tarsal-metatarsal joint and increased

stability. In general, there is no indication that the hallux of *Paranthropus* was abducted to an ape-like degree (Susman and Brain, 1988; Susman and de Ruiter, 2004). The overall proportions of the shaft and robusticity are similar to humans, while the head displays a mosaic of primitive and derived features. The superior articular surface of the head extends onto the dorsum of the shaft, which is an indication of increased dorsiflexion at the MTPJ during bipedalism (Stokes et al., 1979; Susman and Brain, 1988; Susman and de Ruiter, 2004; Griffin and Richmond, 2005; Griffin et al., 2010). In contrast, the dorsal medio-lateral breadth of the head is narrower than the plantar breadth, suggesting the joint did not close-pack in dorsiflexion, and that *Paranthropus* employed a different, less efficient mode of bipedalism (Susman and Brain 1988; Susman and de Ruiter, 2004).

Specimen SK 1813 is a nearly complete left first metatarsal found in a backfill hole, and is thought to come from Member 1 or 2, but attribution to a specific stratigraphic unit cannot be made with certainty (Susman and de Ruiter, 2004). Presence of an epiphyseal line near the base signals the subadult status of this individual, with an estimated age of approximately 15 years (Susman and de Ruiter, 2004). It bears strong morphological affinities to SKX 5017, albeit the former is smaller. It has the same dorsal mediolateral narrowing on the head, and expansion of the dorsal articular surface onto the dorsum of the shaft (Susman and Brain, 1988; Susman and de Ruiter, 2004). The base is also human-like in its morphology – it is dorsoplantarly expanded, which is more adaptive to a bipedal gait (Proctor et al. 2008, Proctor, 2010). The stout form of SK 1813 and its basal morphology is suggestive of increased tensile forces from well-developed plantar ligaments (Susman and de Ruiter, 2004).

2.6 Trabecular bone studies in extinct hominids

Efforts have been made to look beyond external morphology alone by examining the trabecular bone structure within limited fossil taxa (DeSilva and Devlin, 2012; Su et al., 2013; Barak et al., 2013b; Su and Carlson, 2017). DeSilva and Devlin (2012) analysed the trabecular bone structure of *Australopithecus* tali in relation to modern humans, chimpanzees, gorillas, and orangutans. Generally, they found that despite certain arrangements in the trabecular bone consistent with the compressive loads associated with mode of locomotion (i.e. highly anisotropic trabeculae in humans), the trabecular architecture showed no clear-cut intraspecies or regional differences in architecture that were unique to humans. All trabecular parameters (thickness, number, spacing, and connectivity density) had the same regional relationships across taxa. This is suggestive of a deeply conserved architecture in the primate talus, and limits the extent to which the talar trabeculae can be used to infer positional behaviour (DeSilva and Devlin, 2012). Though they found that *Australopithecus* tali were human-like in many respects, they differed in having more anisotropic trabeculae in the posteromedial quadrant of the talus as opposed to the posterolateral one in humans. However, recent analysis of the trabecular structure within the talus (Su and Carlson, 2017) has contradicted these results by finding clear differences in trabecular strut orientation and shape between taxa. Within the comparative sample of modern great apes and humans, *Paranthropus* tali resembled the human condition in the anterior-medial subregion, with a strut orientation positioned to distribute compressive loads medially and toward the talar head. In *A. africanus*, primary strut orientation in this region appears most similar to that of great apes. This indicates a medial weight shift in *Paranthropus* that *Australopithecus* did not possess.

Relatively later *Homo* specimens become marginally easier to interpret. Specimens from Dmanisi represent some of the earliest hominins outside of Africa (1.77 Ma), and include the

only early Pleistocene hominin population for which a complete femur, tibia, and associated foot bones have been found. The hind limb is described as functionally similar to later members of the genus *Homo*, with the exception of the metatarsals, which have a more primitive morphology and are more similar to OH 8 and earlier hominins rather than modern humans (Pontzer et al., 2010). The first metatarsals associated with the Dmanisi hominins are robust and appear more human-like in morphology, but like the OH 8, SK 1813, and SKX 5017 fossils, show variations that would imply a different type of bipedalism (Pontxer et al. 2010).

Ultimately, these interpretations will always suffer because many elements of external morphology can be subjectively interpreted. If a strong link is found between trabecular morphology and principal load patterns in a comparative sample of extant primates and humans, then this methodology can be applied to fossil hominins to obtain a more objective interpretation. By looking at the first metatarsal, an element which has an important evolutionary role, and has shown promise in trabecular bone studies, my project could shed light on the actual behavioural patterns of fossil hominins.

Chapter 3. Manuscript

3.1 Introduction

One of the central questions within the study of human evolution is how and when obligate bipedalism emerged. The forefoot is of particular importance in addressing this question because it directly reflects the extent to which a species is capable of terrestrial versus arboreal locomotion. The first metatarsal has arguably undergone the most dramatic transformation within the forefoot, from a digit used primarily for grasping, to a digit used mainly for weight-bearing, stabilization, and propulsion in modern humans. Using a comparative sample of modern human and non-human primates, this study will address how trabecular structure is reflective of locomotor mode, with the ultimate goal of comparing them to fossil hominins to help resolve debates about earlier forms of bipedalism.

3.1.1 Bone functional adaptation

Functional interpretations of fossil hominin locomotion largely vary because of a lack of consensus on the functional significance of various external skeletal features. Because fossil hominins often possess a mosaic of primitive and derived features, it remains unclear whether they continued to engage in arboreal locomotion, or if they used a form of bipedalism similar to modern humans (Stern and Susman, 1983; Latimer et al., 1987; Clarke and Tobias, 1995; Harcourt-Smith and Aiello, 2004; Zipfel et al., 2009, 2011; Haile-Selassie et al., 2012; DeSilva et al., 2013; Harcourt-Smith et al., 2015). This problem can be overcome by studying aspects of bone that are more responsive to external loading. While articular surfaces indicate the joint positions an individual was able to adopt, internal bone is more likely to show how the joint was actually loaded (Ruff and Runestad, 1992; Kivell, 2016). Cortical bone has been shown to respond to mechanical stress, and is known to

respond to tension and compression in the shaft (Ruff, 1983; Cowin et al., 1985; Doden, 1993; Carlson, 2005; Ruff et al., 2006), however, it is less evident in inferring joint positioning at the epiphyses. Trabecular bone remodels at a faster rate than cortical bone (Eriksen, 2010), and can provide evidence of in vivo loading that may be more useful at reconstructing predominant joint position and associated behaviours (Rubin et al., 2002; Pontzer et al., 2006; Barak et al., 2011; but see Bertram and Swartz, 1991).

The current study focuses on two main structural properties of trabecular bone: bone volume fraction (BV/TV), which is affected by both trabecular thickness and spacing, and degree of anisotropy (DA), which measures the degree to which the trabecular struts are oriented in the same direction. These parameters account for 87-89% of the variance in a bone's strength (Young's modulus) (Maquer et al., 2015) and have been shown to change in relation to changes in magnitude, frequency, and direction of load within *in vivo* studies (Lanyon, 1974; Hodgskinson and Currey, 1990; Biewener et al., 1996; Rubin et al., 2002; Mittra et al., 2005; Pontzer et al., 2006; Barak et al. 2011) and to separate taxa that employ different modes of locomotion (MacLatchy and Muller, 2002; Ryan and Ketcham, 2002, 2005; Ryan and Shaw, 2012; Scherf et al., 2013; Tsegai et al., 2013, 2017; but see Ryan and Ketcham, 2010). BV/TV is an informative parameter to study because it is less likely to scale allometrically (Barak et al., 2013), and is known to be higher in areas that experience greater load, and DA is known to adapt to the direction of an element's range of movement (Biewener et al., 1996; Ryan and Ketcham, 2002; Pontzer et al., 2006, Barak et al., 2011; but see Ruff et al., 2005). It should be noted that the exact functional adaptation of trabecular bone is not fully understood. It is known that there is a genetic component to its structure (Havill et al., 2010), and that different elements might show differential trabecular adaptation (Räth et al. 2015). There is also uncertainty about the role of frequency vs. magnitude of load on trabecular remodelling (Skerry and Lanyon, 1995; Lambers et al. 2013).

3.1.2 MT1 biomechanics

In order to make predictions about trabecular distribution within the metatarsal, a knowledge of the loading regime of the foot must be understood. Modern humans are adapted for a uniquely bipedal mode of locomotion, and possess a forefoot structure in which each metatarsophalangeal joint (MTPJ) acts as a largely weight bearing and propulsive structure during the push-off part of the stance phase (Stokes et al.,1979; Christensen and Jennings, 2009; Griffin et al., 2015). It is during this phase that the MTPJs dorsiflex, moving the proximal phalanges on to the dorsum of their respective metatarsal heads. This causes tightening of the plantar aponeurosis, stabilizing the foot and elevating the longitudinal arch, changing its conformation to a stiff lever for propulsion and ultimately toe-off (Hicks, 1954; Bojsen-Moller, 1979; Susman, 1983; Caravaggi et al. 2010; Griffin et al., 2015). As shown by *in vivo* studies of plantar pressure distribution within the human foot, it is during dorsiflexion that the medial forefoot shows a spike in loading (Hutton and Dhanendran, 1981; Katoh et al., 1983; Soames, 1985; Munro, 1987; Lee and Farley, 1998; Hunt et al., 2001; Nester et al., 2007; Griffin et al., 2010). The first metatarsal (MT1) bears a large portion of this compressive load, which is evident in its external morphology. The MT1 head in humans is generally larger than that of other great apes, due to the greater amount of loading it incurs during push-off. The superior aspect of the articular surface of the head expands to the dorsum of the bone, resulting in a raised appearance in relation to its shaft, which is thought to increase the range of dorsiflexion at the MTPJ (Stokes et al., 1979; Susman and Brain, 1988; Susman and deRuiter, 2004; Griffin and Richmond, 2005; Griffin et al., 2010). Finally, it is medio-laterally wide on the dorsal aspect of the head, which has been argued to enhance joint stability during push-off and facilitate close-packing of the MTPJ (Susman & Brain, 1988; Hetherington et al., 1989; Susman & de Ruiter, 2004; Pontzer et al., 2010, Fernandez et al., 2015).

The non-human primate MT1 head does not experience loading in the same way as in modern humans, as demonstrated by *in vivo* studies of bonobos (Vereecke et al., 2003; d'Août et al., 2004; Griffin et al., 2010) and chimpanzees (Wunderlich and Ischinger, 2017). During terrestrial quadrupedalism, the lateral midfoot shows a higher spike in loading at push-off than the medial aspect, minimizing the strain inflicted upon the MT1 (Vereecke et al., 2003). Instead, the MT1 incurs increased loading during vertical climbing, when the MTPJ is plantarflexed (Wunderlich and Ischinger, 2017). This is reflected within the shape of the MT1 head, which is mediolaterally expanded on the plantar aspect (Susman, 1983; Latimer and Lovejoy, 1990; Griffin and Richmond, 2010; Marchi, 2005, 2010; Fernandez et al., 2015). The same mechanism that allows for close-packing of the MTPJ during dorsiflexion within humans allows for close-packing during plantarflexion in non-human primates, increasing stability during pedal grasping (Susman, 1983; Susman and de Ruiter, 1984; Griffin et al., 2010). Within non-human primates, there is variation in how the hallux is used for locomotion. Though comparative plantar pressure distribution data between *Gorilla*, *Pongo*, and *Pan* does not exist, a substantial amount of information can be obtained through observational studies (Sarmiento, 1994; Remis, 1995), and skeletal morphology (Susman, 1979; Shea, 1981; Inouye, 1992; Doran 1997; Richmond, 1998; Marchi, 2005; Drapeau and Harmon, 2008; Congdon, 2012; Jashashvili et al. 2015). *Pongo* generally do not use the hallux in suspension, whereas *Pan* generally does (Oishi et al., 2012). Although gorillas can locomote arborearly, their size restricts them to supports of larger diameters, and they typically do not use their feet for suspension. Their feet are instead used for vertical climbing or walking, and because the supports they use for climbing are usually large relative to their foot size, there is little flexion of the metatarsophalangeal and interphalangeal joints (Sarmiento, 1994; Remis, 1995).

The proximal articular surface of the MT1 is equally reflective of locomotor behaviour. Within modern humans, it is relatively broad and flat, corresponding to a stable tarsometatarsal joint complex that reduces mediolateral mobility of the hallux, and keeps it in line with the other

metatarsals. (Morton, 1924; Susman and Brain, 1988; Proctor et al. 2008; Proctor, 2010; Gill et al. 2015). Its broad mediolateral width is related to the bending stresses experienced near the base, and its increased cross-sectional area is a response to high compressive forces at the joint, and high tensile forces inflicted upon the ligaments (Stokes et al., 1979; Griffin and Richmond, 2005). In all other living great apes, the proximal MT1 does not experience such high loading, resulting in a proximal surface that is dorso-plantary and medio-laterally narrower. The tarsometarsal joint is instead adapted for a wider range of movement associated with grasping. The proximal articular surface of the MT1 is concave, and the distal articular surface of the medial cuneiform is convex, allowing for multiaxial movement of the hallux that is more effective for climbing and grasping (Berillon, 1999; McHenry and Jones, 2006; Tocheri et al., 2011; Drapeau and Harmon, 2013).

3.1.2 Previous trabecular analysis of the MT1

Predictions about how mechanical loading affects the trabecular bone within the MT1 can be made *a priori* based on already known patterns within the MT1 head of modern *Homo*, *Pan troglodytes*, *Pan paniscus*, and *Gorilla gorilla* (Griffin et al., 2010). Using a VOI-based method of analysis, modern humans exhibit significantly higher DA values in the dorsal aspect of the metatarsal head, consistent with a more tightly constrained joint that has a more uniaxial direction of movement. BV/TV has been shown to be less effective at differentiating locomotor behaviour between species, but this may be caused by the methodological limitations of using VOIs in analysing trabecular structure. Overall, these results suggest that within trabecular bone properties, the degree of anisotropy is the most indicative factor of a forefoot habitually used for propulsion during gait (Griffin et al. 2010).

3.1.3 Fossil MT1s

Among more recent hominin taxa (*H. antecessor, H. heidelbergensis, H. neanderthalensis*), there is general agreement that they were fully adapted to obligate bipedalism (Trinkaus 1983; Lorenzo et al. 1999). Despite known differences in lower limb proportions in these taxa, most of the debate concerning the evolution of bipedalism revolves around earlier taxa, including pre-australopiths, australopiths, and early *Homo*. The most complete hominin pedal remains from the Pliocene and Pleistocene are attributed to *Ardipithecus ramidus* (White et al., 1994; Lovejoy et al., 2009), *Australopithecus afarensis* (Johanson et al., 1989), *Australopithecus africanus* (Clarke and Tobias, 1995), and *Homo habilis* (Leakey et al., 1964), all of which possess complete or partial MT1s.

The earliest of the aforementioned species, *Ar. ramidus* (~4.5 mya) possessed a foot with a range of primitive and derived features, likely capable of hallucal grasping due to its abducted MT1 and a lateral foot that potentially acted as an effective lever for toe-off during bipedalism (Lovejoy et al., 2009; White et al., 2015). Later australopiths show clearer adaptations for habitual bipedalism. Though retaining some features for arboreal locomotion (Stern, 200; Ward, 2002), The *A. afarensis* MT1 is adducted and shows dorsal doming of the head (Tuttle, 1981), and maintains ape-like features (Stern and Susman, 1983; Susman et al., 1984, McHenry and Coffing, 2000). Like *A. afarensis*, *A. africanus* shows a range of features adapted for bipedal and arboreal locomotion, but the two show different combinations of morphologies within the foot (see Harcourt-Smith, 2002). Locomotor diversity within Plio-Pleistocene hominins is further emphasized by pedal remains from Ethiopia dated to 3.4 mya. The Burtele foot (Haile-Selassie et al., 2012) is described as similar to *Ar. ramidus* in its abducted hallux and degree of MT2 torsion, with a lateral foot that was efficient in bipedalism. Despite the fact that it is contemporaneous to *A. afarensis*, the two taxa do not share many similarities, and they are interpreted as having highly different modes of locomotion. This has been suggested as indicating the presence of more

than one hominin species during the Late Pliocene of eastern Africa, and of the persistence of species with a similar mode of locomotion to *Ar. ramidus*.

Given its more recent age (2.4-1.4 mya), The OH 8 foot, attributed to *Homo habilis*, has been crucial in our understanding of the evolution of bipedalism in the Pleistocene (Leakey, Tobias, and Napier, 1964). The MT1 is short, and its base shows no indication of abduction, but the overall morphology of the metatarsals indicates a more robust overall structure than *Homo sapiens.* (Day and Napier, 1964; Day and Wood, 1968; Susman and Stern, 1982; Wood, 1992). Its ankle morphology is described as similar to contemporaneous *P. robustus,* and different from KNM-ER 813 (*Homo ergaster*), which has a more modern overall structure. This implies that there were different hominin pedal morphologies at the same time (Harcourt-Smith, 2002).

Of particular relevance to this study are the postcranial remains of South African robust australopiths attributed to *Paranthropus robustus*. *Paranthropus* is mainly represented by cranial remains (Grine, 1993; Grine and Daegling, 1993; Wood and Constantino, 2007), and postcranial remains are sparse. Based on available elements, the gait of *P. robustus* has been described as adapted to bipedalism, but with a 'waddling gait' and an inability to transfer body weight from one foot to another when walking (Napier, 1964; Robinson, 1974). However, recent research has shed light on *P. robustus* gait through the inner structural morphology of pedal elements from Swartkrans (Su and Carlson, 2017; Dowdeswell et al., 2017). Trabecular analysis of the talus (Su and Carlson, 2017) and diaphyseal cortical bone properties within the fifth metatarsal (Dowdeswell et al., 2017) indicate a medial weight transfer of the foot during push-off, and loading of the lateral column in a human-like way. Two complete metatarsals from Swartkrans contribute to our understanding of *P. robustus* locomotion.

Specimen SKX 5017 is an isolated left MT1 recovered from the lower bank deposit of Swartkrans Member 1, which is dated to approximately 1.5-1.8 Ma (Susman & Brain, 1988; Susman & de Ruiter, 2004). Along with the other fossils found within this level, SKX 5017 is

attributed to *Paranthropus robustus*. The specimen is described as short, and closely resembling OH 8 in overall size, and similar in length to female bonobos (Susman and Brain, 1988). The base of the metatarsal has a mildly concave and ovoid shape, similar to modern great apes (Susman and Brain, 1988), though the morphology of the base and proximal shaft provide evidence that human-like plantar ligaments (and perhaps an aponeurosis) were present. The head displays a mosaic of primitive and derived features. The superior articular surface of the head extends onto the dorsum of the shaft, which is seen in humans, and is an indication of increased dorsiflexion at the MTPJ. In contrast, the dorsal medio-lateral breadth of the head is narrower than the plantar breadth, suggesting the joint did not close-pack in dorsiflexion, and thus was less stable during push-off (Susman & Brain 1988). Based on the degree of torsion between the head and base, and the shape of the proximal articular facet, there is no indication that the hallux of SKX 5017 was abducted to an ape-like degree (Susman and Brain, 1988).

Specimen SK 1813 is a nearly complete right MT1 found in a backfill hole of Swartkrans, and is thought to come from Member 1 or 2, but attribution to a specific stratigraphic unit or taxon cannot be made with certainty (Susman and de Ruiter, 2004). Presence of an epiphyseal line near the base signals the subadult status of this individual, with an estimated age of approximately 15 years (Susman and de Ruiter, 2004). It bears strong morphological affinities to SKX 5017, albeit the former is smaller. It has the same dorsal mediolateral narrowing on the head, and expansion of the dorsal articular surface onto the dorsum of the shaft. The base is also dorsoplantarly expanded, which is more reflective of increased tensile forces from well-developed plantar ligaments in response to a bipedal gait (Susman and de Ruiter, 2004; Proctor et al. 2008, Proctor, 2010). The shape of the proximal articular surface is difficult to discern due to post-mortem damage, but it is nonetheless described as concave and ovoid, typical of non-human primates (Susman and de Ruiter, 2004). Studying trabecular bone structure within extant primates has a direct utility in reconstructing locomotion within fossil taxa that have been described as ‘intermediate’ and ‘mosaic-like’ in

their external morphology. If specific trabecular parameters within the comparative sample can separate modes of locomotion, inferences about the locomotion of SKX 5017 and SK 1813 can be made with reasonable confidence.

3.1.4 Aims and predictions

Based on what we know about loading patterns within the forefoot of comparative modern taxa and the adaptation of BV/TV and DA in response, the following hypotheses can be made about the comparative sample:

1. Modern humans will have a higher BV/TV within the dorsal aspect of the MT1 head and base, and non-human primates will display the opposite pattern. This corresponds to the position in which the joint close-packs and incurs the highest loads.
2. DA within non-human primates will be lower because of a multiaxial range of motion within the joint, whereas modern humans will show higher DA because of the tightly constrained nature of the joint and its uniaxial range of motion.
3. Based on previous studies on *P. robustus* pedal elements and on the external morphology of SKX 5017 and SK1813, which bear strong affinities to modern humans, it is hypothesized that the two specimens will show similar BV/TV distribution to modern *Homo*. Based on the relatively more concave proximal articular facet it is predicted that DA will be lower in this region compared to modern humans.

3.2 Methods

3.2.1 Sample

The comparative sample consists of thirty-nine MT1s from modern non-human great apes and modern humans: six *Pongo pygmaeus*, ten *Gorilla gorilla*, ten *Pan troglodytes*, and eleven *Homo sapiens* (Table 1). All non-human apes were wild-caught, with the exception of one captive male *Pongo pygmaeus* (for additional information see Supplementary Information, Table 1). The modern human sample is composed of 19th – 20th century, likely sedentary and shod individuals from a single archaeological collection (see SI, Table 1). Specimens were chosen if they were adult, free from signs of pathology, and if the trabecular bone was well-preserved. Adult status was determined based on external morphology of the associated postcrania and dental eruption (as well as examination of the internal structure and absence of epiphyseal lines). Additional information on individual specimens is provided within the Supplementary Information. Two fossil metatarsals were obtained from Swartkrans, South Africa, one of which is attributed to *Paranthropus robustus* (SKX 5017), and the other being of unassigned taxonomic status (SK 1813). Both preserve the entire bone morphology, but because of extensive cortical and trabecular damage to the base of SK 1813, only its head was analysed.

Table 1. Study sample composition

Taxon	Side (R/L)	Sex (M/F/?)	Locomotor mode
Pongo pygmaeus	6 (3/3)	1/4/1	Suspensory (torso-orthogrady)
Gorilla gorilla	10 (6/4)	5/5/0	Knuckle-walker
Pan troglodytes	10 (5/5)	6/4/0	Knuckle-walker
Homo sapiens	11 (9/2)	6/5/0	Bipedal
Paranthropus robustus (?) SKX 5017	(0/1)		Bipedal/arboreal (?)
SK 1813 (Hominin indet.)	(1/0)		Bipedal/arboreal (?)

3.2.2 Image Acquisition

Specimens were scanned at the Max Plank Institute for Evolutionary Anthropology in Leipzig and at Cambridge University. The modern *Homo* and *Pongo* specimens were scanned using the Diondo d3 high-resolution micro-CT system in Leipzig with an acceleration voltage of 140 kV, 120 mA and 140 µA respectively, using a 0.5 mm brass filter. The images were reconstructed as 3000 x 3000 16 bit tiff image stacks from 2400 projections with two frame averaging. The Tai Forest *Pan troglodytes* sample was scanned using a Skyscan 1173 with an acceleration voltage of 100 kV and 62 µA using a 1.0 mm aluminium filter. The images were reconstructed from 2240 x 2240 16 bit tiff image stacks from 2400 projections with two frame averaging. *Gorilla gorilla* and *Pan troglodytes* specimens from the Powell-Cotton Museum were scanned using a Nikon Metrology XT H 225 ST High resolution CT scanner in Cambridge University. They were scanned at an acceleration voltage of 135 kV and 135 µA with no filter. The images were reconstructed as 2000 x 2000 16 bit tiff image stacks from 1080 projections with one frame averaging. All specimens were scanned with an isometric voxel resolution of between 27 and 42 µm.

3.2.3 Specimen segmentation

Scans were segmented into binary format using the Ray Casting Algorithm (Scherf and Tilgner, 2009). This method is most effective where there is clear separation between bone and air, and where there is little matrix within the epiphysis. All extant taxa, along with SKX 5017 were segmented using this method. Due to a large amount of matrix within the epiphysis of SK 1813, it was segmented using a machine learning clustering algorithm that is most effective where there is matrix that falls within the greyscale range of trabecular bone. This algorithm assigns voxels in an image to one three predefined classes, based on the probability that its greyscale value would be in each class. Therefore, it allows for segmentation of problematic areas that the RCA does not handle effectively.

3.2.4 Medtool

The segmented images were processed through a customised script within medtool, a python-based script manager (Pahr and Zysset, 2009). Each step of this method has been described by Pahr and Zysset (2009) and tested by Gross et al. (2014). Using the segmented image (Fig. 3.a), the outer surface (Fig. 3.b), and inner surface (Fig. 3.c) were defined and subtracted from one another to create an image of the cortex only (Fig. 3.d). An image of the trabecular bone (Fig. 3.e) only was obtained by subtracting the cortex image from the original segmented image. A series of mask overlays were created to separate the cortical and trabecular bone, and ‘inside air’ from ‘outside air’ by assigning them to different grey values (Fig. 4).

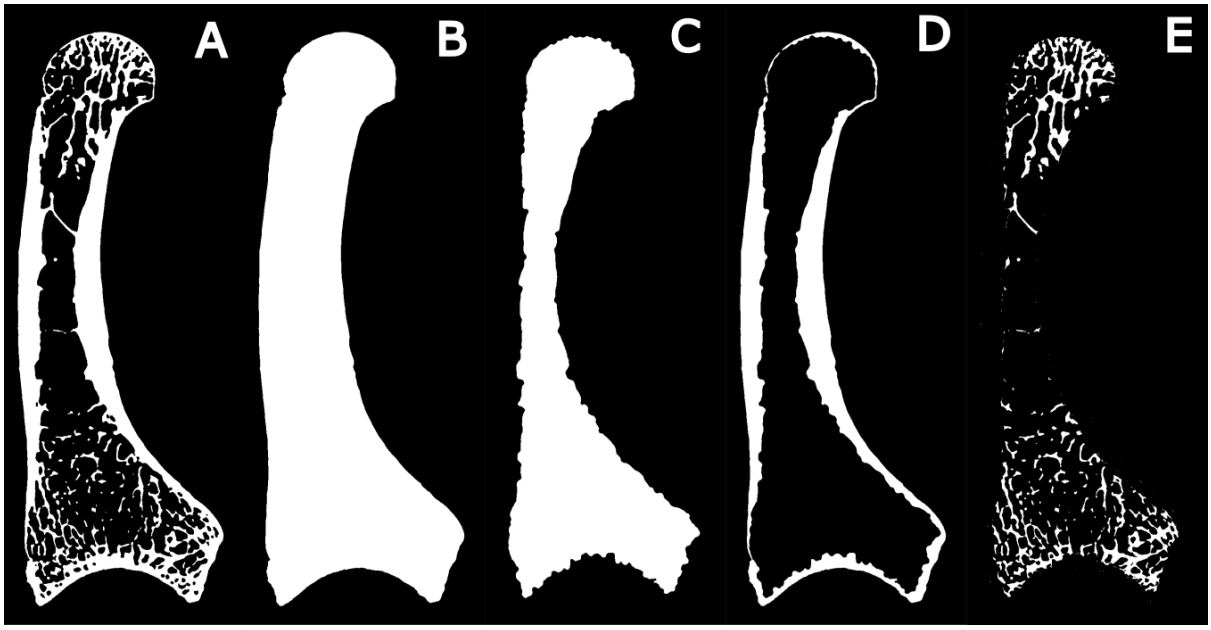

Figure 3. Masking procedure. From left to right: (a) segmented image; (b) outer mask; (c) inner mask; (d) cortical mask; (e) trabecular only image.

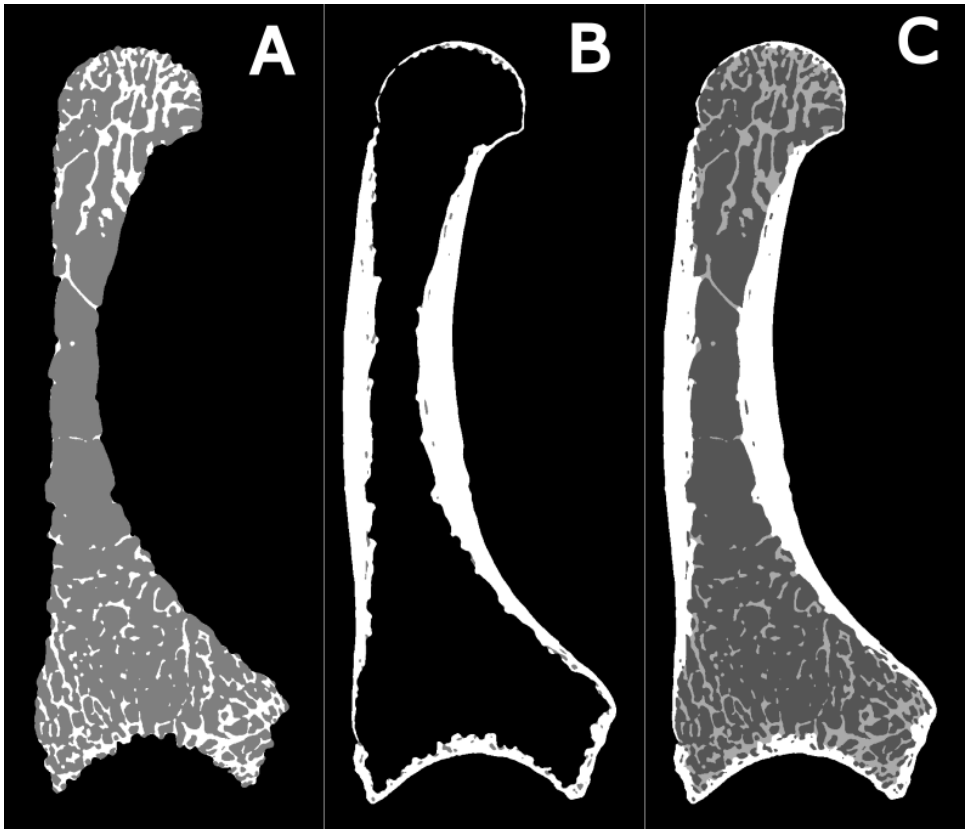

Figure 4. Mask overlays. From left to right: (a) MaskSeg In; (b) MaskSeg Out; (c) MaskSeg

A 3D mesh of the specimens was obtained using the computation geometry algorithms library (CGAL), a mesher that creates a 3D finite element model using 3D Delauney triangulation (Delaunay, 1934). Trabecular bone was analysed through the placement of multiple spherical volumes of interest (VOI) onto a rectangular background grid of 2.5 mm grid spacing over the MaskSegIn image (Fig. 4a). VOIs are placed at each node with a set diameter of 5 mm to ensure overlap. Trabecular parameters were measured within each VOI, and then assigned values to each node, which were interpolated to the tetrahedral elements, resulting in BV/TV and DA colour maps that were visualized using Paraview 3.14.1 (Sandia Corporation, Kitware. Inc).

Within each VOI, bone volume fraction (BV/TV) was calculated as the ratio of bone voxels to bone and air voxels. The trabecular orientation (second rank fabric tensor) is calculated using the Mean Intercept Length (MIL) method (Whitehouse, 1974; Odgaard, 1997). This gave results for first, second, and third eigenvectors and eigenvalues. The values within each VOI were averaged to obtain results for the entire section. Using these mean values, fabric degree of anisotropy (DA) was calculated as 1 minus (eigenvalue 3/eigenvalue 1), which describes the degree of trabecular orientation. In addition to BV/TV and DA, trabecular thickness (Tb.th., mm), trabecular number (Tb.N, mm^{-1}), and trabecular spacing (Tb.S, mm) were calculated within each VOI using the method described by Lazenby et al. (2011).

3.2.5 Statistical analysis

Because the focus was on the base and head of the metatarsals, these sections were separated from the shaft, which would skew overall results because of its lack of trabecular bone. For each scan, the head was separated where the articular surfaces on the plantar aspect terminated, as they are clearly delimitated from the shaft. When viewing the plantar surface of the element, each metatarsal possesses a pronounced curvature on the medial aspect of the shaft towards the base. Where this curvature is most pronounced is where the

cut for the base was made. The base and the head were further split into dorsal and plantar regions by diving in half their maximum dorso-plantar widths.

All trabecular variables were tested for allometry in R using reduced major axis regression. Data for body size was unavailable for the study sample, and instead the geometric mean for each specimen was calculated using five linear measurements of the metatarsal as proposed by De Groote and Humphrey (2011) and used as a proxy for body size. Measurements included maximum MT1 length, and dorsoplantar and mediolateral length of the proximal and distal articular surfaces.

Pair-wise comparisons using Mann-Whitney U tests were conducted to investigate differences between the dorsal and plantar sections within the head and base of each taxon. To compare differences between taxa, the ratio of dorsal to plantar BV/TV and DA within the head and base was analysed using a pairwise Wilcoxon rank sum test with a Bonferroni correction. Additionally, the dorsal and plantar BV/TV and DA values were compared between species to measure absolute differences in values. In addition to traditional non-parametric tests, differences between the BV/TV ratios of each species were evaluated for statistical significance using a standard resampling method (i.e., bootstrapping), which is well-suited to examine differences between means of groups with varying and small sample sizes (Efron and Tibshirani, 1993). Within each taxon, ten thousand means for the BV/TV ratios were generated after sampling with replacement from the original sample. A pairwise comparison was conducted between the differences of the means between each possible species combination. For each pairwise comparison, the ten thousand means from one taxon were aligned with the ten thousand means from the other taxon, and the ten thousand differences between the two sets of means were calculated. These differences were then compared with the difference between the means of the original samples. The number of times the difference between the bootstrapped means exceeded the difference between the original sample means represents a proportion that is analogous to a p-value of a one-tailed

test. The bootstrap analysis was applied to the fossil sample to determine the likelihood that their BV/TV ratios fell within the resampled and replaced BV/TV ratio means of the extant taxa. In this case, the fossil mean was included within the extant taxon's sample which was then resampled and replaced. Just as with the pairwise extant comparisons, the number of times the fossil's absolute BV/TV ratio fell within the range of bootstrapped mean BV/TV ratios represented the likelihood that this value would be part of the comparative sample.

3.3 Results

3.3.1 Whole bone BV/TV distribution

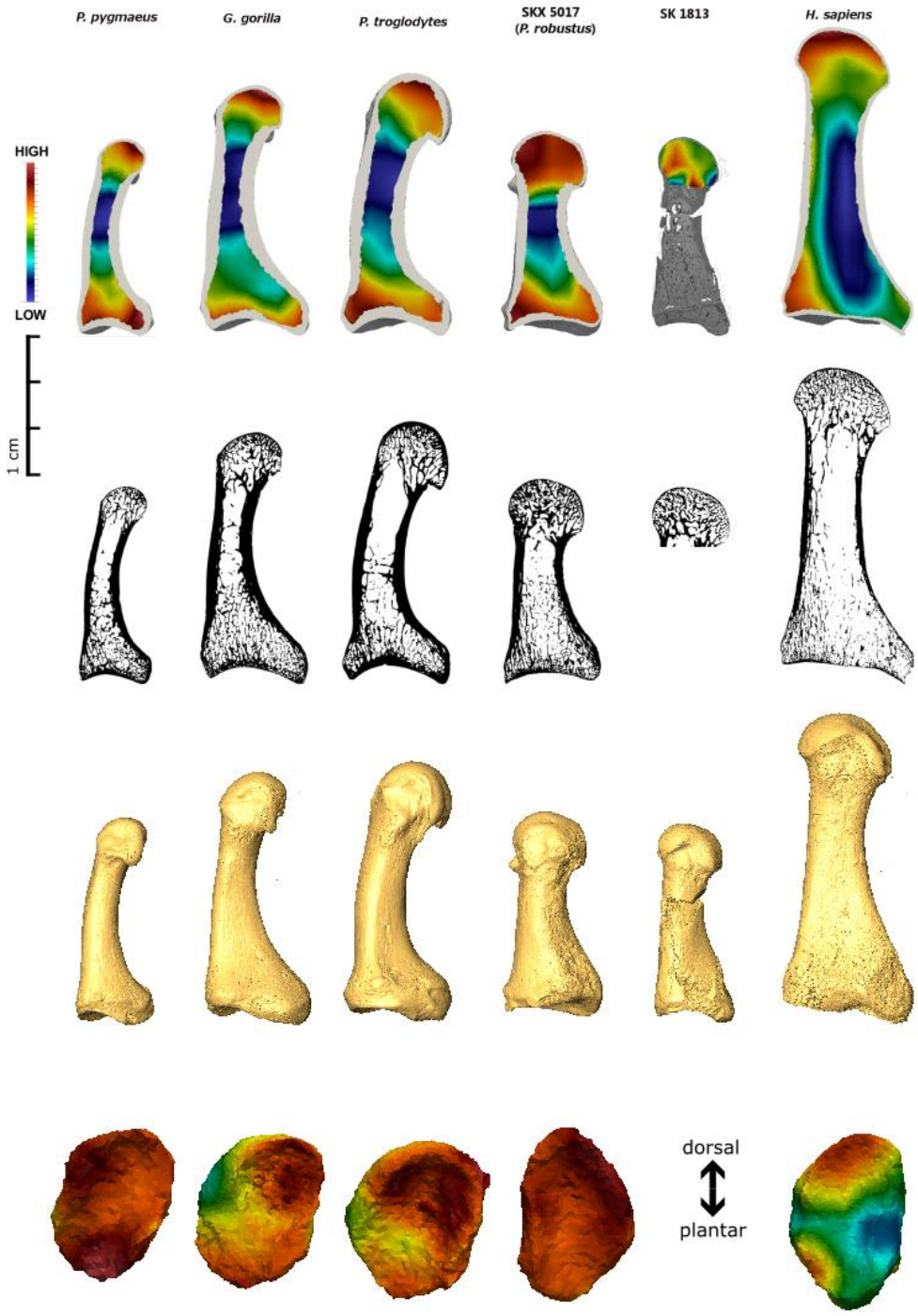

Figure 5. Representative specimens from each taxon. From top to bottom: BV/TV colour maps of bone cross-section, segmentation images, isosurfaces of external bone, and BV/TV colour maps of proximal articular surfaces. BV/TV colour maps are scaled to individual specimen ranges. First three rows are scaled to size.

Figure 5 shows BV/TV colour maps of a representative specimen from each taxon within the sample (images of the full sample are shown within the Supplementary information). Modern humans consistently show a greater distribution of trabecular bone within the distodorsal aspect of the head; although the extent to which BV/TV is higher in the dorsal region varies between individuals, as does the exact position of the highest distribution. Some individuals show higher BV/TV values closer to the centre of the epiphysis, whereas others show higher values near the cortical/trabecular boundary. BV/TV tends to be higher on the lateral side of the dorsal aspect, corresponding with the slightly valgus orientation of the phalanges in relation to the metatarsal shaft. Additionally, specimens show a consistent pattern on the plantar surface of the head whereby the trabecular bone directly below the articular surface for the sesamoid bones shows lower BV/TV. The ventral keel between the articular surfaces has generally higher BV/TV. All modern humans show an area of higher BV/TV on the dorsal half of the MT1 base to varying degrees. The plantar aspect has relatively little trabecular bone, with the exception of increased BV/TV near the insertion site of the peroneus longus tendon, which is more pronounced in modern humans than in non-human primates.

All non-human primates within the sample tend to exhibit a higher concentration of trabecular bone within the plantar region of the head. *Pongo* shows the most plantar concentration, with *Pan* and *Gorilla* showing relatively similar distributions to each other. Like within the modern human sample, the extent to which the trabecular bone extends into the centre of the epiphysis varies: some individuals show fairly localized concentration near the subchondral bone, but other show a much deeper distribution within the entire epiphysis (for e.g., see SI: fig 1. Pp_ZSM_0203, fig. 2 Gg_PC_MER_372, fig. 3 Ptv_MPITC_11800). The pattern of trabecular bone distribution within the base is variable, but overall it is evenly distributed across the dorsal and plantar regions. *Pongo* shows a pattern in which the edges of the articular surface show higher BV/TV (see fig. 5), with relatively less trabecular bone within the centre of the epiphysis. The trabecular bone follows an oblique plane in relation to

the shaft (concentrated within the lateral-plantar and medio-dorsal aspects), and corresponding to the plane in which the metatarsal dorsiflexes and plantarflexes.

Within all taxa, there is variation in how far the trabecular bone from the epiphyses extends into the shaft (see Supplementary Information, figures 1-4). In each taxon, there are individuals with a higher distribution within the shaft. However, modern humans generally show higher a distribution within the dorsal aspect of the shaft, meaning BV/TV is not only higher in the dorsal regions of the head and base, but that it is a widespread trend in the entire element.

Figures 6 and 7 illustrate the external morphology and BV/TV distribution in SKX 5017 and SK 1813, respectively. Like modern humans, the dorsal region of the metatarsal head in SKX 5017 exhibits a higher distribution of trabecular bone than the plantar region; although it is located more dorsally than is generally found within humans. This region of high BV/TV is lateralized and corresponds to a slightly valgus orientation of the phalanges in relation to the shaft. The remainder of the head shows an even distribution of trabecular bone, with an area of slightly higher BV/TV on the plantar aspect on the ventral keel between the articular surfaces for the sesamoid bones (this is also seen in some modern humans). The base of SKX 5017 shows a pattern that appears more like what is seen in non-human primates. The area of highest BV/TV is near the dorso-medial border of the articular surface, similar to where it is seen in several non-human apes, but without a corresponding area of high BV/TV on the plantar-lateral aspect. Both plantar and dorsal regions show high BV/TV, in contrast to modern humans that show a markedly higher and more localized trabecular bone distribution within the dorsal region.

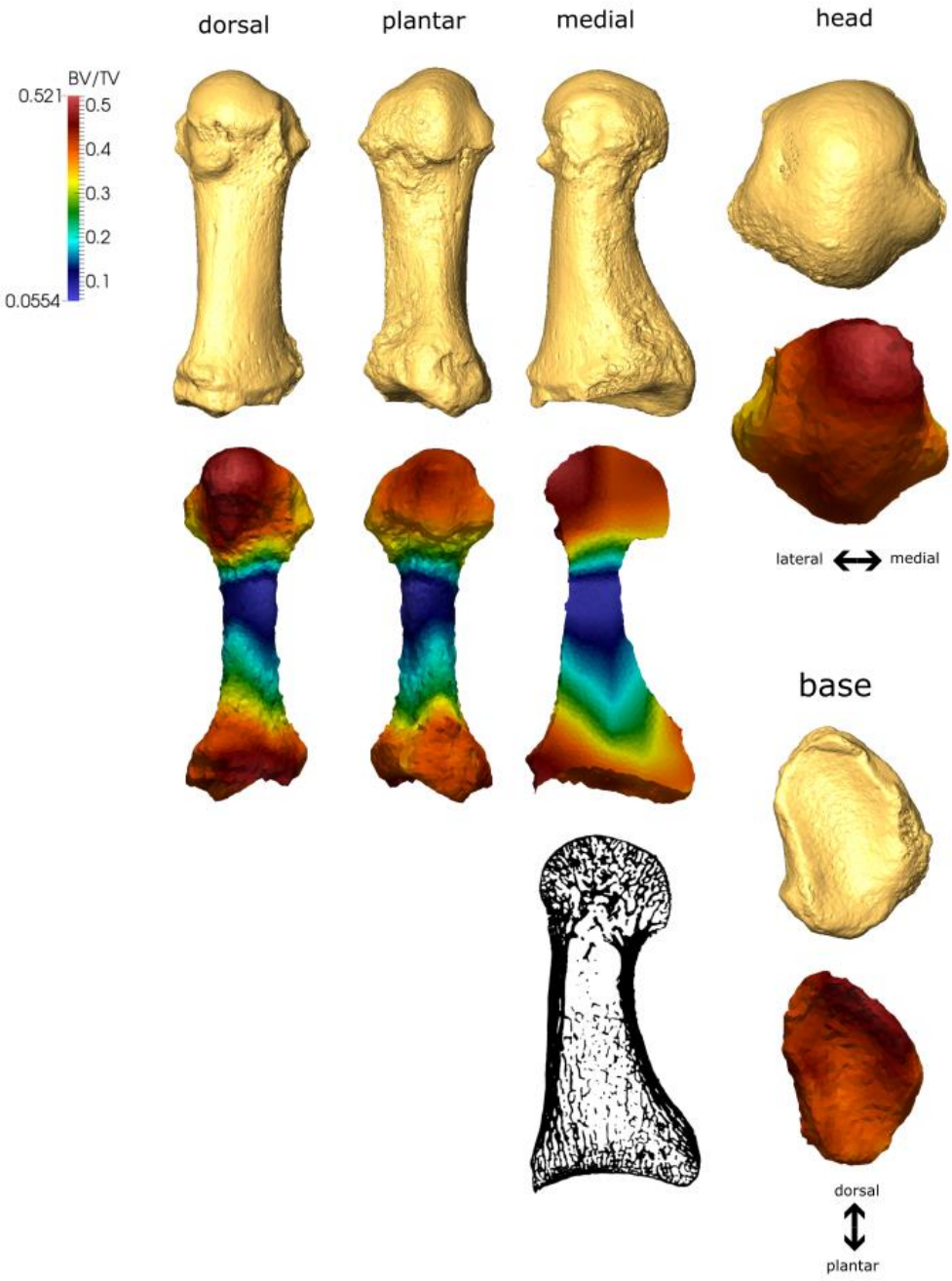

Figure 6. SKX_5017. View of BV/TV colour maps beside cortical isosurface (yellow), and segmentation

SK 1813 (see Figure 7) also shows higher trabecular bone distribution within the dorsal aspect of the head, though it is more centralized within the epiphysis than in SKX 5017 or the modern human specimens. Additionally, the area immediately below the cortical/trabecular boundary shows a sharp decrease in BV/TV. On the plantar aspect, where the shaft meets the head, there is another area of high BV/TV. When comparing the colour map to the

original CT scan, it becomes apparent that this area of high BV/TV is the result of cortical bone from the shaft extending into thick trabecular struts within the head, similar to *Pan* and *Gorilla*. However, SK 1813 shows relatively less trabecular bone within the plantar surface, resulting in a different overall distribution.

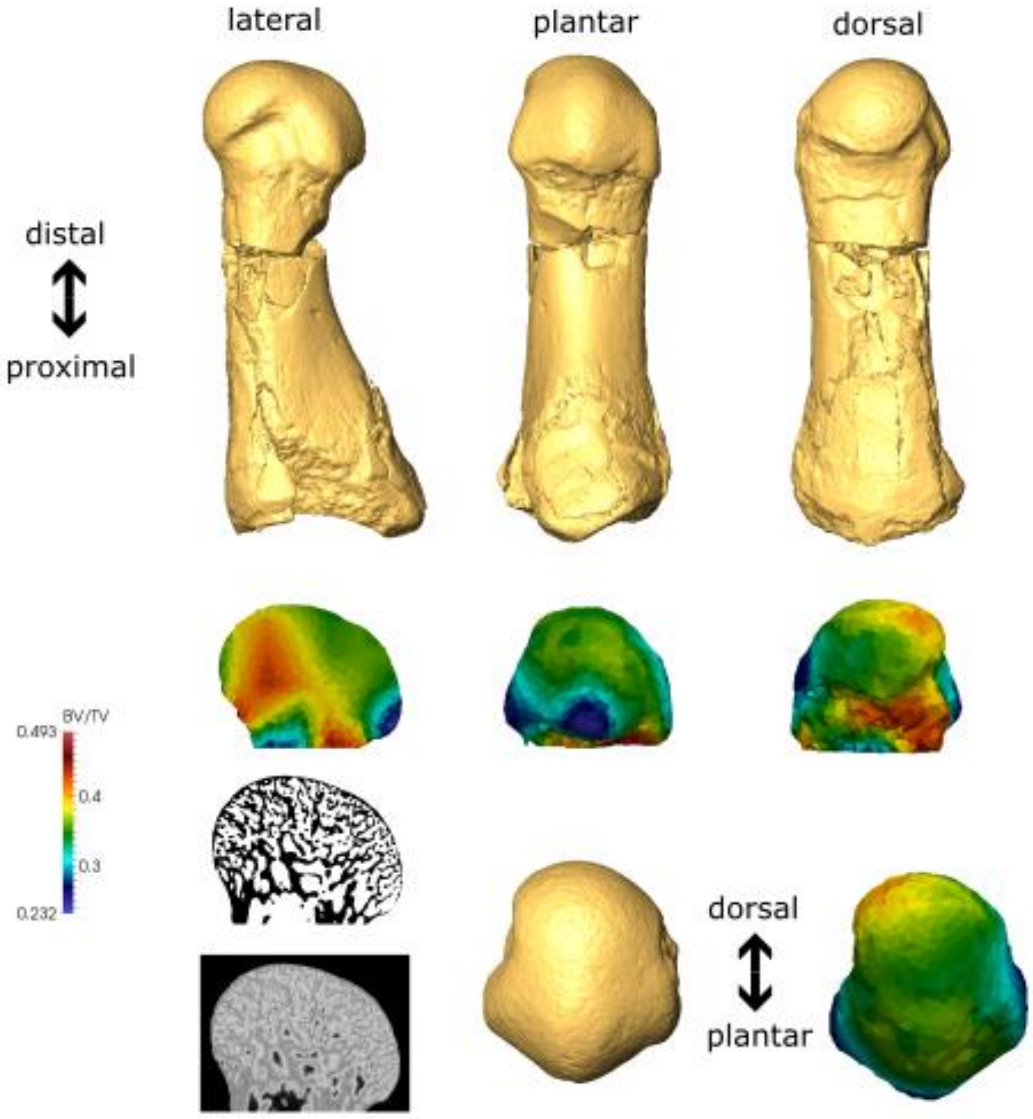

Figure 7. SK 1813. View of BV/TV colour maps beside cortical isosurface (yellow), segmentation, and the original scan.

3.3.2 Allometry

Most parameters showed no significant within species allometric scaling (see Table 2). *Gorilla* showed positive allometric scaling of trabecular thickness, a positive correlation between spacing and body size, along with a negative correlation with trabecular number. However, of these parameters, only trabecular thickness showed significant scaling ($p<0.05$) and the confidence intervals of the slope contained the isometric scaling value. The same pattern is seen in *Homo,* though none of the scaling is significant, and in *Pan*, which shows significant positive and negative allometric scaling of trabecular spacing and number, respectively. BV/TV and DA both show a positive relationship with increased body size, although without any significant positive allometric scaling, allowing for the conclusion that BV/TV and DA are ultimately unaffected by body size. Given the fact that BV/TV does not scale allometrically in any taxon, it can be concluded that body size, and by extension sex do not affect patterns of trabecular distribution to a significant degree.

Table 2. Results from reduced major axis regression analysis.

	variable	Isometric slope value	slope	CL -	CL +	*y*-int	r^2	*p*-value	result
Pongo									
	BV/TV	0	1.94	0.66	5.69	-6.61	0.13	0.48	+
	Tb.Th	1	1.27	0.44	3.62	-4.97	0.18	0.39	+
	Tb.Sp	1	-1.28	-3.81	-0.43	3.14	0.09	0.56	-
	Tb.N	0	0.54	0.18	1.68	-1.39	0.01	0.88	+
	DA	0	1.40	0.45	4.31	-5.28	0.01	0.84	+
Gorilla									
	BV/TV	0	0.89	0.43	1.81	-3.96	0.09	0.40	+
	Tb.Th	1	1.18	0.70	1.98	-5.05	0.56	**0.01**	+
	Tb.Sp	1	1.43	0.69	2.98	-4.89	0.03	0.62	+
	Tb.N	0	-0.99	-1.91	-0.51	3.17	0.24	0.16	-
	DA	0	1.15	0.63	2.11	-4.89	0.37	0.06	+
Pan									
	BV/TV	0	-1.42	-2.90	-0.69	3.35	0.08	0.42	-
	Tb.Th	1	1.87	0.92	3.79	-7.13	0.12	0.33	+
	Tb.Sp	1	3.21	1.90	5.41	-10.39	0.55	**0.01**	+
	Tb.N	0	-2.10	-3.74	-1.18	6.66	0.44	**0.04**	-
	DA	0	1.25	0.59	2.63	-4.90	<0.01	0.94	+
Homo									
	BV/TV	0	2.74	1.37	5.49	-10.42	<0.01	0.82	+
	Tb.Th	1	1.41	0.72	2.75	-6.17	0.08	0.39	+
	Tb.Sp	1	2.56	1.28	5.13	-8.92	<0.01	0.85	+
	Tb.N	0	-1.84	-3.67	-0.92	6.23	0.01	0.78	-
	DA	0	1.26	0.65	2.41	-5.07	0.14	0.26	+

3.3.3 Regional trabecular distribution

Mean species values for all parameters are show in Table 3. Within extant taxa, BV/TV tends to be highest in *Pan* and lowest in modern humans. Modern humans show the highest overall DA values, and *Pongo* shows the lowest. Within modern humans, DA is similar in the head and base, whereas non-human apes show higher DA in the base. Trabecular thickness is highest within *Gorilla* and lowest within modern humans. The highest number of trabeculae is exhibited within modern humans, and the lowest is seen in *Gorilla*. Within all extant non-human apes, there is a higher number and smaller spacing of trabeculae within the base than the head. Modern humans show a relatively equal distribution between the head and the base. *Gorilla* shows the highest overall trabecular spacing, which corresponds with its lowest number of trabeculae. Additionally, coefficients of variation (CV) for all means show that *Pongo* has the most variable BV/TV and DA values (except for modern human base BV/TV). CV values for all other parameters vary.

The two fossils show a different trabecular bone structure from each other and the extant sample. SKX 5017 shows the highest overall BV/TV as a result of a higher number of thicker and closely spaced trabeculae. SK 1813 has a BV/TV value between *Gorilla* and *Pan*, with the highest number of trabeculae that are more closely spaced, and are similar in thickness to *Pongo* (i.e. thinner than *Gorilla* and *Pan*). Disregarding their absolutely thicker trabeculae than modern humans, the two fossils have relatively a relatively higher number of closely spaced trabeculae, a pattern seen in *Pongo* and modern humans. Additionally, though BV/TV is generally equal in the head and base of all taxa, non-human apes exhibit a higher number of thinner and closely spaced trabeculae within the base, and a lower number of thicker, more widely trabeculae in the head. This pattern is not seen in modern humans, which have consistent values between the head and base. SKX 5017 shows a unique trabecular pattern wherein spacing and thickness are lower in the base than the head, but

contrary to the non-human apes, trabecular bone is also thicker in the base. Like in modern non-human apes, DA is higher in its base than in its head.

Table 3. Summary statistics for all analyzed parameters and taxa.

		Pongo pygmaeus	*Gorilla gorilla*	*Pan troglodytes*	SKX 5017	SK 1813	*Homo sapiens*
BV/TV							
Head	Mean	0.324 ± 0.07	0.346 ± 0.05	0.376 ± 0.02	0.410	0.360	0.285 ± 0.04
	Range	0.186 - 0.234	0.279 - 0.421	0.288 - 0.439			0.225 - 0.340
	CV	22.7	13.1	13.4			15.5
Base	Mean	0.318 ± 0.09	0.330 ± 0.02	0.350 ± 0.03	0.383		0.237 ± 0.05
	Range	0.252 - 0.470	0.283 - 0.368	0.313 - 0.395			0.163 - 0.329
	CV	26.8	7.00	7.8			30.0
	DA						
Head	Mean	0.243 ± 0.03	0.299 ± 0.04	0.331 ± 0.04	0.265	0.202	0.401 ± 0.04
	Range	0.188 - 0.280	0.246 - 0.350	0.269 - 0.390			0.334 - 0.460
	CV	13.1	12.8	12.6			9.00
Base	Mean	0.282	0.328 ± 0.04	0.373 ± 0.02	0.365		0.395 ± 0.04
	Range	0.188 - 0.338	0.250 - 0.395	0.347 - 0.408			0.337 - 0.454
	CV	18.5	13.0	5.30			8.90
	Trabecular thickness (mm)						
Head	Mean	0.256 ± 0.04	0.311 ± 0.04	0.286 ± 0.04	0.302	0.262	0.237 ± 0.02
	Range	0.204 - 0.309	0.262 - 0.372	0.217 - 0.341			0.203 - 0.286
	CV	16.9	12.0	14.0			10.5
Base	Mean	0.244 ± 0.04	0.276 ± 0.04	0.231 ± 0.02	0.252		0.199 ± 0.02
	Range	0.213 - 0.310	0.215 - 0.337	0.192 - 0.261			0.166 - 0.241
	CV	14.6	14.0	10.1			9.8
	Trabecular number (mm^{-1})						
Head	Mean	1.0817 ± 0.07	0.876 ± 0.12	1.045 ± 0.20	1.147	1.320	1.126 ± 0.13
	Range	1.019 - 1.206	0.717 - 1.026	0.804 - 1.436			0.971 - 1.386
	CV	6.3	14.0	19.7			11.4
Base	Mean	1.214 ± 0.09	1.107 ± 0.11	1.393 ± 0.12	1.324		1.241 ± 0.17
	Range	1.108 - 1.337	0.986 - 1.338	1.229 - 1.579			0.914 - 1.511
	CV	7.6	9.7	8.9			13.6
	Trabecular spacing (mm)						
Head	Mean	0.696 ± 0.11	0.905 ± 0.200	0.751 ± 0.21	0.571	0.495	0.662 ± 0.10
	Range	0.526	0.691 - 1.193	0.481 - 1.116			0.494 - 0.819
	CV	15.8	22.0	28.1			14.9
Base	Mean	0.583 ± 0.09	0.6334 ± 0.05	0.492 ± 0.05	0.504		0.626 ± 0.14
	Range	0.451 - 0.657	0.532 - 0.705	0.427 - 0.569			0.483 - 0.928
	CV	15.0	8.20	9.40			21.8

Regional summary statistics for all analyzed trabecular parameters can be seen in the supplementary information. Figure 8 presents results from Mann-Whitney U tests that reveal significant differences in raw BV/TV values between the dorsal and plantar regions of the

MT1 heads of all studied taxa. Non-human apes show a higher BV/TV within the plantar region, whereas modern humans show the opposite pattern. Within the base of the metatarsal, only modern humans show significant differences in BV/TV between the dorsal and plantar regions, with higher absolute values in the dorsal region. SKX 5017 shows higher BV/TV in the dorsal regions of the head and base, similar to modern humans, but with overall higher BV/TV. The SK 1813 head displays this pattern as well, though it has absolutely lower BV/TV than SKX 5017.

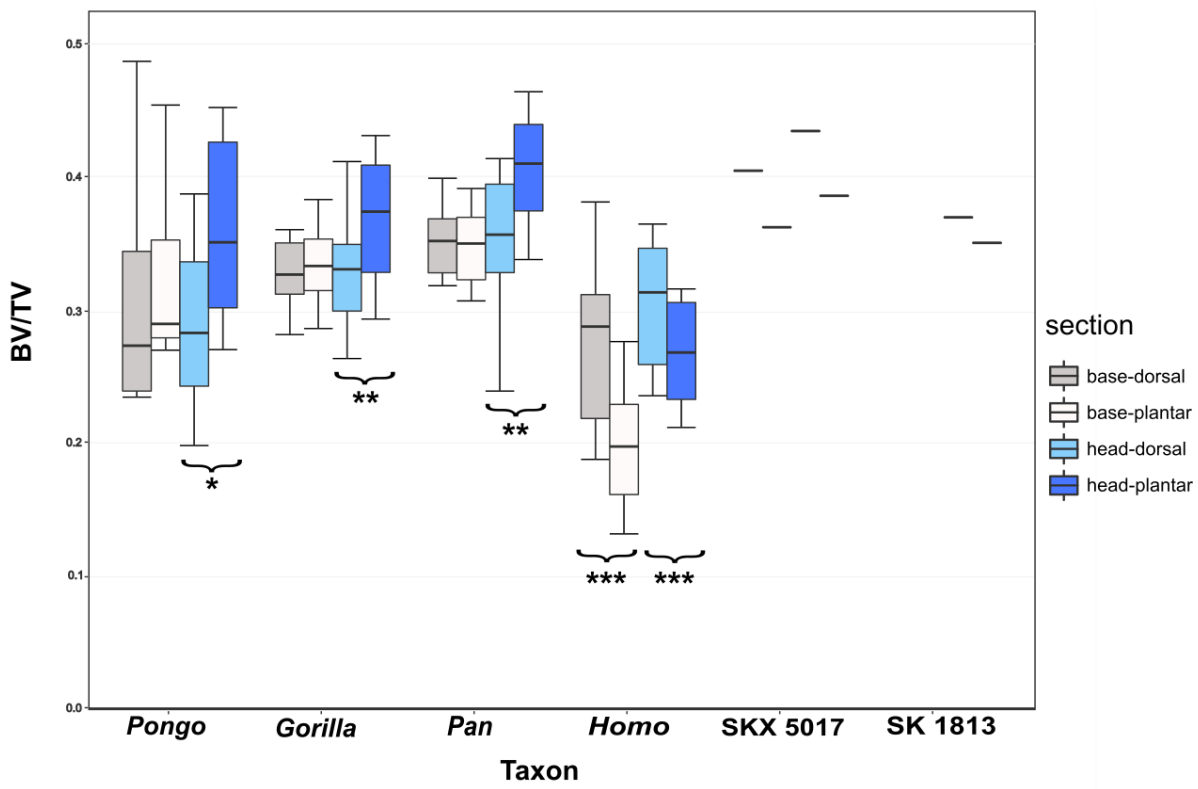

Figure 8. Boxplot showing raw BV/TV values within each analysed region and each taxon and significant differences in pairwise comparisons. (*) = p<0.05; (**) = p<0.005; (***) = p<0.001).

Figure 9 presents differences in raw DA values between the dorsal and plantar regions within the head and the base. Each taxon shows significant differences between DA in the plantar and dorsal regions, with modern humans showing the absolute highest values, and *Pongo* the lowest. There is no statistically significant interspecies difference in the ratio of

DA between the dorsal and plantar regions. All show a pattern of higher DA in the dorsal regions, as well as values in the dorsal regions of the head and base, and plantar regions of the head and base showing similar values. SKX 5017 conforms to the pattern of higher DA in the dorsal regions, though DA in the dorsal region of the base is absolutely higher than DA in the dorsal region of the base, and DA in the plantar region of the base is absolutely higher than the plantar region of the head. The plantar region of the base and the dorsal region of the head show very similar values, a pattern not seen in the extant sample. SK 1813 shows a similar DA pattern to the extant taxa, with higher values in the dorsal region than in the plantar region, though it has the absolute lowest values. All modern taxa display DA values that are significantly higher in the dorsal aspect than the plantar aspect.

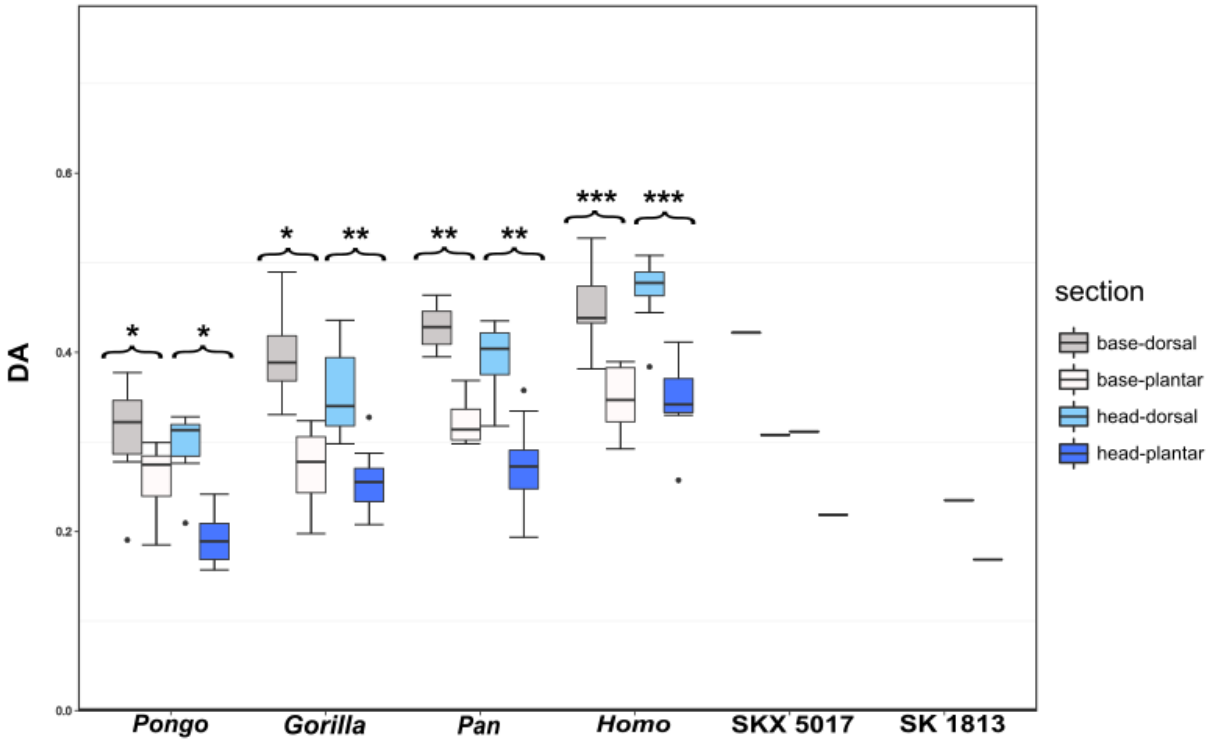

Figure 9. Boxplot showing raw DA values within each analysed region and each taxon and significant differences in pairwise comparisons. (*) = p<0.05; (**) = p<0.005; (***) = p<0.001).

Figure 10 presents ratios of dorsal-to-plantar BV/TV within the heads and bases of all taxa. Within all non-human apes, the base of the metatarsal shows a BV/TV ratio approximating a value of one, indicating relatively equal BV/TV between the dorsal and plantar regions. In

contrast, modern humans show a much higher value, indicating relatively higher BV/TV within the dorsal section of the base. Within the head of the metatarsal, all extant non-human apes show a ratio below one, indicating relatively higher BV/TV within the plantar region, whereas modern humans retain a higher proportion of trabecular bone within the dorsal region. Results from post-hoc pairwise Wilcoxon rank sum tests from the head show significant differences between the BV/TV ratio of modern humans and all extant non-human apes ($p<0.0005$), and between *Gorilla* and *Pongo* ($p<0.01$) (see Table 4). No statistically significant differences were found between *Pongo* and *Pan*, or between *Gorilla* and *Pan*. Within the base, no statistically significant differences were found in BV/TV ratio between the non-human primates, but all showed significant differences from modern humans ($p<0.0005$). Bootstrap analyses support these results, showing a similar distribution of trabecular bone within the base of all non-human primates (see Supplementary information).

Both the head and base of SKX 5017 show a BV/TV ratio over one, indicating a higher distribution of trabecular bone within the dorsal regions. The head falls within the range of modern humans, but the value from the base is lower, indicating an overall higher distribution within the dorsal region, but not to the same extent as modern humans. SK 1813 also shows a higher distribution of trabecular bone within the dorsal region of the head, although the value is lower than in modern humans.

.

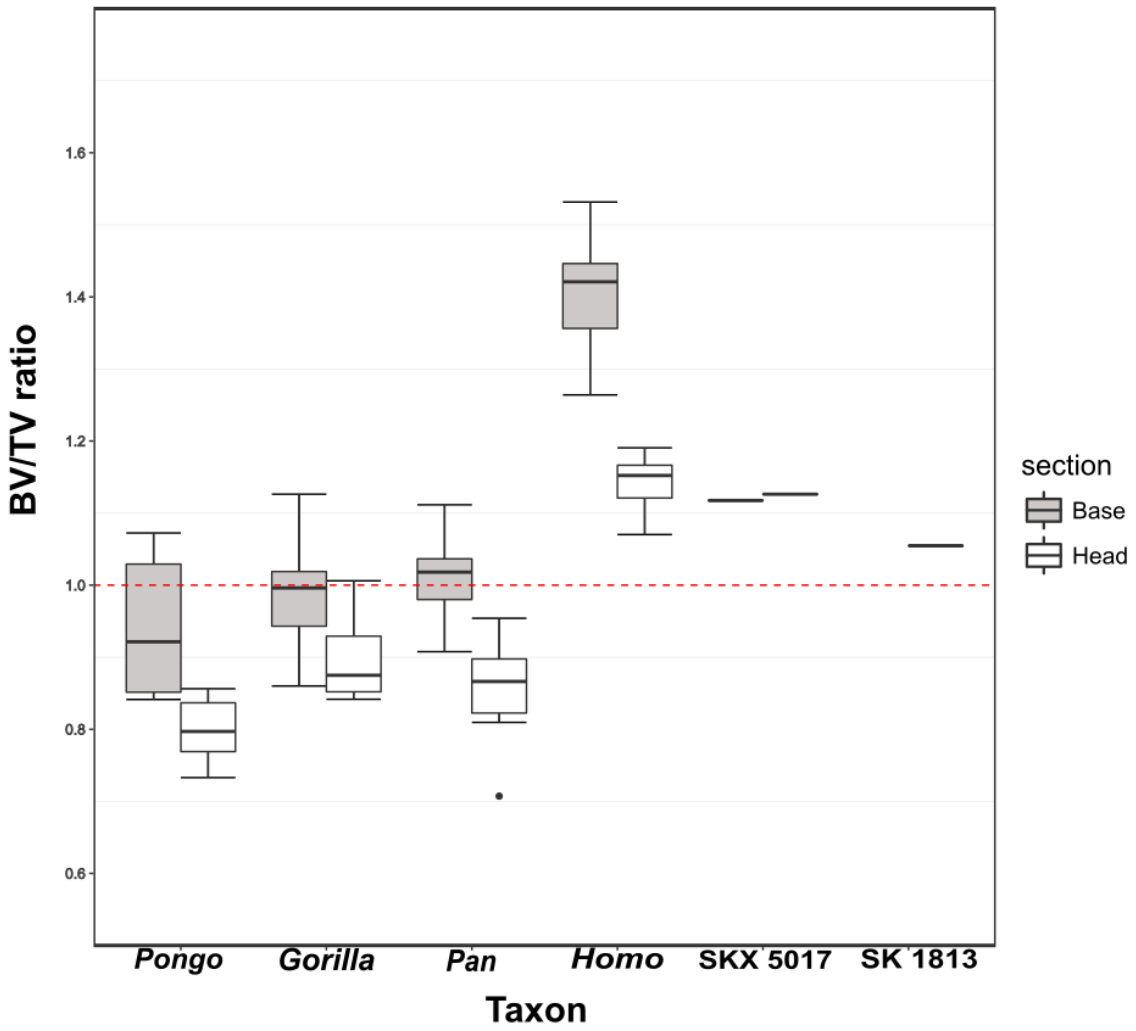

Figure 10. Boxplot of BV/TV ratio within the base and head of each taxon. Red dotted line represents an equal dorso-plantar distribution of trabecular bone.

Table 4. Results from Kruskal-Wallis post hoc tests in interspecies BV/TV and DA ratio. Boxes on top rows represent the head and boxes on bottom rows represent the base. (*) Indicates insignificant p-values.

	Pongo	*Gorilla*	*Pan*	*Homo*
BV/TV				
Pongo		0.0285	*	<0.001
Gorilla	*		*	<0.001
Pan	*	*		<0.001
Homo	<0.001	<0.001	<0.001	
DA				
Pongo		*	*	*
Gorilla	0.045		*	*
Pan	*	*		*
Homo	*	*	*	

Figure 11 shows results from bootstrap analyses that compare the extant taxon BV/TV ratio means of the base to the BV/TV ratio of SKX 5017. Results confirm significant differences between the BV/TV ratio between SKX 5017 and all extant taxa ($p<0.001$), with a value lower than modern *Homo* ($p<0.01$), and higher than *Pongo* ($p<0.01$)*, Gorilla* ($p<0.01$)*,* and *Pan* ($p<0.01$). In contrast, the metatarsal head falls within the range of modern *Homo* ($p>0.05$). The BV/TV ratio within the head of SK 1813 falls outside the range of all extant taxa ($p<0.01$) (see Figure 12). The distribution, though more dorsal than plantar, falls below the range seen in modern *Homo*, and above the range seen *Pongo, Gorilla,* and *Pan*.

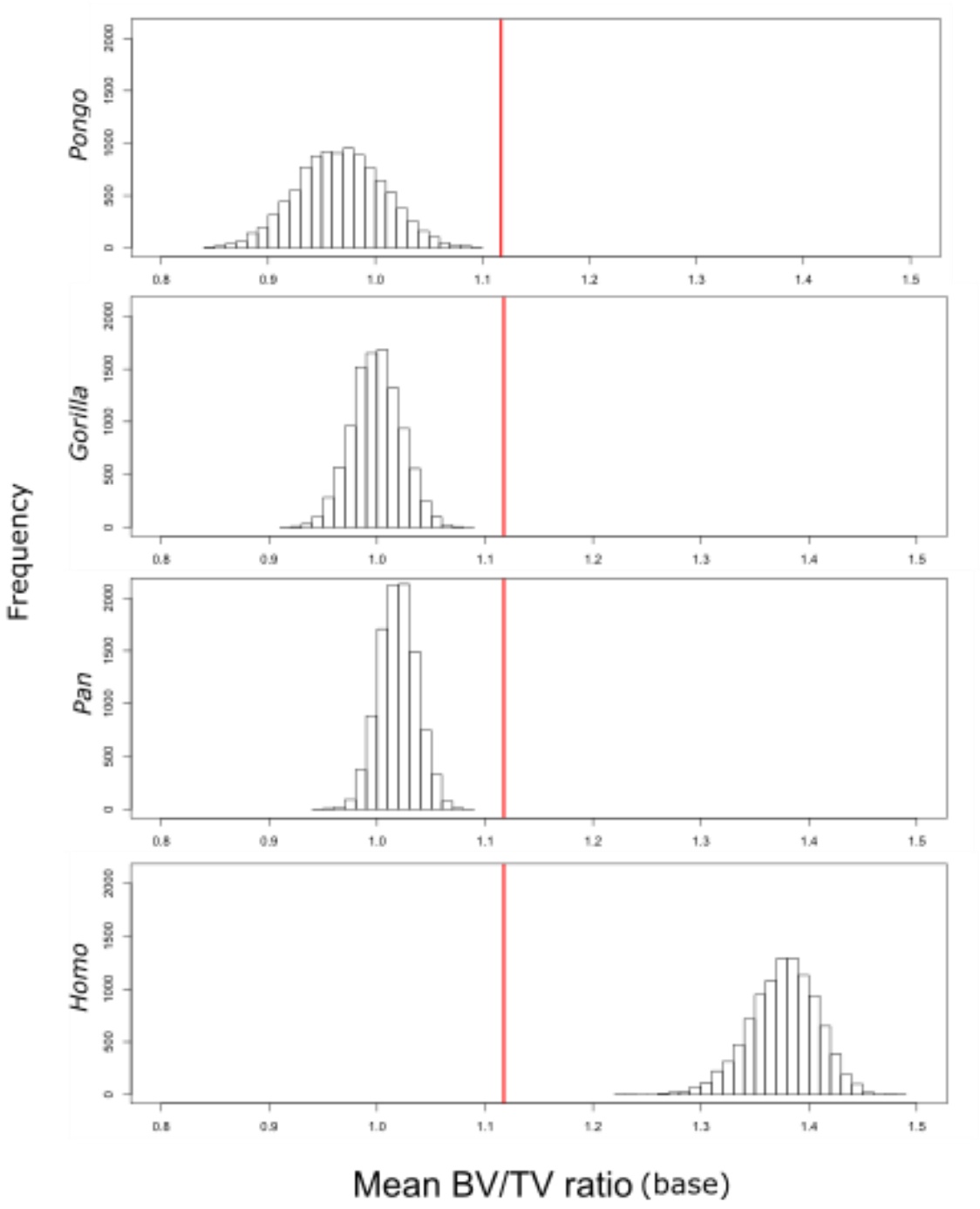

Figure 11. Bootstrap plots showing the resampled and redistributed sample means of BV/TV ratio within the base of each taxon. Red line represents the original BV/TV ratio of SKX 5017.

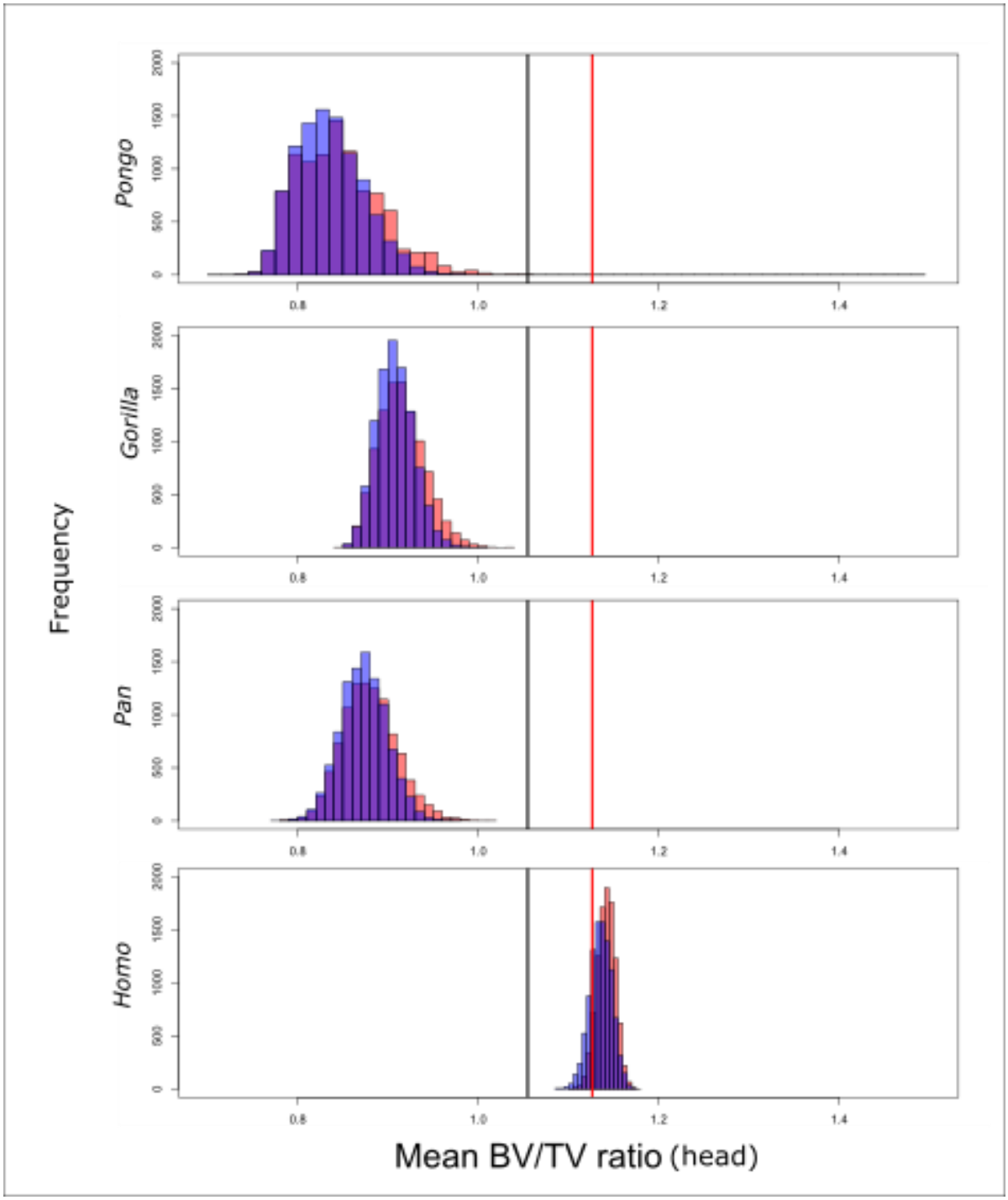

Figure 12. Bootstrap plots showing the sample means of BV/TV ratio within the head of each taxon. Pink bars represent the modern samples resampled and redistributed with SKX 5017; blue bars represent modern samples resampled and redistributed with SK 1813; purple bars represent overlap between the two samples. Red line represents the original BV/TV ratio of SKX 5017; black line represents the original BV/TV ratio of SK1813.

Figure 13 presents a bi-variate plot of BV/TV and DA values of the combined head and base in the study sample. General patterns include lower BV/TV and higher DA within modern humans, and overlapping BV/TV values within all non-human apes. Within the non-human apes, *Pan* shows overall higher DA, followed by *Gorilla* and *Pongo*, respectively. As mentioned earlier, *Pongo* shows the widest range of BV/TV values. BV/TV values in both SKX 5017 and SK1813 are well above modern *humans*, and within the range of the non-human apes**.** DA values are lower in SK 1813 and SKX 5017 than in modern humans, with the former showing the absolute lowest values, within the range of *Pongo*.

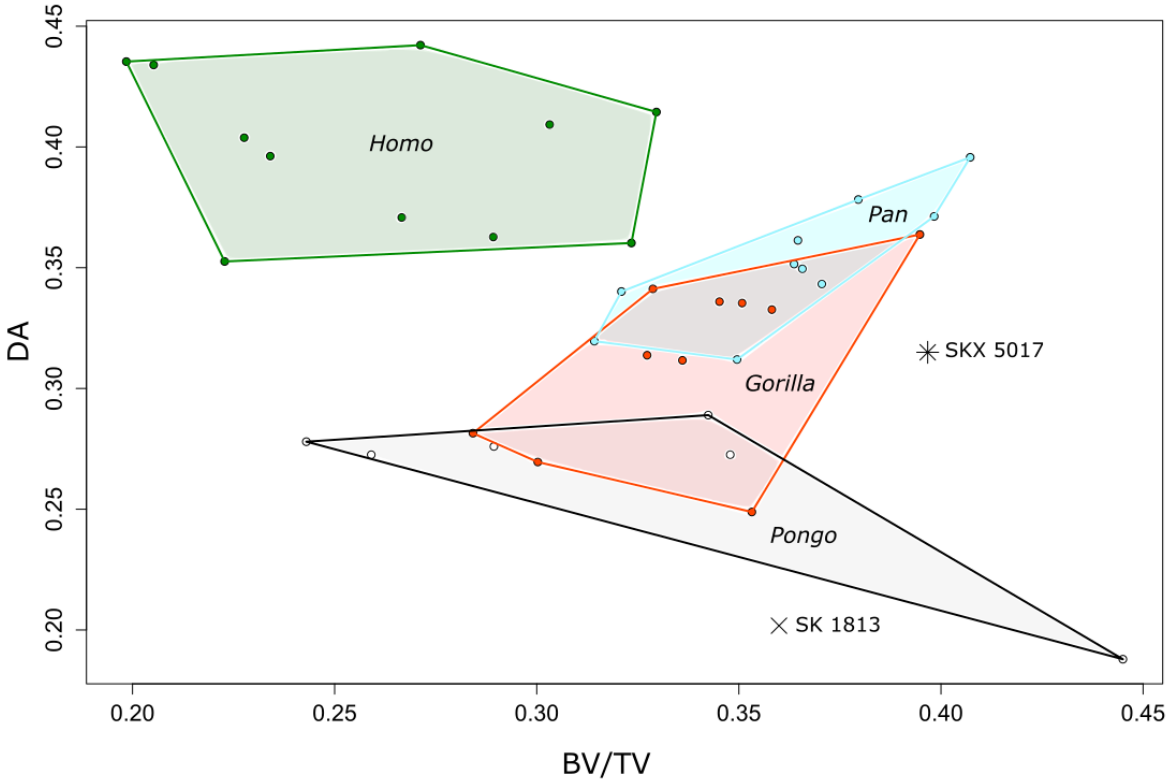

Figure 13. Scatterplot showing the DA vs. BV/TV of all specimens. DA and BV/TV values represent both the head and the base.

Overall, modern humans are characterized by dorsal distribution of trabecular bone within the head and base, whereas non-human apes show a plantar distribution within the head, and a relatively even distribution within the base. Modern humans show the absolute highest

DA and lowest BV/TV, as well as a suite of trabecular parameters that differentiate them from non-human apes. There is considerable overlap within the non-human apes, though BV/TV colour maps show subtle differences that are not apparent from analyses of dorsal and plantar regions. SKX 5017 and SK 1813 show certain modern-human like features. Trabecular bone is distributed more dorsally in the head and base, though statistical analysis shows that the bases fall outside the range of all extant taxa. DA in both fossils is lower than in modern humans, but both show Tb.Sp. and Tb.N values that are within the range of modern humans (see Table 3).

3.4 Discussion

3.4.1 Effect of body size on trabecular bone structure

Most trabecular parameters were found not to scale allometrically with a correlate of size. Like other studies (Ryan and Shaw, 2013), results from this analysis show positive scaling of BV/TV, but no allometric scaling. The only taxon to show positive allometric scaling of trabecular thickness is *Gorilla*, supporting previous findings (Doube et al., 201). However, the confidence intervals of the slope contained the isometric scaling value. All other taxa show no allometric scaling of trabecular thickness, supporting other studies (Mullender et al., 1996; Swartz et al., 1998). The only other trabecular parameters to show allometric scaling were spacing and number in *Pan*, with positive and negative allometry, respectively. This is contrary to other findings of negative allometry of spacing (Ryan and Shaw, 2013), which also show negative allometry of thickness. Results from this study may be different from others because it observes intraspecies allometry, rather than comparing different species to each other. Therefore, results reflect sex-variation as well as body-size variation. Given the overall insignificant results, it would imply that within species, body size does not play in

important role in trabecular structure, and that perhaps trabecular bone between different species responds to changes in body size differentially.

3.4.2 Trabecular distribution within humans and non-human primates

Within the extant sample, the trabecular parameters that most effectively separate each locomotor mode are relative BV/TV and absolute DA. *The first hypothesis* is that modern humans show higher BV/TV within the dorsal aspect of the base. This is supported here based on significantly higher BV/TV ratio within modern humans than all other extant taxa. Since the modern human forefoot mainly experiences high compressive loads as it dorsiflexes, a higher proportion of trabecular bone within the base and head is distributed within the dorsal aspect. The human tarsometatarsal joint, which is more limited in mobility than the MTPJ, is stable and experiences one range of motion (Morton, 1924; Susman and Brain, 1988; Proctor et al. 2008; Gill et al. 2015). Therefore, it consistently shows one tightly constrained pattern within the base of the MT1. Taxa that have a more mobile tarsometatarsal joint (i.e., *Pongo, Gorilla*, and *Pan*) show evenly distributed BV/TV within the entire base which provides trabecular support for loading in multiple directions, though *Pongo* has a slightly more plantar distribution of trabecular bone. BV/TV is known to increase where there is higher loading (Rubin et al., 2002; Barak et al., 2011), therefore trabecular bone that is located in the plantar region offers support for high compressive loading during plantarflexion, and dorsally located trabecular bone offers support for loading during dorsiflexion. The fact that there is no clear distinction in the BV/TV ratio between the non-human primates could be reflective of the variable way in which each species loads the forefoot, resulting in a generalized trabecular structure adapted for a wide range of motion and loading. BV/TV colour maps show differences in the distribution of trabecular bone within the base of *Pongo* and *Gorilla* and *Pan.* As mentioned earlier, trabecular bone within the base of the *Pongo* MT1 shows a higher distribution near the edges of the articular

surface, whereas *Gorilla* and *Pan* show an equal distribution throughout the epiphysis. This could be related to relatively low compressive or tensile forces inflicted upon the *Pongo* MT1 base, resulting in trabecular bone that does not extended as far into the centre of the bone. The equal distribution within *Pan* and *Gorilla* could be an indication that the base experiences higher loading in these two taxa compared to *Pongo*. This is suggestive of the fact that BV/TV ratio is better at differentiating broad locomotor patterns (i.e., between bipedalism and vertical climbing), whereas BV/TV colour maps better capture subtle differences in joint positioning and loading between types of terrestrial quadrupedalism or arboreal locomotion.

Within the head, non-human apes show a plantar distribution of trabecular bone associated with high compressive loading during plantar flexion. Since the joint does not have the same range of dorsal excursion as modern humans, it is limited in its potential degree of dorsiflexion. Therefore, even during terrestrial locomotion, when the MTPJ dorsiflexes, the trabecular bone would not be concentrated as dorsally as in modern humans. Based on studies of plantar pressure distribution in *Pan troglodytes*, peaks occur on the plantar aspect during vertical climbing (Wunderlich and Ischinger, 2017), which is consistent with the results that the plantar aspect of the head displays significantly higher BV/TV. *Pongo* is considered the most arboreal taxon (Cant, 1987; Gebo, 1996; Thorpe and Crompton, 2005) and shows the most marked plantar concentration of trabecular bone compared to *Gorilla* and *Homo*. The opposite condition is found in modern humans. The dorsal region of the MT1 head shows significantly higher BV/TV, corresponding to the position in which the joint incurs maximum loading. These results contradict previous analysis of MT1 trabecular bone structure, which showed no significant difference in the distribution of trabecular bone within the dorsal and plantar regions of the metatarsal head between species (Griffin et al., 2010). This could be based on the different methodologies used for the studies. Oftentimes the area of highest BV/TV is seen at the cortical/trabecular boundary, and VOIs fail to encompass this region.

The second hypothesis is that modern humans show higher absolute DA within the dorsal aspect of the head than other non-human primates. This is the case, however, all taxa show the same pattern of relatively higher DA in the dorsal aspect of the head. Nevertheless, the higher absolute DA within modern humans corresponds with the hypothesis that a more uniaxial range of movement will results in stereotypically oriented trabeculae. Similarly, the base of humans shows the highest DA, though the difference between modern humans and *Pan* is not statistically significant. Because all taxa show the same *pattern* of DA, where the dorsal aspect of the head is more anisotropic, DA ratio is not particularly effective at differentiating between modes of locomotion. The absolute DA values within the head can clearly separate modern humans from non-human apes, but with the apes only distinguish between *Pan* and *Pongo*. Similarities in trabecular patterning between non-human primates are emphasized when plotting DA against BV/TV. Humans show no overlap with the non-human primate pattern, with the latter showing considerable overlap between each other (within the non-human primates, *Gorilla* and *Pan* are more similar to each other than to *Pongo.* Similarities are also seen when comparing trabecular parameters between the two epiphyses. Non-human apes all show more anisotropic bone within the base than the head, which is reflective of multiaxial movement of the MTPJ, and a more tightly constrained tarsometatarsal joint. In contrast, modern humans, which have a limited range of mobility at both joints, show relatively consistent DA values between the two epiphyses.

Although BV/TV is generally equal within the head and base of all taxa, the base exhibits a higher number of thinner and closely spaced trabeculae, and the head exhibits a lower number of thicker, more widely trabeculae. This pattern is not seen in modern humans, which have consistent values between the head and base. Again, this could be reflective of the relatively consistent range of movement experienced within the modern human MT1, resulting in homogeneous trabecular structure between the epiphyses. The different types of load experienced within the heads and bases of non-human apes could contribute to a different type of trabecular configuration between their epiphyses. Despite broad similarities

in BV/TV and DA between non-human apes, differences can be observed between them when comparing overall trabecular parameters (Tb.Th., Tb.Sp., Tb.N.). *Gorilla* combines relatively few thick, and widely spaced trabeculae. *Pongo* is characterized by relatively more, thinner, and closely spaced trabeculae. *Pan* is intermediate between *Pongo* and *Gorilla*. Of the non-human apes, the overall pattern in *Pongo* is most similar to modern humans, which have the thinnest trabeculae, but are similar in number and spacing. Because most trabecular parameters did not show significant allometric scaling, with the exception of Tb.sp and Tb.N in *Pan* and Tb.th in *Gorilla*, these differences likely represent interspecies variation as opposed to allometry related variation.

It is also worth noting that BV/TV ratio is likely better at differentiating between locomotor modes because absolute BV/TV does not necessarily reflect the magnitude of load applied to an element. Modern humans show systematically lower BV/TV than all other taxa, despite their medial forefoot experiencing higher loading during push-off than non-human apes (Vereecke et al., 2003). Lower overall BV/TV has been previously observed in other studies of cortical and trabecular bone (Ruff et al., 1993; Lieberman, 1996; Chirchir et al., 2015; Tsegai et al., 2017) and has been suggested to be linked to higher sedentism in relation to early hominins and recent hunter-gatherers. Because the sample represented in this study is of likely shod and sedentary modern humans, it is also worth noting that the low overall BV/TV values seen here may not reflect the entire range of human variation. For this reason, in this study, BV/TV is mainly relevant when its *relative* distribution is analysed. Further studies including shod and unshod populations, as well as hunter-gatherers may contribute to our understanding of overall BV/TV within modern humans.

3.4.3 Trabecular distribution within fossils

The third hypothesis is that the two fossil specimens will show similar BV/TV distribution to modern humans, and that based on the relatively more concave proximal articular facet, DA

will be lower in this region compared to the latter. This is partially supported: BV/TV ratio within the head of SKX 5017 is similar to modern humans, but the base shows a lower ratio, outside the range of modern humans. As predicted, DA within the base of SKX 5017 is lower than in modern humans. Like modern humans, SK 1813 shows a dorsal distribution of trabecular bone, but below the range seen in the former.

SKX 5017 shows a trabecular architecture within its head that in certain aspects shows clear similarities to modern humans. As shown by the bootstrapping analysis, the trabecular bone follows a pattern of distribution that is within the range of modern humans, indicative of a metatarsal that was habitually loaded on its dorsal aspect. The external morphology of the head, specifically its raised superior aspect in relation to the dorsum of the shaft, indicates it was capable of a wide range of dorsiflexion at the MTPJ, comparable to modern humans (Susman and Brain, 1988). There is no consensus is on how the joint was loaded; given that it is also mediolaterally narrower on the dorsal aspect, it has been suggested that the joint did not close-pack in dorsiflexion, and as a result was less stable during bipedal locomotion (Susman and Brain, 1988; Susman and de Ruiter, 2004). When compared to modern humans, SKX 5017 shows a distribution of trabecular bone that is much more dorsally distributed. Though modern humans show a higher distribution of bone within the dorsal aspect of the head, most specimens do not show the hyper-dorsal distribution seen in SKX 5017. This could suggest a habitually hyperdorsiflexed and less stable MTPJ, and an increase of BV/TV in this area as a compensatory mechanism. Given the fact that the MT1 possesses low DA within the range of *Gorilla* and *Pan*, it is also possible that the foot could have still been efficient in a form of arboreal locomotion different from that of non-human apes. The hyperdorsal concentration of trabecular bone could be caused by habitual hyperdorsiflexion at the MTPJ from foot placement that is directly against a vertical substrate. This form of arboreal locomotion has been noted in modern human populations that collect resources from trees, and is directly associated with extreme dorsiflexion of the ankle and forefoot (Kraft et al., 2014).

Results from the trabecular structure of the base of the MT1 combined with its external morphology emphasize this different loading pattern from modern humans. The articular surface is more concave than in modern humans (Susman and Brain, 1988; Susman and de Ruiter, 2004), similar to the shape seen in *Pan* and western gorillas (Proctor et al., 2008; Vernon, 2013), and more ovoid in its outline, which contributes to a more mobile tarsometatarsal joint complex. The hallux is nonetheless adducted and the base has been described as human-like overall (Susman and Brain, 1988). However, the base does not adhere to a completely modern human-like trabecular structure. Though it shows a higher ratio of trabecular bone within the dorsal aspect, there is relatively more trabecular bone within the plantar region than is observed in modern humans. As a result, the BV/TV ratio within the base of SKX 5017 is lower than within the observed human range, but higher than is observed in all other non-human primates, resulting in an intermediate proportion of dorsal-to-plantar trabecular bone. This could be reflective of a joint that has retained adaptations for grasping, or trabecular bone distributed plantarly to compensate for a less stable MTPJ during toe-off. DA within the base is within the range of *Gorilla*, *Pan*, and *Homo*, and like these taxa, is higher within the base than the head. This implies that the two epiphyses were capable of differential movement, and that unlike in modern humans, the element was not tightly constrained at both joints. These results could confirm a joint that was habitually loaded in dorsiflexion, but that did not move in a strictly uniaxial direction. Additional trabecular parameters emphasize the unique nature of its trabecular architecture. SKX 5017 has a relatively higher number of closely spaced trabeculae, a pattern seen in *Pongo* and modern humans, but much higher trabecular thickness, though the functional implication of this is not certain. When comparing BV/TV and DA, the element does not fall within the range of any modern taxon.

It is worth noting that there is a prominent osteophyte on the dorsal aspect of the shaft, proximal to the articular surface of the head. This could be the result of a traumatic injury sustained in life, or a condition called hallux rigidus, which produces exostoses on the head

of the first metatarsal (Susman and Brain, 1988). However, this condition is accompanied with flexed phalangeal joints, which is in contrast to the distribution of trabecular bone within the metatarsal head that indicates a dorsiflexed rather than plantar flexed MTPJ.

SK 1813 shows a trabecular structure which, though similar in overall distribution to modern humans, shows certain unique aspects. The higher BV/TV within the dorsal aspect of the head is reflective of a joint that was habitually loaded in dorsiflexion. It has been described by Suman and de Ruiter (2004) as similar in morphology and function to SKX 5017. The trabecular structure reveals considerable differences between the two specimens. SK 1813 displays BV/TV that is absolutely lower than SKX 5017, within the range of *Pongo*, *Gorilla*, and *Pan*, and a lower DA, closer to the range of *Pongo.* The distribution of trabecular bone, though more dorsal than plantar, falls equally between the ranges of modern non-human primates and modern humans, meaning it does not conform to any modern pattern. Additionally, the trabecular bone extending from the plantar aspect of the shaft into the head is very thick, resulting in an area of high BV/TV near the plantar surface of the head. It is difficult to interpret the behaviour of SK 1813 accurately because only the head was analysed, and because it is a subadult. Though modern humans retain a relatively consistent locomotor mode throughout ontogeny (Sutherland et al., 1980; Beck et al., 1981; Raichlen et al., 2015), juvenile and subadult gorillas, chimpanzees, and bonobos display much more arboreal behaviour than adults (Doran, 1997; Sarringhaus et al., 2014). Trabecular structure is known to change throughout ontogeny (Ryan and Krovitz, 2006; Gosman and Ketcham, 2009; Raichlen et al., 2015) especially in regards to DA (Gosman and Ketcham, 2009; Abel and Macho, 2011). Because this specimen does not represent a strictly modern human or ape-like trabecular structure, it is not known whether its locomotor repertoire was as variable throughout ontogeny as modern apes, or as constrained as modern humans. The trabecular evidence shows a predominantly dorsal distribution of bone, indicative of a habitual biped. However, the distribution is outside the range of modern adult humans, meaning it might have used its feet in more variable positions. This is supported by the low DA within the

head, indicative of a joint that experiences variable and multiaxial loading. Based on the head, SK 1813 reflects a truly 'intermediate' specimen between modern humans and great apes, be this related to its young age or not.

3.4.4 Interpretation of fossil locomotion

Debates about australopith and *Paranthropus* locomotion have generally argued for 'mosaic' locomotion based on conflicting morphological evidence that shows derived features adapted for bipedalism, and primitive features indicative of climbing and pedal grasping (Stern and Susman, 1983; Susman et al., 1984; Susman and Brain, 1988; Susman and de Ruiter, 2004). Research on *Paranthropus* locomotion is fairly limited because postcranial fossils are scarce and often not securely attributed to the taxon (but see: Dominguez-Rodrigo et al., 2013). Its postcranial morphology is generally described as gracile and small and of small stature (McHenry, 1991), and its locomotion has been described as bipedal with a 'waddling gait' and an inability to transfer body weight from one foot to another during walking (Napier, 1964; Robinson, 1974). The original descriptions of SKX 5017 and SK 1813 (Susman and Brain, 1988; Susman and de Ruiter, 2004) suggested that both have a combination of primitive and derived features, and that based on multivariate analysis of various linear measurements, both were most similar to modern humans. Research on the proximal articular surface of both specimens has differentiated them from modern humans (Proctor et al., 2010) and from one another (Vernon, 2013). Proctor et al. (2010) measured the curvature of the surface using 3D geometric morphometric analysis, and found that SK 1813 did not group with modern humans but showed affinity to SKX 5017, both of which had 'ape-like' curvature, which were then interpreted as both belonging to *Paranthropus*. Other analyses group SKX 5017 with *Pan* and western gorillas in terms of mediolateral articular surface curvature, and SK 1813 with modern humans and *Papio* (Vernon, 2013). Based on

these conflicting results, it is difficult to determine how ‘human-like’ or ‘ape-like’ the proximal articular surface is, and even less so the locomotor behaviour associated with its shape.

Studies of trabecular bone structure have provided mixed results in its utility in inferring habitual joint positioning (Ryan and Ketcham, 2002; Fajardo et al., 2007; DeSilva and Devlin, 2012). However, it is possible that elements in closer contact to the substrate may be more reflective of locomotor behaviour because they directly absorb compressive loads associated with ground reaction forces (Maga et al., 2006; Kivell, 2016). The MT1 shows particular promise because it is a relatively simple element that shows a consistent range of motion. Results from this study strengthen its application in inferring fossil hominin locomotion by providing evidence that its trabecular structure can be linked to habitual joint positioning and loading of the forefoot within an extant sample. BV/TV reflects the position in which the joint experiences the highest load, and DA reflects its range of motion. Though these parameters do not accurately differentiate variation in non-human primate locomotion, obligate bipedalism presents very clear signals.

Based on patterns of BV/TV and DA within the metatarsal, there is evidence that the *Paranthropus* foot (associated with SKX 5017) possessed a habitually dorsiflexing MTPJ that was capable of a relatively multiaxial range of movement. The head has a similar distribution of trabecular bone to modern humans, but is more dorsally oriented and isotropic, indicating it was loaded in dorsiflexion. This may have been caused by a less stable MTPJ due to its inability to close-pack in dorsiflexion, or it could be reflective of a different type of arboreal locomotion than what is seen in non-human apes. The base is intermediate between humans and non-human primates, showing relatively more trabecular bone within the dorsal aspect, but also retaining isotropic bone within the plantar region, suggesting retained grasping abilities. SK 1813 is not attributed to a specific taxon, and shows an intermediate condition between modern humans and non-human primates, indicating it may have had a varied locomotor repertoire including habitual bipedalism and

arboreal locomotion. Though previous analysis of its proximal articular surface describes it as more modern human-like than SKX 5017 (Vernon, 2013), its lower BV/TV ratio and more isotropic trabecular bone indicate it adopted more arboreal locomotion than the former individual. Beyond BV/TV ratio, trabecular structure in both specimens maintains ape-like and human-like properties. SKX 5017 shows the highest BV/TV of all taxa, with a trabecular structure characterized by a high number of tightly spaced and thicker trabeculae. SK 1813 shows a high number of relatively thinner (compared to SKX 5017), and more tightly spaced trabeculae.

Thick trabecular bone is a pattern seen in modern great apes, but the high number and tight spacing is a pattern seen in modern humans (Ryan and Shaw, 2015). When comparing the two fossils, both show comparable values for spacing and number, but disparate values of thickness. It would appear that although the fossils show absolutely higher BV/TV than modern humans, it is mainly the result of thicker trabecular bone, and that the other trabecular parameters (number and spacing) correspond with those of modern humans. Without proper taxonomic attribution for SK 1813, any firm links between the two specimens cannot be made. However, if the two represent the same species, as suggested by Proctor et al., (2008), these differences would correspond with what we know about ontogenetic changes in trabecular bone: BV/TV increases in life as a result of increasing thickness, but spacing and number stays the same (Partiff et al., 2000; Tanck et al., 2001).

The taxonomic status of SKX 5017 is reasonably-well established. The layer in which it was found (Member 1), is represented by more than 95% *Paranthropus* remains (Susman, 1988), and its external morphology separates it from early *Homo* (Susman, 1988; Proctor, 2008; Vernon, 2013). Therefore, these interpretations of locomotor behaviour can be applied to *Paranthropus robustus* with confidence. Given the partial results from SK 1813, and its subadult status, it is not certain whether this element represents *P. robustus* as well. Trabecular structure within the two specimens is different in BV/TV ratio, DA, and BV/TV

distribution, indicating different habitual joint loading, and two forms of locomotion. *If* the trabecular structure of SK 1813 represents its final adult structure, it could indicate two different species (*P. robustus* and *Homo* sp.). However, if this structure reflects a subadult mode of locomotion that differs from the adult mode of locomotion, it could indicate the same species at different ontogenetic stages.

Recently, the trabecular structure of tali associated with *Paranthropus* have been studied and shown to display increased DA in parts of the element associated with a medial weight shift, and by extension a human-like bipedal gait (Su and Carlson, 2017). They also showed higher BV/TV in the lateral region, indicating a degree of lateral loading intermediate in magnitude between modern human and anthropoid tali. Cumulatively, analyses of *Paranthropus* locomotion based on trabecular structure and external morphology show hallmark features characteristic of habitual bipedalism, with an indication that the overall structure of the foot was less stable, allowing for multiaxial movement at the MTPJ and metatarsocuneiform joint. These results are in line with the current study, and support the idea that *Paranthropus* was adapted for bipedalism, but nonetheless possessed a unique forefoot structure.

Chapter 4. Conclusions

This study has demonstrated that trabecular bone structure within the first metatarsal can effectively reflect habitual joint loading within the MT1, and by extension general locomotor repertoire within extant apes. The most apparent differences are seen between modern humans and all other extant taxa, indicating that the relatively constrained and stable structure of the human foot results in a very specific trabecular patterning. It also highlights the importance of trabecular bone analysis in the context of palaeoanthropology. The two fossil specimens, which have been described as highly similar in external morphology, present very different trabecular bone structure that would imply two different modes of locomotion. Though studies have used the proximal articular surface to differentiate the two specimens, others have grouped the two together based on the structure of the head. Results from trabecular analysis suggest that the MTPJ was loaded differently in the two specimens: one in hyperdorsiflexion, and the other in a manner intermediate between modern humans and non-human primates. Trabecular structure within the two metatarsals suggests a push-off mechanism within the foot that was neither distinctly human-like or ape-like. The observed variability in trabecular parameters – BV/TV corresponding with a human-like push-off mechanism and DA corresponding with a more mobile joint, emphasizes its unique form of locomotion, and the variability in early Pleistocene hominin locomotion.

References

Aerts, P., Van Damme, R., Van Elsacker, L., & Duchêne, V. (2000). Spatio-temporal gait characteristics of the hind-limb cycles during voluntary bipedal and quadrupedal walking in bonobos (*Pan paniscus*). *American Journal of Physical Anthropology, 111*(4), 503-517.

Aeillo, L., & Dean, C. (2002). Chapter fourteen - bipedal locomotion and the postcranial skeleton. In L. Aeillo, & C. Dean (Eds.), *An introduction to human evolutionary anatomy* (pp. 244-274). San Diego: Academic Press.

Alam, I., Sun, Q., Liu, L., Koller, D., Fishburn, T., Carr, L., et al. (2005). Whole-genome scan for linkage to bone strength and structure in inbred fischer 344 and lewis rats. *Journal of Bone and Mineral Research, 20*(9), 1589-1596.

Alexander, R., Ker, R., Bennet, M., Bibby, S., & Kester, R. (1987). The spring in the arch of the human foot. *Nature*, *325*(6100), 147-149.

Alexander, R. M. (1991). Energy-saving mechanisms in walking and running. *Journal of Experimental Biology*, *160*(1), 55-69.

Asfaw, B., White, T., Lovejoy, O., Latimer, B., Simpson, S., & Suwa, G. (1999). *Australopithecus garhi*: A new species of early hominid from ethiopia. *Science (New York, N.Y.), 284*(5414), 629-635.

Barak, M. M., Lieberman, D. E. Raichlen, D., Pontzer, H., Warrener, A. G., & Hublin, J. J. (2013). Trabecular evidence for a human-like gait in *Australopithecus africanus*. *Plos One, 8*(11), 1-9.

Barak, M. M., Lieberman, D. E., & Hublin, J. J. (2011). A Wolff in sheep's clothing: Trabecular bone adaptation in response to changes in joint loading orientation. *Bone, 49*(6), 1141-1151.

Barak, M. M., Lieberman, D. E., & Hublin, J. J. (2013). Of mice, rats and men: Trabecular bone architecture in mammals scales to body mass with negative allometry. *Journal of Structural Biology, 183*(2), 123-131.

Bassey, E. J., & Ramsdale, S. J. (1994). Increase in femoral bone-density in young-women following high-impact exercise. *Osteoporosis International, 4*(2), 72-75.

Beddoe, A. H. (1978). A quantitative study of the structure of trabecular bone in man, rhesus monkey, beagle and miniature pig. *Calcified Tissue Research, 25*(1), 273-281.

Bennett, M. R., Harris, J. W. K., Richmond, B. G., Braun, D. R., Mbua, E., Kiura, P., et al. (2009). Early hominin foot morphology based on 1.5-million-year-old footprints from ileret, Kenya. *Science, 323*(5918), 1197-1201.

Berillon, G. (1999). Geometric pattern of the hominoid hallucal tarsometatarsal complex. Quantifying the degree of hallux abduction in early hominids. *Comptes Rendus De l'Académie Des Sciences - Series IIA - Earth and Planetary Science, 328*(9), 627-633.

Bertram, J., & Swartz, S. (1991). The law of bone transformation - A case of crying Wolff. *Biological Reviews of the Cambridge Philosophical Society, 66*(3), 245-273.

Biewener, A., Fazzalari, N., Konieczynski, D., & Baudinette, R. (1996). Adaptive changes in trabecular architecture in relation to functional strain patterns and disuse. *Bone, 19*(1), 1-8.

Bøjsen-Moller, F. (1979). Calcaneocuboid joint and stability of the longitudinal arch of the foot at high and low gear push off. *Journal of Anatomy, 129*(1), 165-176.

Bojsen-Møller, F., & Lamoreux, L. (1979). Significance of free dorsiflexion of the toes in walking. *Acta Orthopaedica Scandinavica*, *50*(4), 471-479.

Brunet, M. (2002). Palaeoanthropology (communication arising): *Sahelanthropus* or *'Sahelpithecus'*? *Nature, 419*(6907), 582-582.

Cant, J. G. H. (1987). Positional behavior of female bornean orangutans (*Pongo pygmaeus*). *American Journal of Primatology, 12*(1), 71-90.

Cant, J. G. H. (1992). Positional behavior and body size of arboreal primates: A theoretical framework for field studies and an illustration of its application. *American Journal of Physical Anthropology, 88*(3), 273-283.

Caravaggi, P., Pataky, T., Goulermas, J. Y., Savage, R., & Crompton, R. (2009). A dynamic model of the windlass mechanism of the foot: evidence for early stance phase preloading of the plantar aponeurosis. *Journal of Experimental Biology*, *212*(15), 2491-2499.

Caravaggi, P., Pataky, T., Günther, M., Savage, R., & Crompton, R. (2010). Dynamics of longitudinal arch support in relation to walking speed: Contribution of the plantar aponeurosis. *Journal of Anatomy, 217*(3), 254-261.

Carter, D., Van der Meulen, M., & Beaupre, G. (1996). Mechanical factors in bone growth and development. *Bone, 18*(1), S5-S10.

Chang, G., Pakin, S. K., Schweitzer, M. E., Saha, P. K., & Regatte, R. R. (2008). Adaptations in trabecular bone microarchitecture in olympic athletes determined by 7T MRI. *Journal of Magnetic Resonance Imaging, 27*(5), 1089-1095.

Chirchir, H., Kivell, T. L., Ruff, C. B., Hublin, J., Carlson, K. J., Zipfel, B., et al. (2015). Recent origin of low trabecular bone density in modern humans. *Proceedings of the National Academy of Sciences of the United States of America, 112*(2), 366-371.

Christen, P., Ito, K., & van Rietbergen, B. (2015). A potential mechanism for allometric trabecular bone scaling in terrestrial mammals. *Journal of Anatomy, 226*(3), 236-243.

Christensen, J. C., & Jennings, M. M. (2009). Normal and abnormal function of the first ray. *Clinics in Podiatric Medicine and Surgery, 26*(3), 355-371.

Clarke, R. J., & Tobias, P. V. (1995). Sterkfontein member 2 foot bones of the oldest South African hominid. *Science, 269*(5223), 521-524.

Congdon, K. (2012). Interspecific and ontogenetic variation in proximal pedal phalangeal curvature of great apes (gorilla gorilla, pan troglodytes, and pongo pygmaeus). *International Journal of Primatology, 33*(2), 418-427.

Cotter, M. M., Simpson, S. W., Latimer, B. M., & Hernandez, C. J. (2009). Trabecular microarchitecture of hominoid thoracic vertebrae. *Anatomical Record-Advances in Integrative Anatomy and Evolutionary Biology, 292*(8), 1098-1106.

Cowin, S., Hart, R., Balser, J., & Kohn, D. (1985). Functional adaptation in long bones - establishing in vivo values for surface remodeling rate coefficients. *Journal of Biomechanics, 18*(9), 665-&.

Crompton, R. H., Thorpe, S., Weijie, W., Yu, L., Payne, R., Savage, R., et al. (2003). The biomechanical evolution of erect bipedality. *Walking Upright, 243*, 135-146.

Crompton, R. H., Vereecke, E. E., & Thorpe, S. K. S. (2008). Locomotion and posture from the common hominoid ancestor to fully modern hominins, with special reference to the last common panin/hominin ancestor. *Journal of Anatomy, 212*(4), 501-543.

Cunningham, C. A., & Black, S. M. (2009a). Anticipating bipedalism: Trabecular organization in the newborn ilium. *Journal of Anatomy, 214*(6), 817-829.

Cunningham, C. A., & Black, S. M. (2009b). Development of the fetal ilium - challenging concepts of bipedality. *Journal of Anatomy, 214*(1), 91-99.

D'Août, K., Aerts, P., De Clercq, D., De Meester, K., & Van Elsacker, L. (2002). Segment and joint angles of hind limb during bipedal and quadrupedal walking of the bonobo (*Pan paniscus*). *American Journal of Physical Anthropology, 119*(1), 37-51.

D'Août, K., Vereecke, E., Schoonaert, K., De Clercq, D., Van Elsacker, L., & Aerts, P. (2004). Locomotion in bonobos (*Pan paniscus*): Differences and similarities between bipedal and quadrupedal terrestrial walking, and a comparison with other locomotor modes. *Journal of Anatomy, 204*(5), 353-361.

De Cock, A., Vanrenterghem, J., Willems, T., Witvrouw, E., & De Clercq, D. (2008). The trajectory of the centre of pressure during barefoot running as a potential measure for foot function. *Gait & Posture, 27*(4), 669-675.

De Groote, I., & Humphrey, L. T. (2011). Body mass and stature estimation based on the first metatarsal in humans. *American Journal of Physical Anthropology*, *144*(4), 625-632.

Deloison, Y. (1999). L'homme ne descend pas d'un primate arboricole! une évidence méconnue. *Biométrie Humaine Et Anthropologie, 17*(3-4), 147-150.

Demes, B., & Jungers, W. (1993). Long bone cross-sectional dimensions, locomotor adaptations and body size in prosimian primates. *Journal of Human Evolution, 25*(1), 57-74.

Dempster, D. W. (2000). The contribution of trabecular architecture to cancellous bone quality. *Journal of Bone and Mineral Research, 15*(1), 20-23.

DeSilva, J. M. (2010). Revisiting the midtarsal break. *American Journal of Physical Anthropology, 141*(2), 245-258.

DeSilva, J. M., & Devlin, M. J. (2012). A comparative study of the trabecular bony architecture of the talus in humans, non-human primates, and *Australopithecus*. *Journal of Human Evolution, 63*(3), 536-551.

Ding, M., & Hvid, I. (2000). Quantification of age-related changes in the structure model type and trabecular thickness of human tibial cancellous bone. *Bone*, *26*(3), 291-295.

Doden, E. (1993). The relationship between the function and the inner cortical structure of metacarpal and phalangeal bones. In H. Preuschoft, & D. J. Chivers (Eds.), *Hands of primates* (pp. 271-284). Vienna: Springer Vienna.

Domínguez-Rodrigo, M., Pickering, T. R., Baquedano, E., Mabulla, A., Mark, D. F., Musiba, C., ... & Pérez-González, A. (2013). First partial skeleton of a 1.34-million-year-old Paranthropus boisei from Bed II, Olduvai Gorge, Tanzania. *PLoS One*, *8*(12), e80347.

Donahue, S. W., & Sharkey, N. A. (1999). Strains in the metatarsals during the stance phase of gait: Implications for stress fractures. *The Journal of Bone and Joint Surgery.American Volume, 81*(9), 1236-1244.

Doran, D. M. (1993a). Comparative locomotor behavior of chimpanzees and bonobos - the influence of morphology on locomotion. *American Journal of Physical Anthropology, 91*(1), 83-98.

Doran, D. M. (1993b). Sex-differences in adult chimpanzee positional behavior - the influence of body size on locomotion and posture. *American Journal of Physical Anthropology, 91*(1), 99-115.

Doran, D. M. (1997). Ontogeny of locomotion in mountain gorillas and chimpanzees. *Journal of Human Evolution, 32*(4), 323-344.

Doube, M., Klosowski, M. M., Wiktorowicz-Conroy, A. M., Hutchinson, J. R., & Shefelbine, S. J. (2011). Trabecular bone scales allometrically in mammals and birds. *Proceedings of the Royal Society B-Biological Sciences, 278*(1721), 3067-3073.

Dowdeswell, M. R., Jashashvili, T., Patel, B. A., Lebrun, R., Susman, R. L., Lordkipanidze, D., et al. (2017). Adaptation to bipedal gait and fifth metatarsal structural properties in *Australopithecus*, *Paranthropus*, and *Homo*. *Comptes Rendus Palevol.*

Drapeau, M., & Harmon, E. (2008). Metatarsal head torsion in apes, humans and A. afarensis. Paper presented at the *American Journal of Physical Anthropology,* pp. 92-92.

Drapeau, M. S. M., & Harmon, E. H. (2013). Metatarsal torsion in monkeys, apes, humans and australopiths. *Journal of Human Evolution, 64*(1), 93-108.

Duncan, A., Kappelman, J., & Shapiro, L. (1994). Metatarsophalangeal joint function and positional behavior in *Australopithecus afarensis*. *American Journal of Physical Anthropology, 93*(1), 67-81.

Elftman, H., & Manter, J. (1935). The evolution of the human foot, with especial reference to the joints. *Journal of Anatomy, 70*, 56-67.

Eriksen, E. F. (1986). Normal and pathological remodeling of human trabecular bone: Three dimensional reconstruction of the remodeling sequence in normals and in metabolic bone disease. *Endocrine Reviews, 7*(4), 379-408.

Eriksen, E. F. (2010). Cellular mechanisms of bone remodeling. *Reviews in Endocrine & Metabolic Disorders, 11*(4), 219-227.

Fajardo, R. J., & Müller, R. (2001). Three-dimensional analysis of nonhuman primate trabecular architecture using micro-computed tomography. *American Journal of Physical Anthropology, 115*(4), 327-336.

Fajardo, R. J., Muller, R., Ketcham, R. A., & Colbert, M. (2007). Nonhuman anthropoid primate femoral neck trabecular architecture and its relationship to locomotor mode. *Anatomical Record (Hoboken, N.J.: 2007), 290*(4), 422-436.

Ferguson, W. W. (1989). A new species of the genus *Australopithecus* (primates: Hominidae) from Plio/Pleistocene deposits west of Lake Turkana in Kenya. *Primates, 30*(2), 223-232.

Fernández, P. J., Almécija, S., Patel, B. A., Orr, C. M., Tocheri, M. W., & Jungers, W. L. (2015). Functional aspects of metatarsal head shape in humans, apes, and old world monkeys. *Journal of Human Evolution, 86*, 136-146.

Fleagle, J. G., Stern, J. T., Jungers, W. L., Susman, R. L., Vangor, A. K., & Wells, J. P. (1981). Climbing: A biomechanical link with brachiation and bipedalism. *Symposia of the Zoological Society of London, 48*, 359.

Frost, H. (1987). Bone mass and the mechanostat - a proposal. *Anatomical Record, 219*(1), 1-9.

Gomberg D. N. (1981). Form and Function of the Hominoid Foot. Ph.D. thesis, University of Massachusetts, Amherst.

Gebo, D. L. (1985). The nature of the primate grasping foot. *American Journal of Physical Anthropology, 67*(3), 269-277.

Gebo, D. (1992). Plantigrady and foot adaptation in African apes - implications for hominid origins. *American Journal of Physical Anthropology, 89*(1), 29-58.

Gebo, D. L. (1996). Climbing, brachiation, and terrestrial quadrupedalism: Historical precursors of hominid bipedalism. *American Journal of Physical Anthropology, 101*(1), 55-92.

Gibson, L. (1985). The mechanical behaviour of cancellous bone. *Journal of biomechanics*, *18*(5), 317-328.

Gill, C. M., Bredella, M. A., & DeSilva, J. M. (2015). Skeletal development of hallucal tarsometatarsal joint curvature and angulation in extant apes and modern humans. *Journal of Human Evolution, 88*, 137-145.

Goodship, A., Lanyon, L., & McFie, H. (1979). Functional adaptation of bone to increased stress. An experimental study. *Jbjs, 61*(4), 539-546.

Griffin, N. L., D'Août, K., Richmond, B., Gordon, A., & Aerts, P. (2010a). Comparative in vivo forefoot kinematics of *Homo sapiens* and *Pan paniscus*. *Journal of Human Evolution, 59*(6), 608-619.

Griffin, N. L., D'Août, K., Ryan, T. M., Richmond, B. G., Ketcham, R. A., & Postnov, A. (2010b). Comparative forefoot trabecular bone architecture in extant hominids. *Journal of Human Evolution, 59*(2), 202-213.

Griffin, N. L., & Richmond, B. G. (2005). Cross-sectional geometry of the human forefoot. *Bone, 37*(2), 253-260.

Griffin, N. L., & Richmond, B. G. (2010). Joint orientation and function in great ape and human proximal pedal phalanges. *American journal of physical anthropology*, *141*(1), 116-123.

Griffin, N. L., Miller, C. E., Schmitt, D., & D'Août, K. (2015). Understanding the evolution of the windlass mechanism of the human foot from comparative anatomy: Insights, obstacles, and future directions. *American Journal of Physical Anthropology, 156*(1), 1-10.

Grine, F. E., & Susman, R. L. (1991). Radius of *Paranthropus robustus* from member 1, Swartkrans formation, South Africa. *American Journal of Physical Anthropology, 84*(3), 229-248.

Grine, F. E. (1993). Description and preliminary analysis of new hominid craniodental fossils from the Swartkrans formation. *Swartkrans: A Cave's Chronicle of Early Man.Transvaal Museum, Pretoria,* 75-116.

Grine, F. E., & Daegling, D. J. (1993). New mandible of *Paranthropus robustus* from member 1, Swartkrans formation, South Africa. *Journal of Human Evolution, 24*(4), 319-333.

Guldberg, R., Caldwell, N., Guo, X., Goulet, R., Hollister, S., & Goldstein, S. (1997). Mechanical stimulation of tissue repair in the hydraulic bone chamber. *Journal of Bone and Mineral Research, 12*(8), 1295-1302.

Guy, F., Lieberman, D. E., Pilbeam, D., de Leon, M. P., Likius, A., Mackaye, H. T., et al. (2005). Morphological affinities of the *Sahelanthropus tchadensis* (late miocene hominid from Chad) cranium. *Proceedings of the National Academy of Sciences of the United States of America, 102*(52), 18836-18841.

Haile-Selassie, Y. (2001). Late Miocene hominids from the middle awash, Ethiopia. *Nature, 412*(6843), 178-181.

Halstead, J., Turner, D. E., & Redmond, A. C. (2005). The relationship between hallux dorsiflexion and ankle joint complex frontal plane kinematics: a preliminary study. *Clinical Biomechanics*, *20*(5), 526-531.

Harcourt-Smith, W. E. H., Aiello, L. C., & O'Higgins, P. (2002). From Lucy to Littlefoot: a three dimensional analysis of Plio-Pleistocene hominin tarsal remains. *American Journal of Physical Anthropology*, 34 (Suppl.), 82.

Harcourt-Smith, W. E. H., & Aiello, L. C. (2004). Fossils, feet and the evolution of human bipedal locomotion. *Journal of Anatomy, 204*(5), 403-416.

Harrison, L. C., Nikander, R., Sikio, M., Luukkaala, T., Helminen, M. T., Ryymin, P., et al. (2011). MRI texture analysis of femoral neck: Detection of exercise load-associated differences in trabecular bone. *Journal of Magnetic Resonance Imaging: JMRI, 34*(6), 1359-1366.

Havill, L. M., Allen, M. R., Bredbenner, T. L., Burr, D. B., Nicolella, D. P., Turner, C. H., et al. (2010). Heritability of lumbar trabecular bone mechanical properties in baboons. *Bone, 46*(3), 835-840.

Hetherington, V. J., Carnett, J., & Patterson, B. A. (1989). Motion of the first metatarsophalangeal joint. *The Journal of Foot Surgery, 28*(1), 13-19.

Hicks, J. H. (1954). The mechanics of the foot: II. The plantar aponeurosis and the arch. *Journal of Anatomy, 88*, 25-30.1.

Hodgskinson, R., & Currey, J. D. (1990). Effects of structural variation on young's modulus of non-human cancellous bone. *Proceedings of the Institution of Mechanical Engineers.Part H, Journal of Engineering in Medicine, 204*(1), 43-52.

Holowka, N. B., O'Neill, M. C., Thompson, N. E., & Demes, B. (2017). Chimpanzee and human midfoot motion during bipedal walking and the evolution of the longitudinal arch of the foot. *Journal of Human Evolution, 104*, 23-31.

Huiskes, R., Ruimerman, R., van Lenthe, G., & Janssen, J. (2000). Effects of mechanical forces on maintenance and adaptation of form in trabecular bone. *Nature, 405*(6787), 704-706.

Hunt, K. D., Cant, J. G., Gebo, D. L., Rose, M. D., Walker, S. E., & Youlatos, D. (1996). Standardized descriptions of primate locomotor and postural modes. *Primates, 37*(4), 363-387.

Hunt, A. E., Smith, R. M., Torode, M., & Keenan, A. M. (2001). Inter-segment foot motion and ground reaction forces over the stance phase of walking. *Clinical Biomechanics (Bristol, Avon), 16*(7), 592-600.

Hunt, K. D. (1991). Mechanical implications of chimpanzee positional behavior. *American Journal of Physical Anthropology, 86*(4), 521-536.

Hunt, K. D. (1992). Social rank and body size as determinants of positional behavior in *Pan troglodytes*. *Primates, 33*(3), 347-357.

Hunt, K. D. (1994). Body size effects on vertical climbing among chimpanzees. *International Journal of Primatology, 15*(6), 855-865.

Hutton, W. C., & Dhanendran, M. (1981). The mechanics of normal and hallux valgus feet--a quantitative study. *Clinical Orthopaedics and Related Research, (157)*(157), 7-13.

Nguyen, N. H., Pahr, D. H., Gross, T., Skinner, M. M., & Kivell, T. L. (2014). Micro-finite element (μFE) modeling of the siamang (*Symphalangus syndactylus*) third proximal phalanx: the functional role of curvature and the flexor sheath ridge. *Journal of human evolution*, *67*, 60-75.

Inouye, S. E. (1992). Ontogeny and allometry of African ape manual rays. *Journal of Human Evolution*, *23*(2), 107-138. Jashashvili, T., Dowdeswell, M. R., Lebrun, R., & Carlson, K. J. (2015). Cortical structure of hallucal metatarsals and locomotor adaptations in hominoids. *PLOS One, 10*(1)

Jashashvili, T., Dowdeswell, M. R., Lebrun, R., & Carlson, K. J. (2015). Cortical structure of hallucal metatarsals and locomotor adaptations in hominoids. *Plos One, 10*(1), e0117905.

Johanson, D. C., & White, T. D. (1979). A systematic assessment of early african hominids. *Science (New York, N.Y.), 203*(4378), 321-330.

Jouffroy, F. K., & Lessertisseur, J. (1960). Les spécialisations anatomiques de la main chez les singes à progression suspendue. *Mammalia*, *24*(1), 93-151.

Jenkins, F. A. (1974). *Primate locomotion*. Academic Press.

Jungers, W. L. (1982). Lucy's limbs: Skeletal allometry and locomotion in *Australopithecus afarensis*. *Nature, 297*(5868), 676-678.

Jungers, W. L., & Stern, J. T. (1983). Body proportions, skeletal allometry and locomotion in the hadar hominids: A reply to wolpoff. *Journal of Human Evolution, 12*(7), 673-684.

Jungers, W. L. (1984). Aspects of size and scaling in primate biology with special reference to the locomotor skeleton. *American Journal of Physical Anthropology, 27*(S5), 73-97.

Kanamoto, S., Ogihara, N., & Nakatsukasa, M. (2011). Three-dimensional orientations of talar articular surfaces in humans and great apes. *Primates, 52*(1), 61-68.

Katoh, Y., Chao, E. Y., Laughman, R. K., Schneider, E., & Morrey, B. F. (1983). Biomechanical analysis of foot function during gait and clinical applications. *Clinical Orthopaedics and Related Research,* (177), 23-33.

Kerschnitzki, M., Kollmannsberger, P., Burghammer, M., Duda, G. N., Weinkamer, R., Wagermaier, W., et al. (2013). Architecture of the osteocyte network correlates with bone material quality. *Journal of Bone and Mineral Research, 28*(8), 1837-1845.

Khazzam, M., Long, J. T., Marks, R. M., & Harris, G. F. (2007). Kinematic changes of the foot and ankle in patients with systemic rheumatoid arthritis and forefoot deformity. *Journal of Orthopaedic Research, 25*(3), 319-329.

Kidder, S. M., Abuzzahab, F. S., Harris, G. F., & Johnson, J. E. (1996). A system for the analysis of foot and ankle kinematics during gait. *IEEE Transactions on Rehabilitation Engineering*, *4*(1), 25-32.

Kimura, T., Okada, M., & Ishida, H. (1977). Dynamics of primate bipedal walking as viewed from the force of foot. *Primates, 18*(1), 137-147.

Kitaoka, H. B., Crevoisier, X. M., Hansen, D., Katajarvi, B., Harbst, K., & Kaufman, K. R. (2006). Foot and ankle kinematics and ground reaction forces during ambulation. *Foot & Ankle International, 27*(10), 808-813.

Kivell, T. L., Skinner, M. M., Lazenby, R., & Hublin, J. J. (2011). Methodological considerations for analyzing trabecular architecture: An example from the primate hand. *Journal of Anatomy, 218*(2), 209-225.

Kivell, T. L. (2016). A review of trabecular bone functional adaptation: What have we learned from trabecular analyses in extant hominoids and what can we apply to fossils? *Journal of Anatomy, 228*(4), 569-594.

Kraft, T. S., Venkataraman, V. V., & Dominy, N. J. (2014). A natural history of human tree climbing. *Journal of human evolution*, *71*, 105-118.

Lambers, F. M., Koch, K., Kuhn, G., Ruffoni, D., Weigt, C., Schulte, F. A., et al. (2013). Trabecular bone adapts to long-term cyclic loading by increasing stiffness and normalization of dynamic morphometric rates. *Bone, 55*(2), 325-334.

Lanyon, L. E. (1973). Analysis of surface bone strain in the calcaneus of sheep during normal locomotion. *Journal of Biomechanics, 6*(1), 41-49.

Lanyon, L. E. (1974). Experimental support for the trajectorial theory of bone structure. *The Journal of Bone and Joint Surgery. British Volume, 56*(1), 160-166.

Latimer, B. M., Lovejoy, C. O., Johanson, D. C., & Coppens, Y. (1982). Hominid tarsal, metatarsal, and phalangeal bones recovered from the hadar formation: 1974–1977 collections. *American Journal of Physical Anthropology, 57*(4), 701-719.

Latimer, B., & Lovejoy, C. O. (1989). The calcaneus of *Australopithecus afarensis* and its implications for the evolution of bipedality. *American Journal of Physical Anthropology, 78*(3), 369-386.

Latimer, B., & Lovejoy, C. O. (1990). Hallucal tarsometatarsal joint in australopithecus afarensis. *American Journal of Physical Anthropology, 82*(2), 125-133.

Latimer, B., Ohman, J. C., & Lovejoy, C. O. (1987). Talocrural joint in african hominoids: Implications for australopithecus afarensis. *American Journal of Physical Anthropology, 74*(2), 155-175.

Leakey, L. S., Tobias, P. V., & Napier, J. R. (1964). A new species of the genus homo from Olduvai Gorge. *Nature, 202*(4927), 7-9.

Leakey, L. (1960). Recent discoveries at Olduvai Gorge. *Nature, 188*(4755), 1050-1052.

Leakey, M. G., Feibel, C. S., McDougall, I., & Walker, A. (1995). New four-million-year-old hominid species from Kanapoi and Allia bay, Kenya. *Nature, 376*(6541), 565.

Leakey, M. G., Feibel, C. S., McDougall, I., Ward, C., & Walker, A. (1998). New specimens and confirmation of an early age for *Australopithecus anamensis*. *Nature, 393*(6680), 62.

Leakey, M., & Hay, R. (1979). Pliocene footprints in the Laetolil beds at Laetoli, northern Tanzania. *Nature, 278*(5702), 317-323.

Leardini, A., Benedetti, M. G., Berti, L., Bettinelli, D., Nativo, R., & Giannini, S. (2007). Rear-foot, mid-foot and fore-foot motion during the stance phase of gait. *Gait & posture*, *25*(3), 453-462.

Lee, C. R., & Farley, C. T. (1998). Determinants of the center of mass trajectory in human walking and running. *Journal of Experimental Biology, 201*(21), 2935-2944.

Lieberman, D. E., Polk, J. D., & Demes, B. (2004). Predicting long bone loading from cross-sectional geometry. *American Journal of Physical Anthropology, 123*(2), 156-171.

Lieberman, D. (1996). How and why humans grow thin skulls: Experimental evidence for systemic cortical robusticity. *American Journal of Physical Anthropology, 101*(2), 217-236.

Lieberman, D. (1997). Making behavioral and phylogenetic inferences from hominid fossils: Considering the developmental influence of mechanical forces. *Annual Review of Anthropology, 26*, 185-210.

Liu, X. S., Sajda, P., Saha, P. K., Wehrli, F. W., Bevill, G., Keaveny, T. M., et al. (2008). Complete volumetric decomposition of individual trabecular plates and rods and its morphological correlations with anisotropic elastic moduli in human trabecular bone. *Journal of Bone and Mineral Research, 23*(2), 223-235.

Lockwood, C., Richmond, B., Jungers, W., & Kimbel, W. (1996). Randomization procedures and sexual dimorphism in *Australopithecus afarensis*. *Journal of Human Evolution, 31*(6), 537-548.

Lorenzo, C., Arsuaga, J. L., & Carretero, J. M. (1999). Hand and foot remains from the Gran Dolina Early Pleistocene site (Sierra de Atapuerca, Spain). *Journal of Human Evolution, 37*(3-4), 501-522.

MacLatchy, L., & Muller, R. (2002). A comparison of the femoral head and neck trabecular architecture of galago and perodicticus using micro-computed tomography (microCT). *Journal of Human Evolution, 43*(1), 89-105.

MacWilliams, B. A., Cowley, M., & Nicholson, D. E. (2003). Foot kinematics and kinetics during adolescent gait. *Gait & posture*, *17*(3), 214-224.

Maga, M., Kappelman, J., Ryan, T., & Ketcham, R. (2006). Preliminary observations on the calcaneal trabecular microarchitecture of extant large-bodied hominoids. *American Journal of Physical Anthropology, 129*(3), 410-417.

Maquer, G., Musy, S. N., Wandel, J., Gross, T., & Zysset, P. K. (2015). Bone volume fraction and fabric anisotropy are better determinants of trabecular bone stiffness than other morphological variables. *Journal of Bone and Mineral Research, 30*(6), 1000-1008.

Marchi, D. (2005). The cross-sectional geometry of the hand and foot bones of the Hominoidea and its relationship to locomotor behavior. *Journal of human evolution*, *49*(6), 743-761.

Marchi, D. (2010). Articular to diaphyseal proportions of human and great ape metatarsals. *American Journal of Physical Anthropology, 143*(2), 198-207.

Martin, R. B., Burr, D. B., Sharkey, N. A., & Fyhrie, D. P. (1998). *Skeletal tissue mechanics*. New York: Springer.

Martin, R. B., Burr, D. B., Sharkey, N. A., & Fyhrie, D. P. (2015). *Skeletal tissue mechanics*. New York: Springer.

Marzke, M. W. (1971). Origin of the human hand. *American Journal of Physical Anthropology, 34*(1), 61-84.

Masao, F. T., Ichumbaki, E. B., Cherin, M., Barili, A., Boschian, G., Iurino, D. A., et al. (2016). New footprints from laetoli (tanzania) provide evidence for marked body size variation in early hominins. *Elife, 5*, e19568.

McHenry, H. M. (1991). Petite bodies of the robust australopithecines. *American Journal of Physical Anthropology, 86*(4), 445-454.

McHenry, H. M., Brown, C. C., & McHenry, L. J. (2007). Fossil hominin ulnae and the forelimb of *Paranthropus*. *American Journal of Physical Anthropology, 134*(2), 209-218.

McHenry, H. M., & Jones, A. L. (2006). Hallucial convergence in early hominids. *Journal of human evolution*, *50*(5), 534-539.

McHenry, H. (1991). Sexual dimorphism in *Australopithecus-afarensis*. *Journal of Human Evolution, 20*(1), 21-32.

Mittra, E., Rubin, C., & Qin, Y. (2005). Interrelationship of trabecular mechanical and microstructural properties in sheep trabecular bone. *Journal of Biomechanics, 38*(6), 1229-1237.

Mittra, E., Rubin, C., Gruber, B., & Qin, Y. (2008). Evaluation of trabecular mechanical and microstructural properties in human calcaneal bone of advanced age using mechanical testing, mu CT, and DXA. *Journal of Biomechanics, 41*(2), 368-375.

Modlesky, C. M., Majumdar, S., & Dudley, G. A. (2008). Trabecular bone microarchitecture in female collegiate gymnasts. *Osteoporosis International, 19*(7), 1011-1018.

Modlesky, C. M., Subramanian, P., & Miller, F. (2008). Underdeveloped trabecular bone microarchitecture is detected in children with cerebral palsy using high-resolution magnetic resonance imaging. *Osteoporosis International*, *19*(2), 169-176.

Morton, D. J. (1922). Evolution of the human foot. *American Journal of Physical Anthropology, 5*(4), 305-336.

Morton, D. J. (1924). Evolution of the human foot II. *American Journal of Physical Anthropology, 7*(1), 1-52.

Morton, D. J. (1964). *The human foot: its evolution, physiology, and functional disorders*. Hafner Pub. Co..

Mullender, M. G., Huiskes, R., Versleyen, H., & Buma, P. (1996). Osteocyte density and histomorphometric parameters in cancellous bone of the proximal femur in five mammalian species. *Journal of Orthopaedic Research*, *14*(6), 972-979.

Munro, C. F., Miller, D. I., & Fuglevand, A. J. (1987). Ground reaction forces in running: a reexamination. *Journal of biomechanics*, *20*(2), 147-155.

Myers, M. J., & Steudel, K. (1985). Effect of limb mass and its distribution on the energetic cost of running. *Journal of Experimental Biology, 116*(1), 363-373.

Nagel, A., Fernholz, F., Kibele, C., & Rosenbaum, D. (2008). Long distance running increases plantar pressures beneath the metatarsal heads - A barefoot walking investigation of 200 marathon runners. *Gait & Posture, 27*(1), 152-155.

Napier, J. R. (1964). The evolution of bipedal walking in the hominids. *Archives of Biological Sciences, 37*, 3.

Nawoczenski, D. A., Baumhauer, J. F., & Umberger, B. R. (1999). Relationship between clinical measurements and motion of the first metatarsophalangeal joint during gait. *JBJS*, *81*(3), 370-6.

Nester, C., Jones, R. K., Liu, A., Howard, D., Lundberg, A., Arndt, A., et al. (2007). Foot kinematics during walking measured using bone and surface mounted markers. *Journal of Biomechanics, 40*, 3412.

Novacheck, T. F. (1998). The biomechanics of running. *Gait & posture*, *7*(1), 77-95.

Oishi, M., Ogihara, N., Endo, H., Une, Y., Ichihara, N., Asari, M., et al. (2012). Muscle dimensions of the foot in the orangutan and the chimpanzee. *Journal of Anatomy, 221*(4), 311-317.

Orr, C. M. (2005). Knuckle-walking anteater: A convergence test of adaptation for purported knuckle-walking features of African hominidae. *American Journal of Physical Anthropology, 128*(3), 639-658.

Oxnard, C. E., & Lisowski, F. P. (1980). Functional articulation of some hominoid foot bones: Implications for the olduvai (hominid 8) foot. *American Journal of Physical Anthropology, 52*(1), 107-117.

Parfitt, A., Travers, R., Rauch, F., & Glorieux, F. (2000). Structural and cellular changes during bone growth in healthy children. *Bone, 27*(4), 487-494.

Perry, J., & Davids, J. R. (1992). Gait analysis: normal and pathological function. *Journal of Pediatric Orthopaedics*, *12*(6), 815.

Pickford, M., Senut, B., Gommery, D., & Treil, J. (2002). Bipedalism in *Orrorin tugenensis* revealed by its femora. *Comptes Rendus Palevol, 1*(4), 191-203.

Pontzer, H., Lieberman, D., Momin, E., Devlin, M., Polk, J., Hallgrimsson, B., et al. (2006). Trabecular bone in the bird knee responds with high sensitivity to changes in load orientation. *Journal of Experimental Biology, 209*(1), 57-65.

Pontzer, H., Rolian, C., Rightmire, G. P., Jashashvili, T., Ponce de León, M. S., Lordkipanidze, D., et al. (2010). Locomotor anatomy and biomechanics of the dmanisi hominins. *Journal of Human Evolution, 58*(6), 492-504.

Preuschoft, H. (1971). Body posture and mode of locomotion in early pleistocene hominids. *Folia Primatologica, 14*(3-4), 209-240.

Proctor, D. J. (2010). Brief communication: Shape analysis of the MT 1 proximal articular surface in fossil hominins and shod and unshod homo. *American Journal of Physical Anthropology, 143*(4), 631-637.

Proctor, D. J., Broadfield, D., & Proctor, K. (2008). Quantitative three-dimensional shape analysis of the proximal hallucial metatarsal articular surface in *Homo*, *Pan*, *Gorilla*, and *Hylobates*. *American Journal of Physical Anthropology, 135*(2), 216-224.

Proctor, D. J. (2013). Proximal metatarsal articular surface shape and the evolution of a rigid lateral foot in hominins. *Journal of human evolution*, *65*(6), 761-769.

Prost, J. H. (1980). Origin of bipedalism. *American Journal of Physical Anthropology, 52*(2), 175-189.

Räth, C., Baum, T., Monetti, R., Sidorenko, I., Wolf, P., Eckstein, F., et al. (2013). Scaling relations between trabecular bone volume fraction and microstructure at different skeletal sites. *Bone, 57*(2), 377-383.

Rafferty, K. L., & Ruff, C. B. (1994). Articular structure and function in *Hylobates*, *Colobus*, and *Papio*. *American Journal of Physical Anthropology, 94*(3), 395-408.

Raichlen, D. A., Gordon, A. D., Harcourt-Smith, W. E. H., Foster, A. D., & Haas, W. R., Jr. (2010). Laetoli footprints preserve earliest direct evidence of human-like bipedal biomechanics. *Plos One, 5*(3), e9769.

Raichlen, D. A., Gordon, A. D., Foster, A. D., Webber, J. T., Sukhdeo, S. M., Scott, R. S., et al. (2015). An ontogenetic framework linking locomotion and trabecular bone architecture with applications for reconstructing hominin life history. *Journal of Human Evolution, 81*, 1-12.

Remis, M. (1995). Effects of body size and social context on the arboreal activities of lowland gorillas in the central african republic. *American Journal of Physical Anthropology, 97*(4), 413-433.

Remis, M. J. (1998). The gorilla paradox. In E. Strasser, J. G. Fleagle, A. L. Rosenberger & H. M. McHenry (Eds.), *Primate locomotion: Recent advances* (pp. 95-106). Boston, MA: Springer US.

Richmond, B. G., & Jungers, W. L. (1995). Size variation and sexual dimorphism in australopithecus afarensis and living hominoids. *Journal of Human Evolution, 29*(3), 229-245.

Richmond, B. G., & Strait, D. S. (2000). Evidence that humans evolved from a knuckle-walking ancestor. *Nature, 404*(6776), 382-385.

Richmond, B. G., Begun, D. R., & Strait, D. S. (2001). Origin of human bipedalism: The knuckle-walking hypothesis revisited. *American Journal of Physical Anthropology, Suppl 33*, 70-105.

Richmond, B. G. (1998). *Ontogeny and biomechanics of phalangeal form in primates.* Unpublished Anthropology Doctor of Philosophy, SUNY Stony Brook,

Richmond, B. (2007). Ontogeny and biomechanics of phalangeal form in primates. (Doctor of Philosophy, SUNY Stony Brook). *Anthropology,*

Richmond, B. G. (2007). Biomechanics of phalangeal curvature. *Journal of Human Evolution, 53*(6), 678-690.

Robinson, J. T. (1972). *Early hominid posture and locomotion* University of Chicago Press.

Rodgers, M. M. (1995). Dynamic foot biomechanics. *Journal of Orthopaedic & Sports Physical Therapy, 21*(6), 306-316.

Rodgers, M., & Cavanagh, P. (1985). Pressure distribution in Morton's foot structure. *Medicine and Science in Sports and Exercise, 17*(2), 223-223.

Rolian, C., Lieberman, D. E., Hamill, J., Scott, J. W., & Werbel, W. (2009). Walking, running and the evolution of short toes in humans. *Journal of Experimental Biology, 212*(5), 713-721.

Rose, M. D. (1984). A hominine hip bone, KNM-ER 3228, from east Lake Turkana, Kenya. *American Journal of Physical Anthropology, 63*(4), 371-378.

Rose, M. D. (1988). Functional anatomy of the cheiridia. *Orang-utan biology*, 299-310.

Rubin, C., Turner, A. S., Mallinckrodt, C., Jerome, C., Mcleod, K., & Bain, S. (2002). Mechanical strain, induced noninvasively in the high-frequency domain, is anabolic to cancellous bone, but not cortical bone. *Bone, 30*(3), 445-452.

Rubin, C. T., & Lanyon, L. E. (1982). Limb mechanics as a function of speed and gait: A study of functional strains in the radius and tibia of horse and dog. *Journal of Experimental Biology, 101*(1), 187-211.

Ruff, C. B., & Hayes, W. C. (1983). Cross-sectional geometry of pecos pueblo femora and tibiae—A biomechanical investigation: I. method and general patterns of variation. *American Journal of Physical Anthropology, 60*(3), 359-381.

Ruff, C. (1983). The contribution of cancellous bone to long-bone strength and rigidity. *American Journal of Physical Anthropology, 61*(2), 141-143.

Ruff, C. (2002). Long bone articular and diaphyseal structure in old world monkeys and apes. I: Locomotor effects. *American Journal of Physical Anthropology, 119*(4), 305-342.

Ruff, C., & Runestad, J. (1992). Primate limb bone structural adaptations. *Annual Review of Anthropology, 21*, 407-433.

Ruff, C., Holt, B., & Trinkaus, E. (2006). Who's afraid of the big bad wolff?: Â€œWolff's lawâ€• and bone functional adaptation. *American Journal of Physical Anthropology, 129*(4), 484-498.

Ryan, T. M., & Ketcham, R. A. (2002). The three-dimensional structure of trabecular bone in the femoral head of strepsirrhine primates. *Journal of Human Evolution, 43*(1), 1-26.

Ryan, T., & Ketcham, R. (2005). Angular orientation of trabecular bone in the femoral head and its relationship to hip joint loads in leaping primates. *Journal of Morphology, 265*(3), 249-263.

Ryan, T. M., & Krovitz, G. E. (2006). Trabecular bone ontogeny in the human proximal femur. *Journal of Human Evolution, 51*(6), 591-602.

Ryan, T. M., & Walker, A. (2010). Trabecular bone structure in the humeral and femoral heads of anthropoid primates. *The Anatomical Record: Advances in Integrative Anatomy and Evolutionary Biology, 293*(4), 719-729.

Ryan, T. M., & Shaw, C. N. (2012). Unique suites of trabecular bone features characterize locomotor behavior in human and non-human anthropoid primates. *Plos One, 7*(7), e41037.

Ryan, T. M., & Shaw, C. N. (2013). Trabecular bone microstructure scales allometrically in the primate humerus and femur. *Proceedings of the Royal Society B-Biological Sciences, 280*(1758), 20130172.

Saparin, P., Scherf, H., Hublin, J., Fratzl, P., & Weinkamer, R. (2011). Structural adaptation of trabecular bone revealed by position resolved analysis of proximal femora of different primates. *The Anatomical Record: Advances in Integrative Anatomy and Evolutionary Biology, 294*(1), 55-67.

Sarmiento, E. (1994). *Terrestrial traits in the hands and feet of gorillas. american museum novitates ; no. 3091*. New York: American Museum of Natural History.

Scherf, H., Harvati, K., & Hublin, J. J. (2013). A comparison of proximal humeral cancellous bone of great apes and humans. *Journal of Human Evolution, 65*(1), 29-38.

Scherf, H., & Tilgner, R. (2009). A new high-resolution computed tomography (CT) segmentation method for trabecular bone architectural analysis. *American Journal of Physical Anthropology, 140*(1), 39-51.

Schilling, A., Tofanelli, S., Hublin, J., & Kivell, T. L. (2014). Trabecular bone structure in the primate wrist. *Journal of Morphology, 275*(5), 572-585.

Schoonaert, K., D'Août, K., Samuel, D., Talloen, W., Nauwelaerts, S., Kivell, T. L., et al. (2016). Gait characteristics and spatio-temporal variables of climbing in bonobos (*Pan paniscus*). *American Journal of Primatology, 78*(11), 1165-1177.

Scott, G., Menz, H. B., & Newcombe, L. (2007). Age-related differences in foot structure and function. *Gait & posture*, *26*(1), 68-75.

Senut, B. (1981). Humeral outlines in some hominoid primates and in Plio-Pleistocene hominids. *American Journal of Physical Anthropology, 56*(3), 275-283.

Senut, B. (1985). Functional aspects of plio-pleistocene hominid limb bones: Implications for taxonomy and phylogeny. *Ancestors: The Hard Evidence*, 193-201.

Senut, B. (1996). Pliocene hominid systematics and phylogeny. *South African Journal of Science, 92*(4), 165-166.

Senut, B., Pickford, M., Gommery, D., Mein, P., Cheboi, K., & Coppens, Y. (2001). First hominid from the Miocene (Lukeino formation, Kenya). *Comptes Rendus De l'Académie Des Sciences-Series IIA-Earth and Planetary Science, 332*(2), 137-144.

Shea, B. T. (1981). Relative growth of the limbs and trunk in the African apes. *American Journal of Physical Anthropology, 56*(2), 179-201.

Shi, X., Liu, X. S., Wang, X., Guo, X. E., & Niebur, G. L. (2010). Effects of trabecular type and orientation on microdamage susceptibility in trabecular bone. *Bone*, *46*(5), 1260-1266.

Simkin, A., Ayalon, J., & Leichter, I. (1987). Increased trabecular bone density due to bone-loading exercises in postmenopausal osteoporotic women. *Calcified Tissue International, 40*(2), 59-63.

Simkin, A., Leichter, I., Swissa, A., & Samueloff, S. (1989). The effect of swimming activity on bone architecture in growing-rats. *Journal of Biomechanics, 22*(8-9), 845-&.

Simmons, D. J., Russell, J. E., Winter, F., Tran Van, P., Vignery, A., Baron, R., et al. (1983). Effect of spaceflight on the non-weight-bearing bones of rat skeleton. *The American Journal of Physiology, 244*(3), R319-26.

Simon, J., Doederlein, L., McIntosh, A. S., Metaxiotis, D., Bock, H. G., & Wolf, S. I. (2006). The Heidelberg foot measurement method: development, description and assessment. *Gait & Posture*, *23*(4), 411-424.

Skedros, J. G., Knight, A. N., Farnsworth, R. W., & Bloebaum, R. D. (2011). Do regional modifications in tissue mineral content and microscopic mineralization heterogeneity adapt trabecular bone tracts for habitual bending? Analysis in the context of trabecular architecture of deer calcanei. *Journal of Anatomy, 220*(3), 242-255.

Skerry, T., & Lanyon, L. (1995). Interruption of disuse by short-duration walking exercise does not prevent bone loss in the sheep calcaneus. *Bone, 16*(2), 269-274.

Skinner, M. M., Stephens, N. B., Tsegai, Z. J., Foote, A. C., Nguyen, N. H., Gross, T., et al. (2015). Human-like hand use in *Australopithecus africanus*. *Science, 347*(6220), 395-399.

Soames, R. W. (1985). Foot pressure patterns during gait. *Journal of biomedical engineering*, *7*(2), 120-126.

Stauber, M., Rapillard, L., van Lenthe, G. H., Zysset, P., & Müller, R. (2006). Importance of individual rods and plates in the assessment of bone quality and their contribution to bone stiffness. *Journal of Bone and Mineral Research*, *21*(4), 586-595.

Stern, J. T. (1975). Before bipedality. Paper presented at the *American Journal of Physical Anthropology, 42.* (2) pp. 331-331.

Stern, J. T., & Susman, R. L. (1983). The locomotor anatomy of *Australopithecus afarensis*. *American Journal of Physical Anthropology, 60*(3), 279-317.

Stern, J. T., Jungers, W. L., & Susman, R. L. (1995). Quantifying phalangeal curvature: An empirical comparison of alternative methods. *American Journal of Physical Anthropology, 97*(1), 1-10.

Stern, J. T. (1999). The cost of bent-knee, bent-hip bipedal gait. A reply to Crompton et al. *Journal of Human Evolution, 36*(5), 567-570.

Stern, J. T. (2000). Climbing to the top: A personal memoir of australopithecus afarensis. *Evolutionary Anthropology: Issues, News, and Reviews, 9*(3), 113-133.

Stokes, I. A., Hutton, W. C., & Stott, J. R. (1979a). Forces acting on the metatarsals during normal walking. *Journal of Anatomy, 129*(Pt 3), 579-590.

Stokes, I., Hutton, W., Stott, J., & Lowe, L. (1979b). Forces under the hallux valgus foot before and after surgery. *Clinical Orthopaedics and Related Research,* (142), 64-72.

Su, A., & Carlson, K. J. (2017). Comparative analysis of trabecular bone structure and orientation in South African hominin tali. *Journal of Human Evolution, 106*, 1-18.

Su, A., Wallace, I. J., & Nakatsukasa, M. (2013). Trabecular bone anisotropy and orientation in an Early Pleistocene hominin talus from East Turkana, Kenya. *Journal of human evolution*, *64*(6), 667-677.

Sumner, D., & Andriacchi, T. (1996). Adaptation to differential loading: Comparison of growth-related changes in cross-sectional properties of the human femur and humerus. *Bone, 19*(2), 121-126.

Susman, R. L. (1979). Comparative and functional-morphology of hominoid fingers. *American Journal of Physical Anthropology, 50*(2), 215-236.

Susman, R. L., & Stern, J. T. (1982). Functional morphology of homo habilis. *Science (New York, N.Y.), 217*(4563), 931-934.

Susman, R. L. (1983). Evolution of the human foot - evidence from plio-pleistocene hominids. *Foot & Ankle, 3*(6), 365-376.

Susman, R. L., Stern, J. T., & Jungers, W. L. (1984). Arboreality and bipedality in the hadar hominids. *Folia Primatologica; International Journal of Primatology, 43*(2-3), 113-156.

Susman, R. L., & Brain, T. M. (1988). New first metatarsal (SKX 5017) from Swartkrans and the gait of *Paranthropus robustus*. *American Journal of Physical Anthropology, 77*(1), 7-15.

Susman, R. L., & de Ruiter, D. J. (2004). New hominin first metatarsal (SK 1813) from Swartkrans. *Journal of Human Evolution, 47*(3), 171-181.

Swartz, S., Parker, A., & Huo, C. (1998). Theoretical and empirical scaling patterns and topological homology in bone trabeculae. *Journal of Experimental Biology, 201*(4), 573-590.

Takemoto, H. (2004). Seasonal change in terrestriality of chimpanzees in relation to microclimate in the tropical forest. *American Journal of Physical Anthropology*, *124*(1), 81-92.

Tanck, E., Homminga, J., Van Lenthe, G., & Huiskes, R. (2001). Increase in bone volume fraction precedes architectural adaptation in growing bone. *Bone, 28*(6), 650-654.

Tardieu, C. (1983). L'articulation de genou: analyse morpho-fonctionnelle chez les primates et les hominidés fossiles. Paris: *Cahiers Paleoanthropologie.* 108 pp.

Thorpe, S. K. S., & Crompton, R. H. (2005). Locomotor ecology of wild orangutans (*Pongo pygmaeus abelii*) in the Gunung Leuser ecosystem, Sumatra, Indonesia: A multivariate analysis using log-linear modelling. *American Journal of Physical Anthropology, 127*(1), 58-78.

Tocheri, M. W., Solhan, C. R., Orr, C. M., Femiani, J., Frohlich, B., Groves, C. P., ... & Jungers, W. L. (2011). Ecological divergence and medial cuneiform morphology in gorillas. *Journal of human evolution*, *60*(2), 171-184.

Tome, J., Nawoczenski, D. A., Flemister, A., & Houck, J. (2006). Comparison of foot kinematics between subjects with posterior tibialis tendon dysfunction and healthy controls. *Journal of Orthopaedic & Sports Physical Therapy, 36*(9), 635-644.

Trinkaus, E. (1983). Functional-aspects of Neandertal pedal remains. *Foot & Ankle, 3*(6), 377-390.

Tsegai, Z. J., Kivell, T. L., Gross, T., Nguyen, N. H., Pahr, D. H., Smaers, J. B., et al. (2013). Trabecular bone structure correlates with hand posture and use in hominoids. *Plos One, 8*(11), e78781.

Tsegai, Z. J., Skinner, M. M., Gee, A. H., Pahr, D. H., Treece, G. M., Hublin, J., et al. (2017). Trabecular and cortical bone structure of the talus and distal tibia in pan and homo (advance online). *American Journal of Physical Anthropology*

Turner, C. H. (1992). On Wolff's law of trabecular architecture. *Journal of Biomechanics, 25*(1), 1-9.

Tuttle, R. H. (1981). Evolution of hominid bipedalism and prehensile capabilities. *Philosophical Transactions of the Royal Society of London. Series B, Biological Sciences,* , 89-94.

Tuttle, R. H. (1969). Quantitative and functional studies on the hands of the anthropoidea. I. the hominoidea. *Journal of Morphology, 128*(3), 309-363.

Tuttle, R. H. (1970). PHYSICAL ANTHROPOLOGY: The life of primates. Adolph H. Schultz. *American Anthropologist, 72*(6), 1563-1564.

Tuttle, R., & Beck, B. B. (1972). Knuckle walking hand postures in an orangutan (*Pongo pygmaeus*). *Nature, 236*(5340), 33-34.

Vaughan, C. L., Davis, B. L., & Jeremy, C. O. (1999). Dynamics of human gait.

Vereecke, E., D'Août, K., Clercq, D. D., Elsacker, L. V., & Aerts, P. (2003). Dynamic plantar pressure distribution during terrestrial locomotion of bonobos (*Pan paniscus*). *American Journal of Physical Anthropology, 120*(4), 373-383.

Wang, W. J., & Crompton, R. H. (2004). Analysis of the human and ape foot during bipedal standing with implications for the evolution of the foot. *Journal of Biomechanics, 37*(12), 1831-1836.

Ward, C. V. (2002). Interpreting the posture and locomotion of *Australopithecus afarensis*: Where do we stand? *American Journal of Physical Anthropology, 119*(S35), 185-215.

Ward, S. C., & Susman, R. W. (1979). Correlates between locomotor anatomy and behavior in two sympatric species of lemur. *American Journal of Physical Anthropology, 50*(4), 575-590.

Washburn, S. L. (1967). Behaviour and the origin of man. *Proceedings of the Royal Anthropological Institute of Great Britain and Ireland,* (1967), 21-27.

Wehrli, F. W. (2007). Structural and functional assessment of trabecular and cortical bone by micro magnetic resonance imaging. *Journal of Magnetic Resonance Imaging, 25*(2), 390-409.

White, T. D., Suwa, G., & Asfaw, B. (1994). *Australopithecus ramidus*, a new species of early hominid from Aramis, Ethiopia. *Nature, 371*(6495), 306-312.

White, T., & Suwa, G. (1987). Hominid footprints at Laetoli - facts and interpretations. *American Journal of Physical Anthropology, 72*(4), 485-514.

Wood, B., & Constantino, P. (2007). *Paranthropus boisei*: Fifty years of evidence and analysis. *American Journal of Physical Anthropology, 134*(S45), 106-132.

Woodburn, J., Nelson, K. M., Siegel, K. L., Kepple, T. M., & Gerber, L. H. (2004). Multisegment foot motion during gait: Proof of concept in rheumatoid arthritis. *The Journal of Rheumatology, 31*(10), 1918-1927.

Wrangham, R. W. (1977). Feeding behavior of chimpanzees in Gombe national park, Tanzania. *Primate ecology* (pp. 504-538). New York: Academic Press; Academic Press.

Wolff, J. (1892) Das Gesetz der Transformation der Knochen. Berlin: A. Hirchwild.

Wunderlich, R.E., 1999. Pedal form and plantar pressure distribution in anthropoid primates. Ph.D. Dissertation. State University of New York at Stony Brook.

Wunderlich, R. E., & Ischinger, S. B. (2017). Foot use during vertical climbing in chimpanzees (*Pan troglodytes*). *Journal of Human Evolution, 109*, 1-10.

Zipfel, B., & Kidd, R. (2006). Hominin first metatarsals (SKX 5017 and SK 1813) from Swartkrans: A morphometric analysis. *Homo-Journal of Comparative Human Biology, 57*(2), 117-131.

Zipfel, B., DeSilva, J. M., Kidd, R. S., Carlson, K. J., Churchill, S. E., & Berger, L. R. (2011). The foot and ankle of *Australopithecus sediba*. *Science, 333*(6048), 1417-1420.

Appendix A

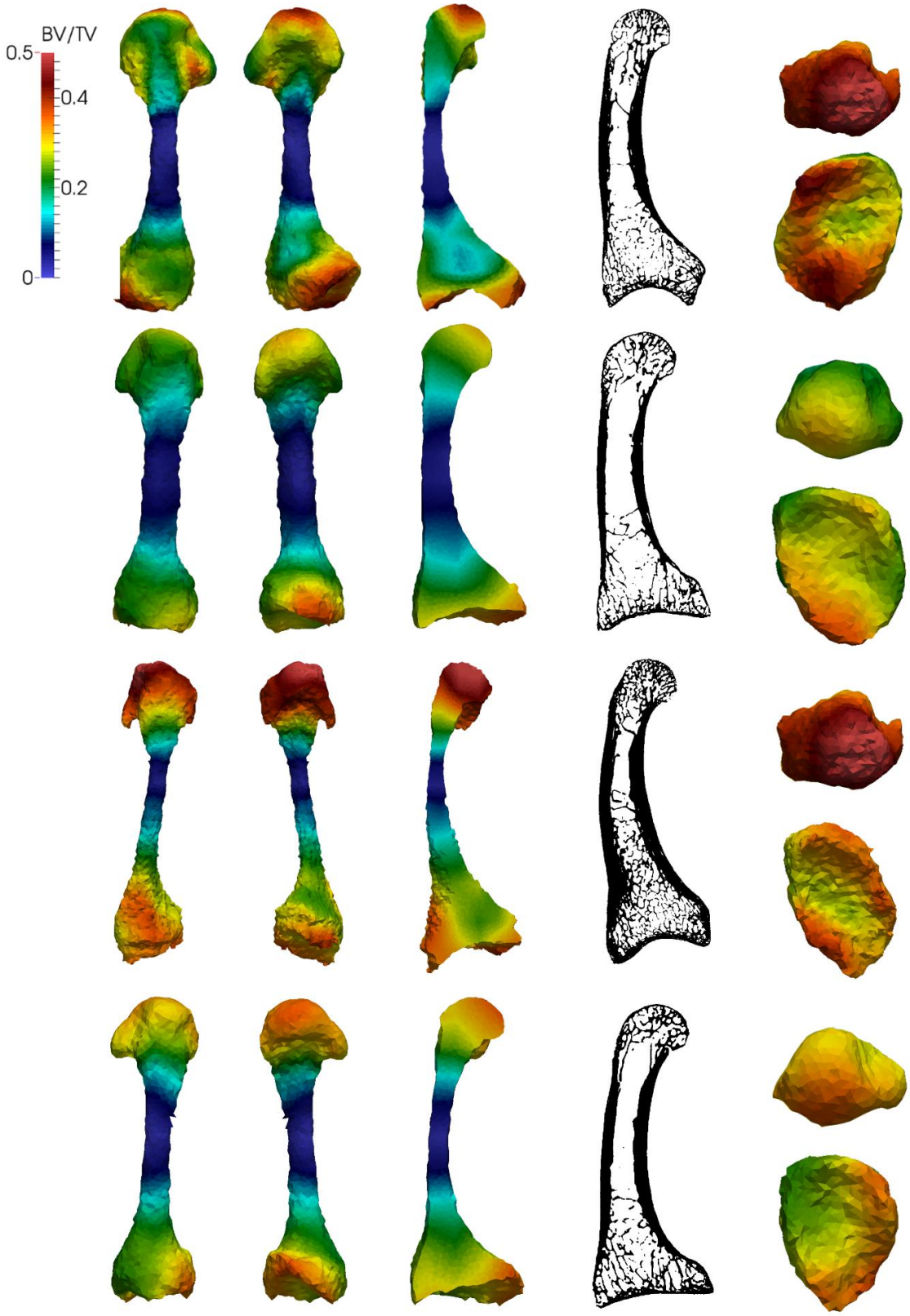

(cont.)

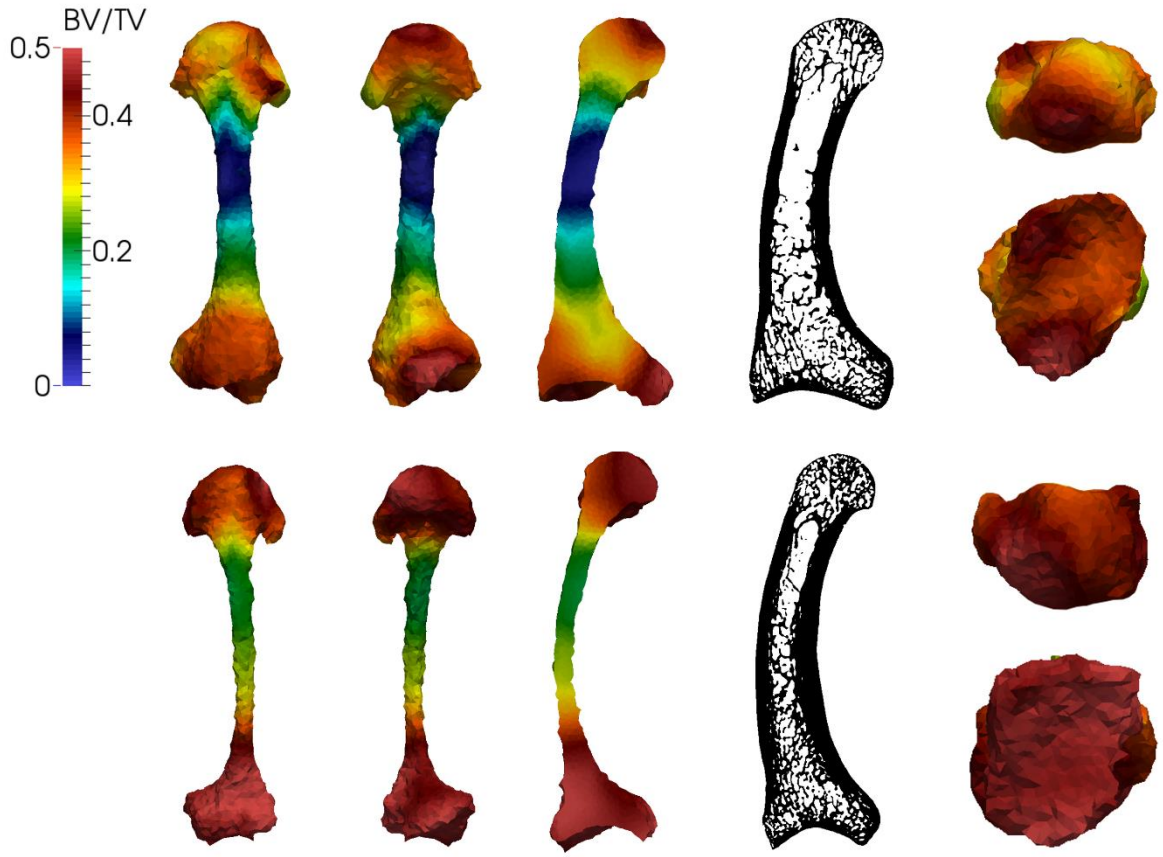

Figure 1. *Pongo pygmaeus* BV/TV colour maps and segmentations. From left to right: Dorsal view, plantar view, parasagittal cross-section, segmentation, (top) distal articular surface, (bottom) proximal articular surface. From top to bottom: Pp_ZSM_1909_0801_MT1R; Pp_ZSM_1907_0660_MT1L; Pp_ZSM_0203_MT1L; Pp_ZSM_1907_0483_MT1L; Pp_ZSM_1907_0633b_MT1R; Pp_ZSM_1982_0092_MT1R.

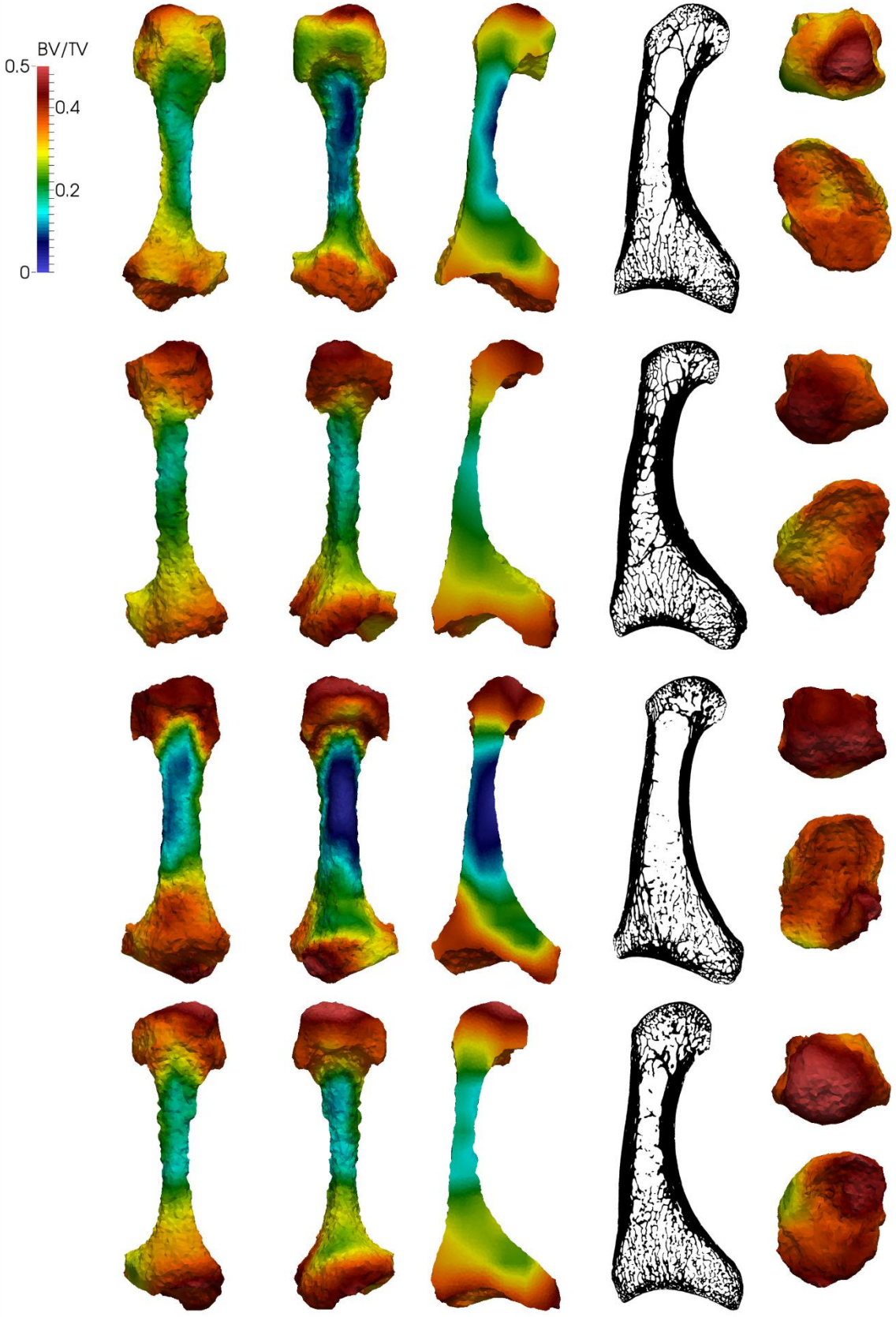
BV/TV
0.5
0.4
0.2
0

(cont.)

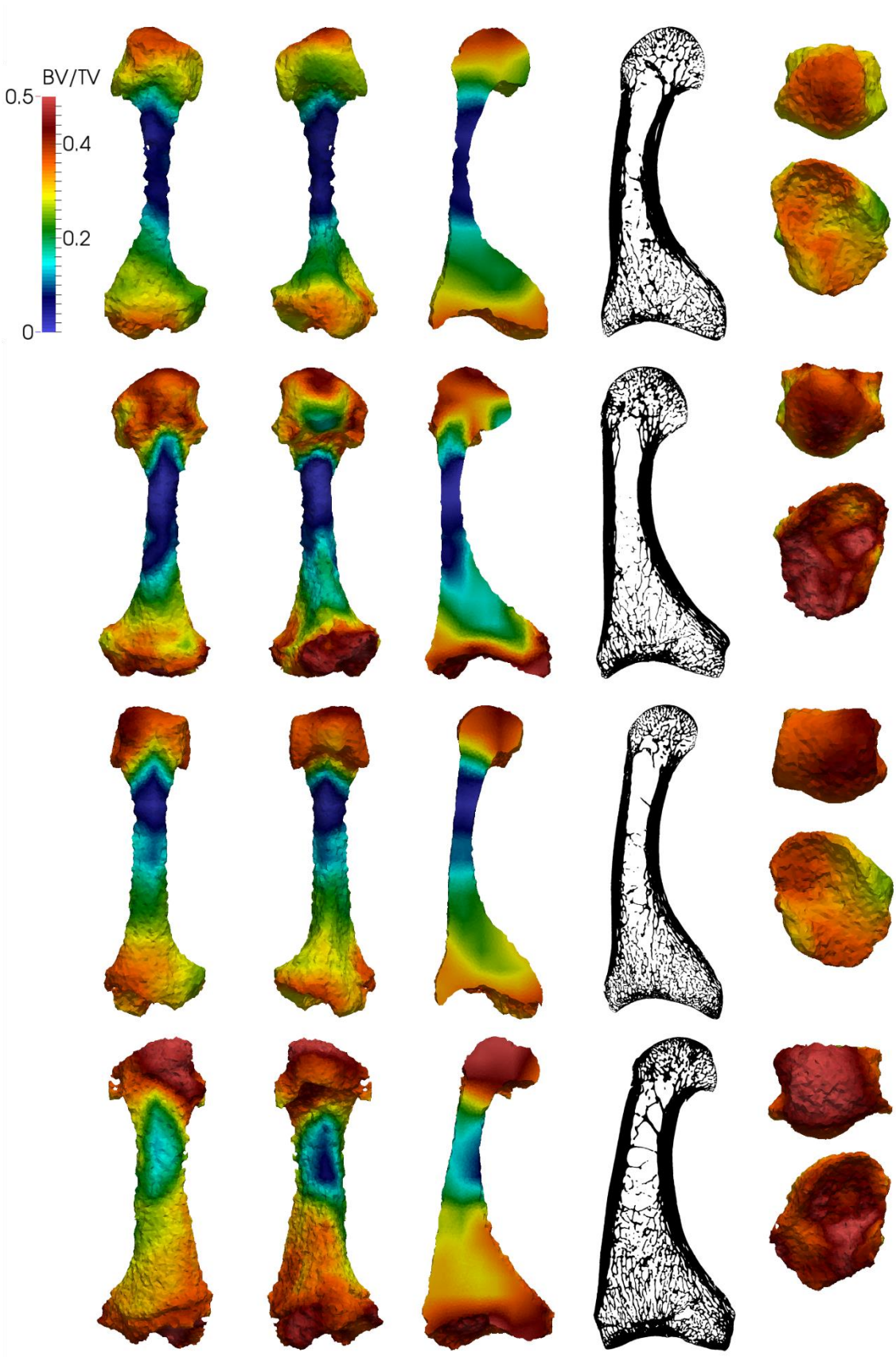

(cont.)

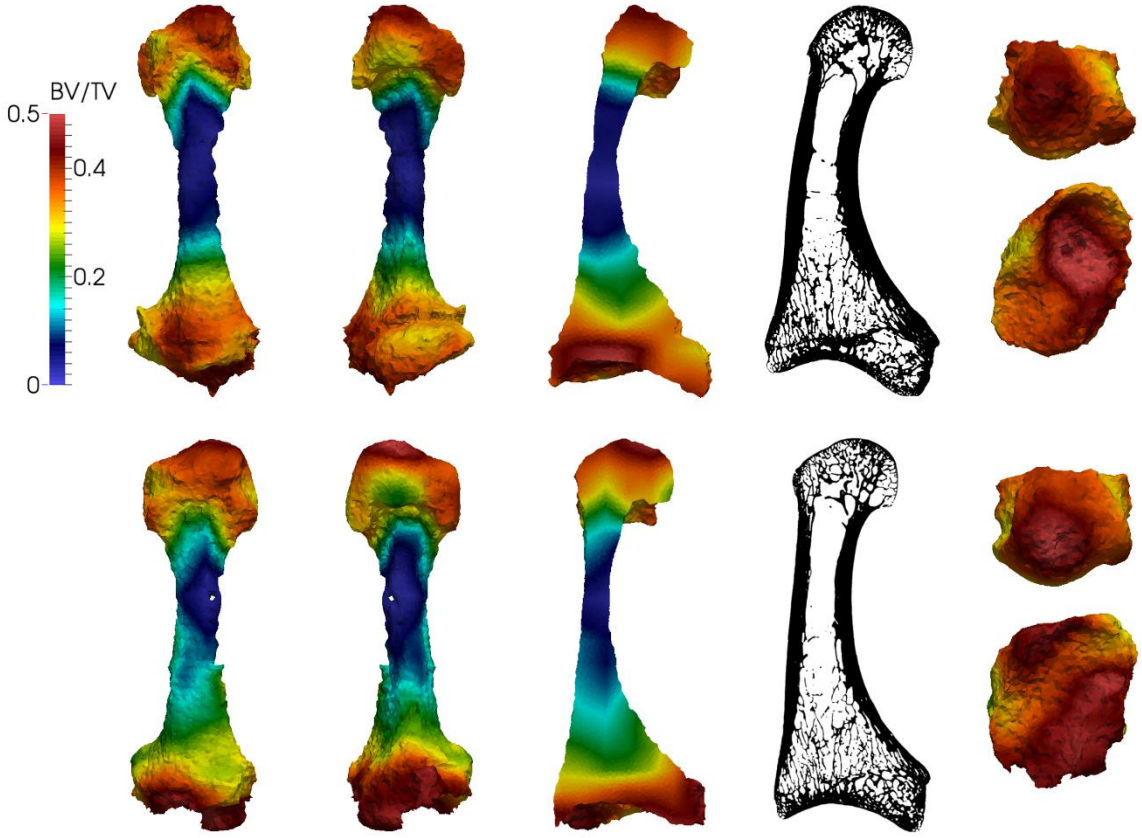

Figure 2. *Gorilla gorilla* BV/TV colour maps and segmentations. From left to right: Dorsal view, plantar view, parasagittal cross-section, segmentation, (top) distal articular surface, (bottom) proximal articular surface. From top to bottom: Gg_PC_MER_95_MT1L; Gg_PC_MER_129_MT1R; Gg_PC_MER_135_MT1R; Gg_PC_MER_136_MT1R; Gg_PC_MER_138_MT1L; Gg_PC_MER_372_MT1R; Gg_PC_MER_696_MT1L; Gg_PC_ZII_64_MT1R.

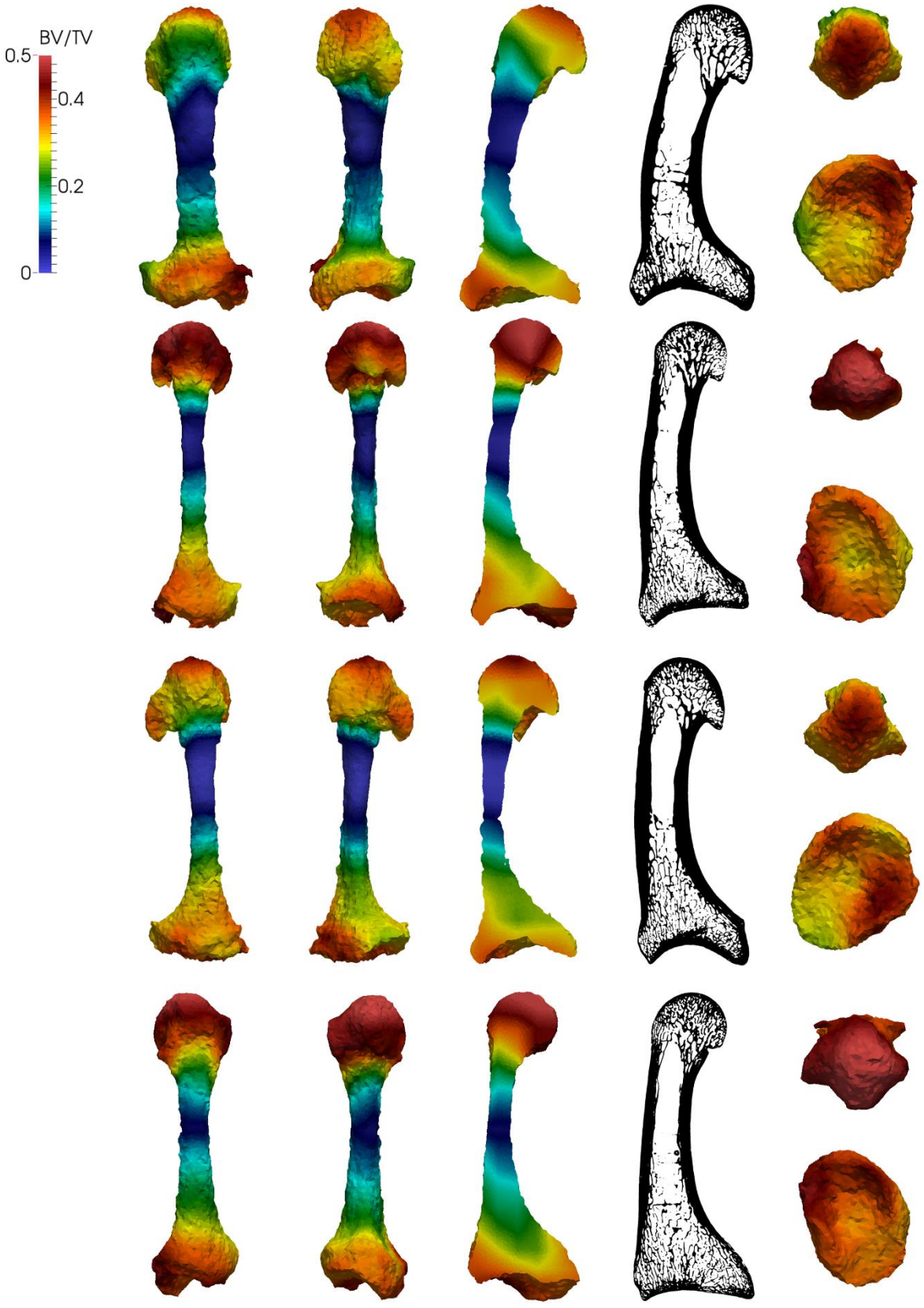
BV/TV
0.5
0.4
0.2
0

(cont.)

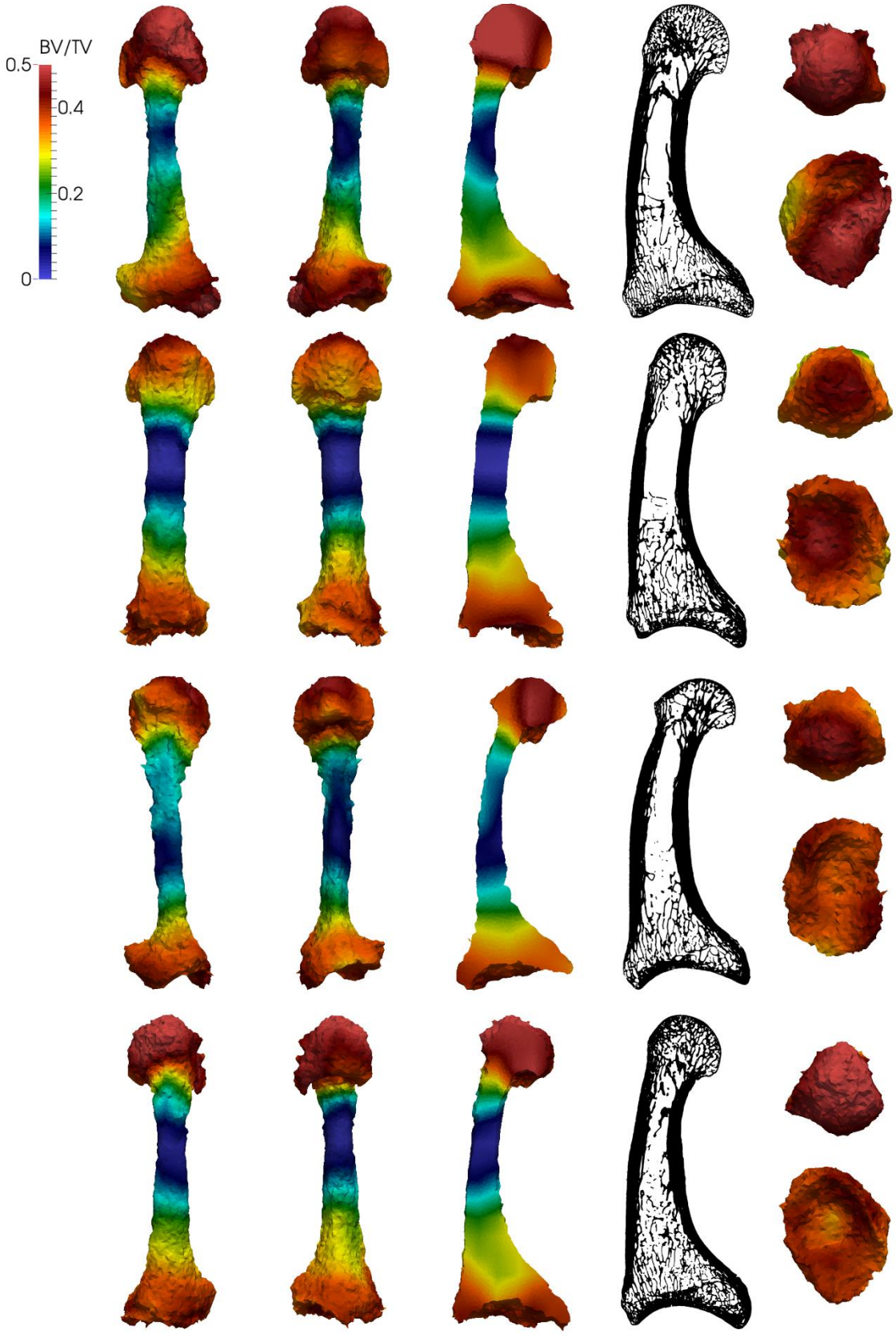

(cont.)

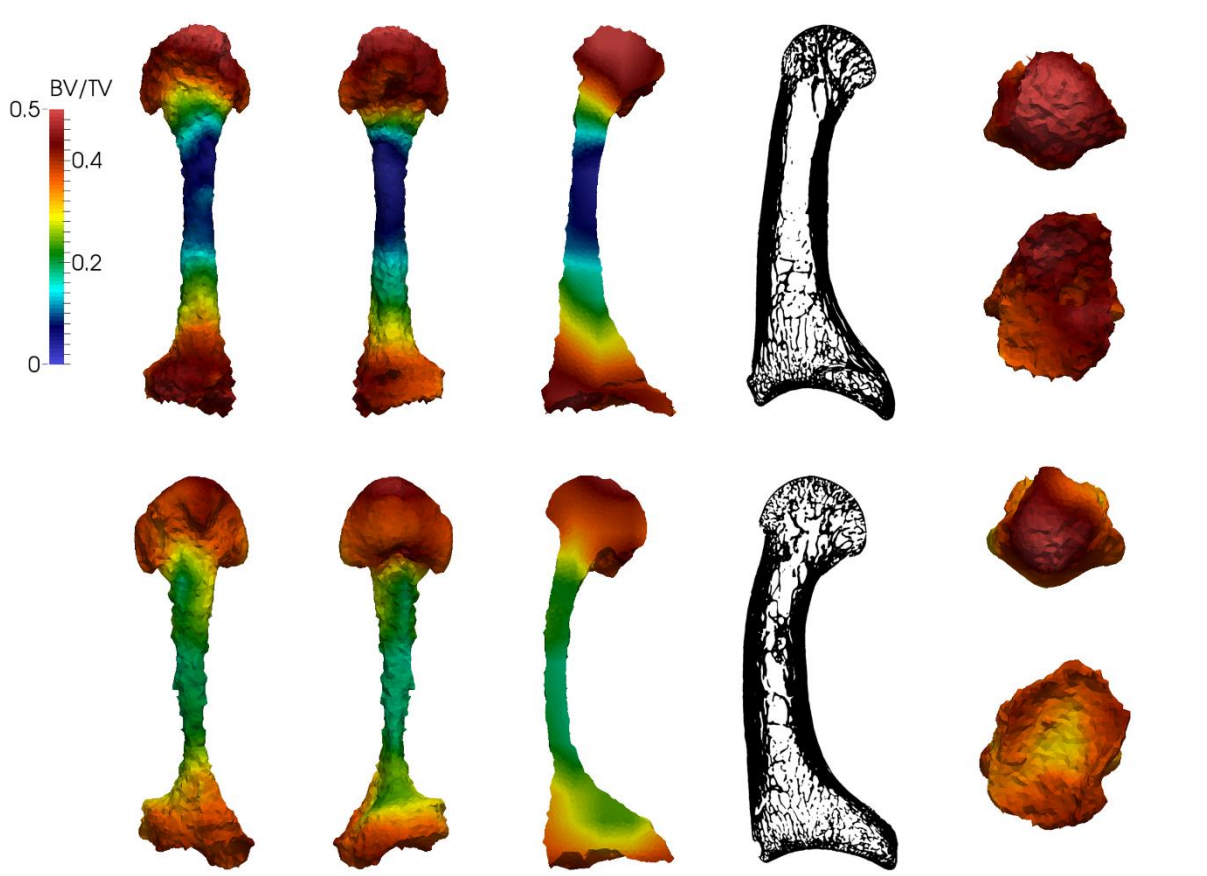

Figure 3. *Pan troglodytes* BV/TV colour maps and segmentations. From left to right: Dorsal view, plantar view, parasagittal cross-section, segmentation, (top) distal articular surface, (bottom) proximal articular surface. From top to bottom: Ptv_MPITC_11781_MT1R; Ptv_MPITC_11800_MT1L; Ptv_MPITC_11903_MT1R; Pt_PC_MER_172_MT1L; Pt_PC_MER_712_MT1R; Pt_PC_ZVI_34_MT1L; Pt_PC_ZVII_24_MT1R; Pt_PC_ZVII_25_MT1L; Pt_PC_ZVIII_10_MT1R; Pt_PC_ZIX_52_MT1R. (Ptv = *Pan troglodytes verus*; Pt = *Pan troglodytes troglodytes*)

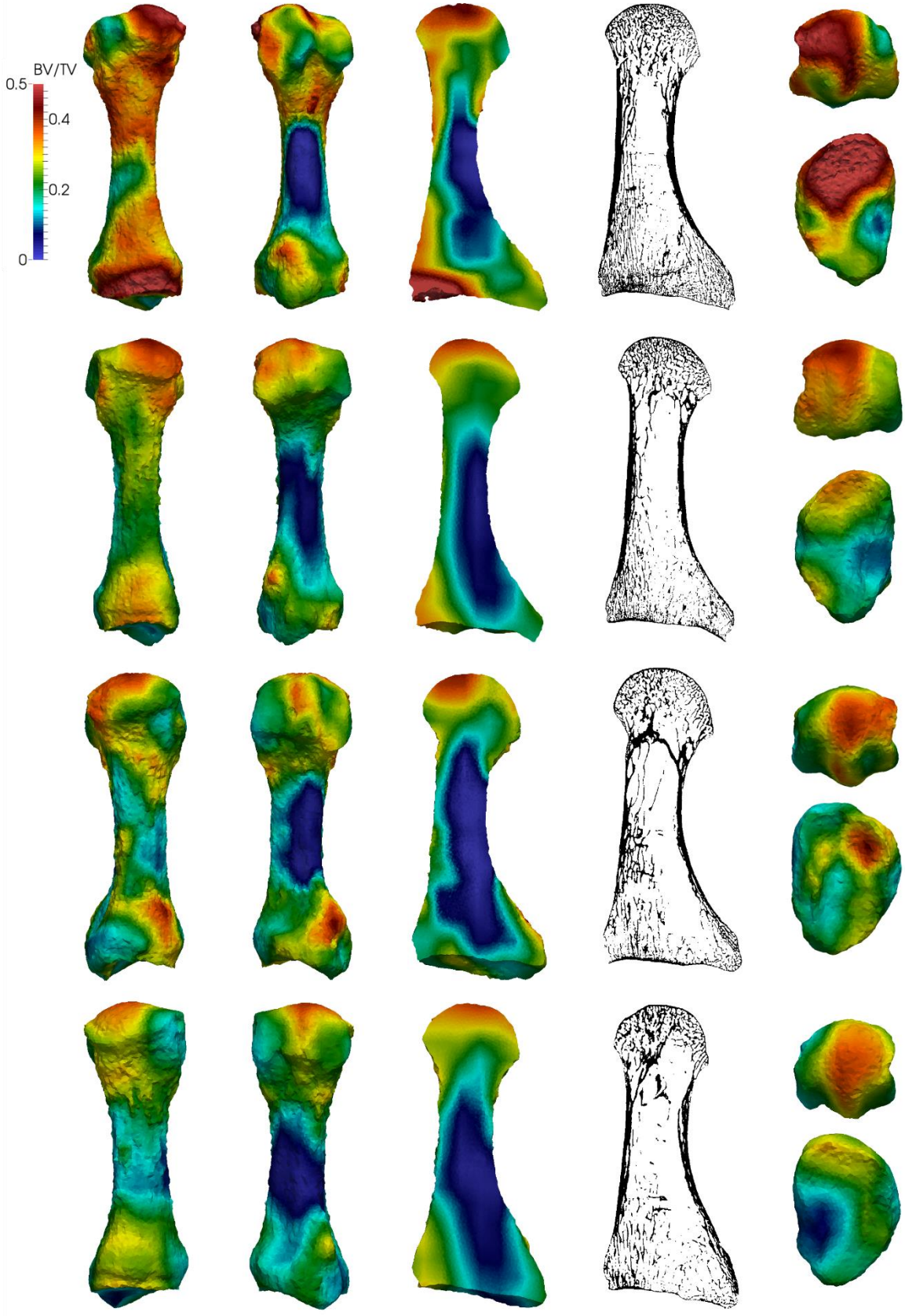
BV/TV
0.5
0.4
0.2
0

(cont.)

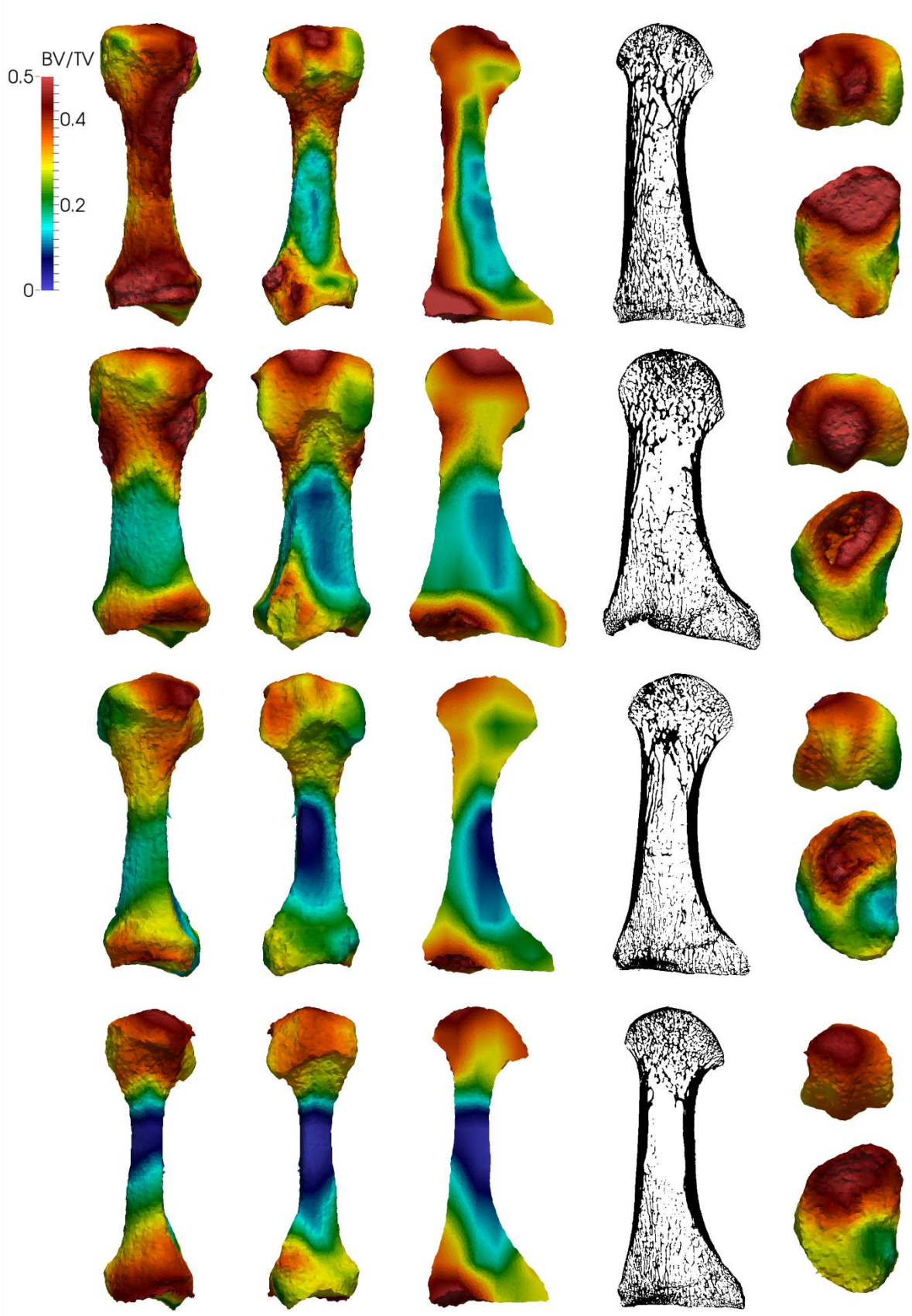

(cont.)

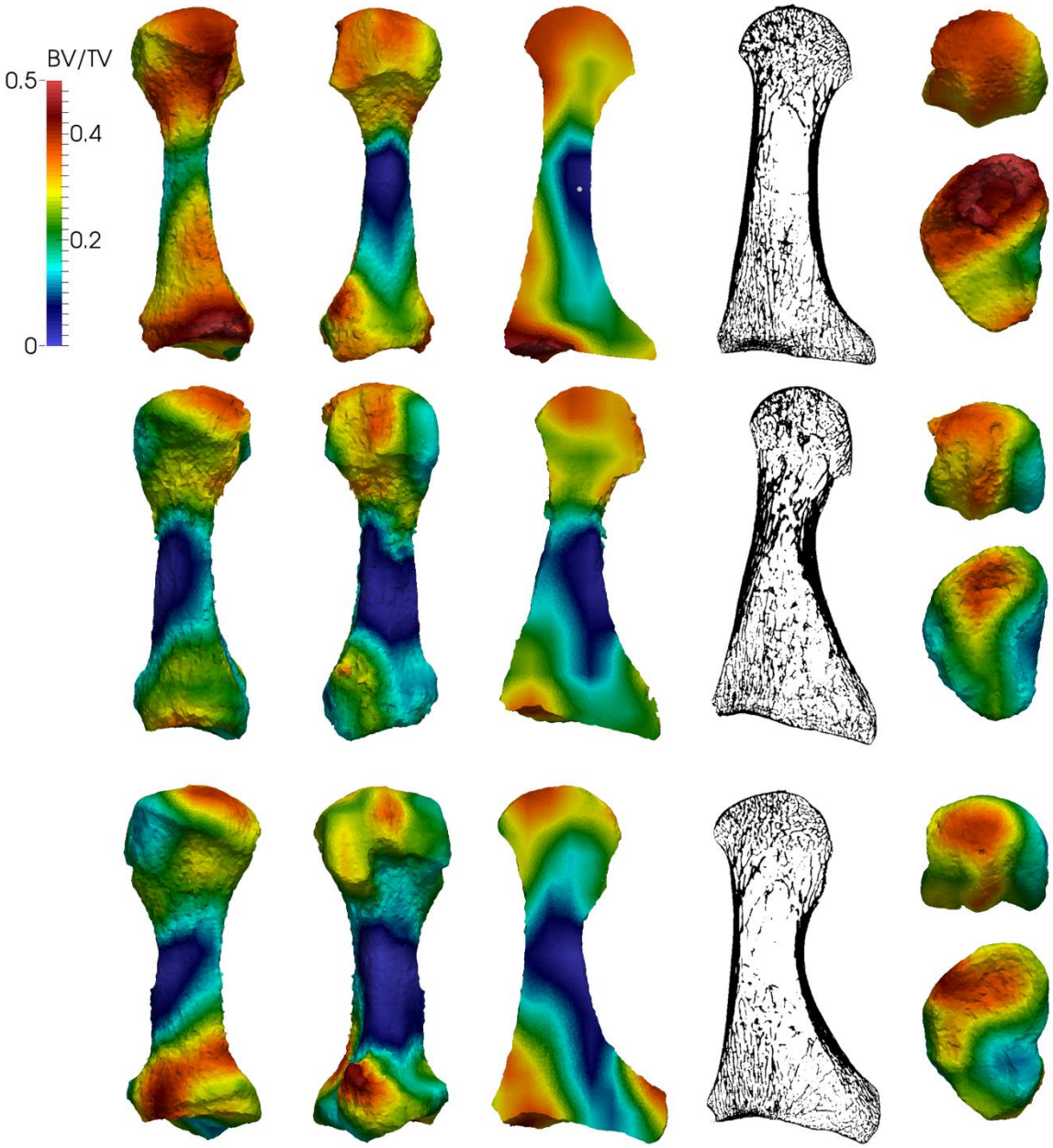

Figure 4. *Homo sapiens* BV/TV colour maps and segmentations. From left to right: Dorsal view, plantar view, parasagittal cross-section, segmentation, (top) distal articular surface, (bottom) proximal articular surface. From top to bottom: Hs_Inden_131_MT1R; Hs_Inden_164_MT1R; Hs_Inden_342_MT1L; Hs_Inden_438_MT1L; Hs_Campus_8_MT1R; Hs_Campus_43_MT1R; Hs_Campus_45_MT1R; Hs_Campus_57_MT1R; Hs_Campus_62_MT1R; Hs_Campus_64_MT1R; Hs_Campus_65_MT1R.

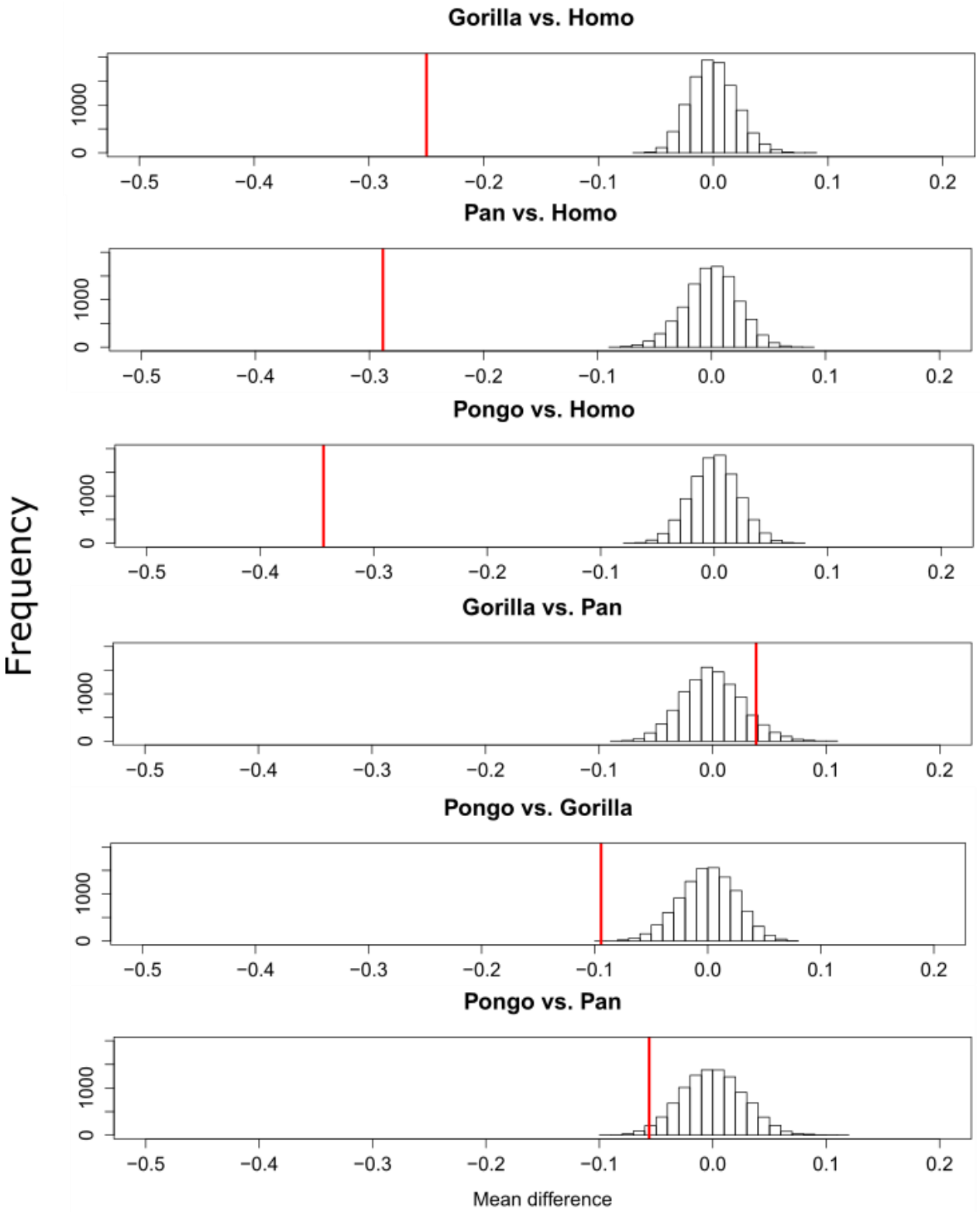

Figure 5. Plots of all extant taxa pairwise bootstrap analyses of BV/TV ratio within the head. Red line represents the actual mean difference between the two samples.

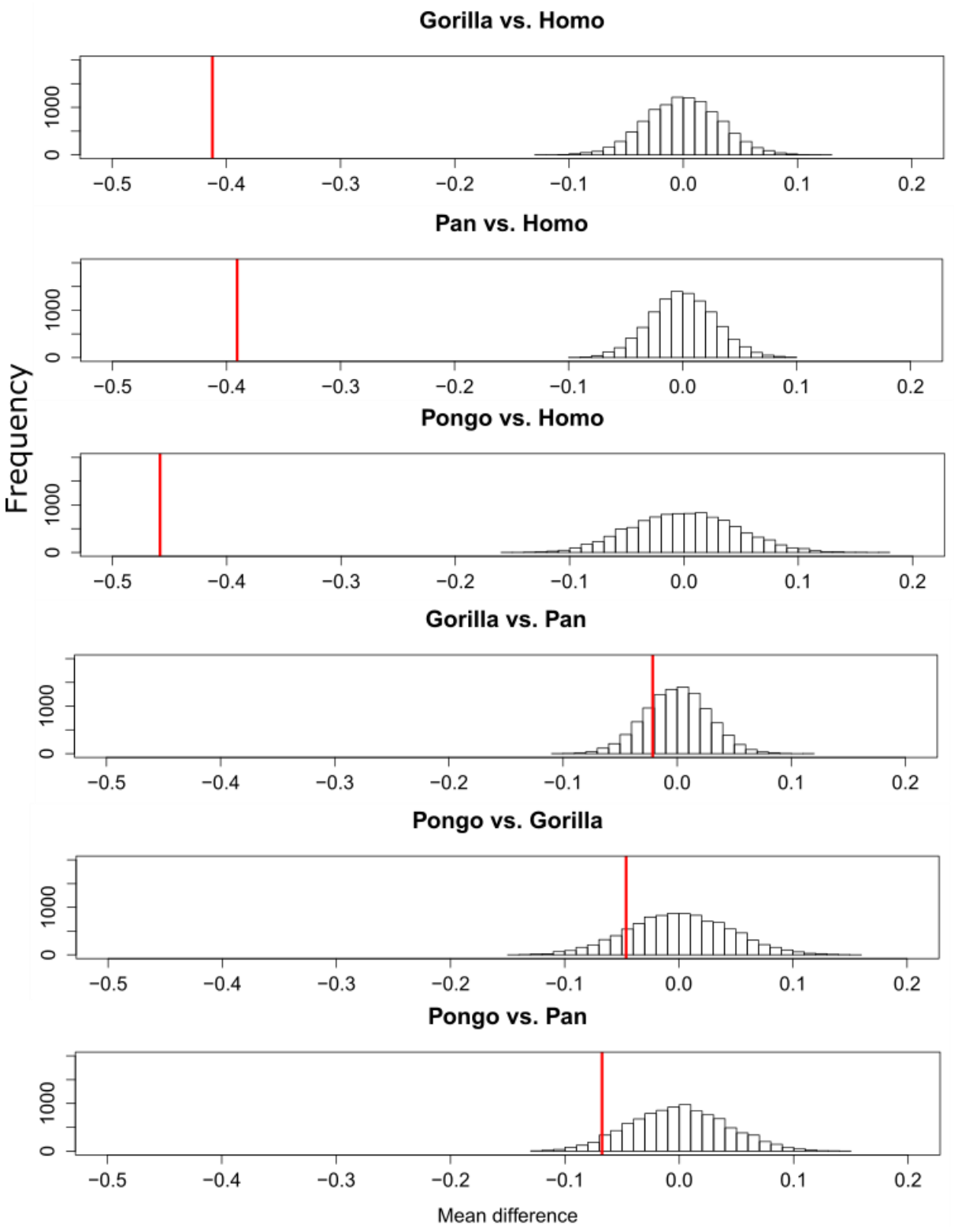

Figure 6. Plots of all extant taxa pairwise bootstrap analyses of BV/TV ratio within the base. Red line represents the actual mean difference between the two samples.

Appendix B

	Side (L/R)	Sex (M/F/?)	Resolution	BV/TV				DA			
				Base		Head		Base		Head	
				dorsal	plantar	dorsal	plantar	dorsal	plantar	dorsal	plantar
Pongo pygmaeus											
1907_0483	L	F	0.028389	0.253	0.299	0.263	0.343	0.351	0.288	0.308	0.157
1907_0633b	R	F	0.028384	0.361	0.370	0.302	0.358	0.332	0.228	0.320	0.211
1907_0660	L	F	0.028382	0.234	0.270	0.198	0.270	0.278	0.274	0.318	0.242
1909_0801	R	M(?)	0.029301	0.234	0.279	0.236	0.288	0.312	0.275	0.328	0.175
1966_0203	L	M	0.028385	0.293	0.280	0.347	0.449	0.377	0.299	0.276	0.203
1982_0092	R	F	0.028376	0.487	0.454	0.387	0.452	0.190	0.185	0.209	0.167
Gorilla gorilla											
MER_95	L	F	0.039137	0.330	0.314	0.263	0.297	0.364	0.243	0.323	0.208
MER_129	R	F	0.042340	0.312	0.332	0.350	0.414	0.424	0.323	0.355	0.287
MER_135	R	M	0.039137	0.355	0.315	0.354	0.421	0.381	0.290	0.395	0.327
MER_136	R	F	0.029658	0.340	0.334	0.347	0.392	0.330	0.198	0.301	0.219
MER_138	L	F	0.032181	0.281	0.286	0.277	0.293	0.346	0.229	0.316	0.236
MER_372	R	M	0.039137	0.323	0.341	0.324	0.322	0.393	0.308	0.298	0.257
MER_696	L	F	0.032749	0.312	0.306	0.337	0.390	0.403	0.266	0.325	0.253
ZII_64	R	M	0.037462	0.354	0.383	0.411	0.431	0.490	0.301	0.391	0.274
ZVI_32	R	M	0.035033	0.360	0.357	0.305	0.358	0.384	0.318	0.409	0.232
FC_123	L	M	0.034671	0.310	0.360	0.297	0.348	0.424	0.244	0.436	0.261
Pan troglodytes											
MPITC_11781	R	M	0.030024	0.372	0.335	0.239	0.338	0.434	0.315	0.368	0.244
MPITC_11800	L	F	0.030024	0.327	0.332	0.402	0.421	0.401	0.309	0.401	0.262
MPITC_11903	R	M	0.030024	0.325	0.319	0.274	0.339	0.440	0.300	0.318	0.221

MER_172	L	F	0.026680	0.318	0.307	0.382	0.461	0.464	0.338	0.396	0.286
MER_712	R	M	0.027041	0.353	0.389	0.326	0.386	0.395	0.300	0.419	0.292
ZVI_34	L	M	0.029628	0.384	0.371	0.333	0.371	0.423	0.332	0.407	0.283
ZVII_24	R	M	0.032139	0.357	0.365	0.359	0.437	0.420	0.313	0.423	0.357
ZVII_25	L	M	0.034088	0.350	0.365	0.414	0.464	0.451	0.340	0.435	0.260
ZVIII_10	R	F	0.032139	0.399	0.391	0.399	0.440	0.448	0.368	0.432	0.334
ZIX_52	R	F	0.029189	0.330	0.316	0.354	0.399	0.405	0.298	0.351	0.194
Fossil specimens											
SKX 5017	L		0.025	0.405	0.362	0.434	0.386	0.422	0.308	0.311	0.219
SK 1813	R		0.013547			0.370	0.350			0.235	0.169
Homo sapiens											
Inden_131	R	M	0.030877	0.298	0.201	0.313	0.273	0.502	0.347	0.508	0.412
Inden_164	R	F	0.030877	0.207	0.146	0.289	0.246	0.441	0.310	0.384	0.330
Inden_342	L	F	0.030877	0.201	0.157	0.251	0.212	0.479	0.390	0.472	0.395
Inden_438	L	F	0.031975	0.188	0.132	0.249	0.219	0.527	0.388	0.498	0.337
Campus_8	R	M	0.031060	0.381	0.276	0.347	0.314	0.438	0.389	0.478	0.352
Campus_43	R	M	0.031060	0.270	0.214	0.360	0.313	0.382	0.292	0.444	0.333
Campus_45	R	F	0.031059	0.287	0.197	0.319	0.268	0.423	0.335	0.477	0.333
Campus_57	R	F	0.030694	0.362	0.252	0.364	0.316	0.429	0.301	0.454	0.257
Campus_62	R	M	0.030694	0.325	0.244	0.345	0.298	0.436	0.377	0.482	0.342
Campus_64	R	M	0.030694	0.230	0.165	0.267	0.249	0.436	0.361	0.476	0.342
Campus_65	R	M	0.0306943	0.291	0.190	0.235	0.214	0.469	0.341	0.497	0.389

Table 1. Details of each specimen, including scan resolution and mean BV/TV and DA values for each section. *P. pygmaeus* - Zoologische Staatsammlung Munich, Germany (ZSM); *P. troglodytes* - Tai Collection of Max Planck Institute for Evolutionary Anthropology, Leipzig, Germany (MPITC), Merfield (MER) and Zenker (Z) Collection from the Powell-Cotton Museum, England; *G. gorilla* – Merfield (MER), Zenker (Z), and French Congo (FC) Collections from the Powell-Cotton Museum, England; *H. sapiens* – Campus and Inden Collections from the Anthropologie der Georg-August-Universität Göttingen, Germany.

Specimen	Tb. N.				Tb. Sp.				Tb. Th.			
	Base		Head		base		Head		Base		Head	
	dorsal	plantar	dorsal	plantar	Dorsal	Plantar	Dorsal	plantar	Dorsal	Plantar	Dorsal	plantar
Pongo pygmaeus												
1907_0483	1.163	1.143	0.762	1.276	0.636	0.627	1.071	0.535	0.224	0.248	0.241	0.249
1907_0633b	1.360	1.314	0.940	1.250	0.495	0.510	0.813	0.556	0.240	0.250	0.251	0.244
1907_0660	1.148	1.186	0.849	1.195	0.662	0.627	0.976	0.631	0.209	0.216	0.203	0.206
1909_0801	1.184	1.233	0.903	1.221	0.636	0.590	0.887	0.595	0.208	0.221	0.221	0.223
1966_0203	1.101	1.115	1.003	1.170	0.661	0.654	0.703	0.531	0.248	0.243	0.293	0.324
1982_0092	1.348	1.282	1.113	1.298	0.434	0.467	0.601	0.456	0.308	0.313	0.297	0.314
Gorilla gorilla												
MER_95	1.125	1.044	0.561	0.873	0.623	0.681	1.485	0.847	0.266	0.277	0.296	0.299
MER_129	1.170	1.188	0.922	1.103	0.618	0.592	0.798	0.608	0.237	0.250	0.287	0.298
MER_135	1.030	0.946	0.535	0.966	0.667	0.742	1.511	0.671	0.304	0.315	0.357	0.365
MER_136	1.191	1.200	0.882	1.097	0.584	0.581	0.845	0.617	0.256	0.252	0.289	0.295
MER_138	1.150	1.133	0.679	0.985	0.639	0.641	1.205	0.758	0.231	0.242	0.268	0.257
MER_372	1.015	1.004	0.694	0.873	0.691	0.685	1.114	0.825	0.294	0.311	0.327	0.321
MER_696	1.332	1.345	0.763	1.164	0.535	0.529	1.034	0.578	0.216	0.214	0.277	0.281
ZII_64	1.099	1.074	0.823	1.057	0.621	0.607	0.823	0.593	0.289	0.324	0.392	0.353
ZVI_32	1.030	1.008	0.573	0.913	0.635	0.653	1.388	0.759	0.335	0.339	0.356	0.336
FC_123	1.077	1.007	1.057	0.994	0.662	0.680	0.686	0.696	0.267	0.313	0.260	0.310
Pan troglodytes												
MPITC_11781	1.232	1.252	0.548	1.060	0.540	0.548	1.563	0.669	0.272	0.251	0.260	0.274
MPITC_11800	1.613	1.545	0.875	1.344	0.422	0.432	0.818	0.456	0.198	0.215	0.326	0.288
MPITC_11903	1.499	1.380	0.542	1.126	0.459	0.491	1.553	0.623	0.208	0.234	0.293	0.265
MER_172	1.472	1.526	1.153	1.457	0.486	0.465	0.632	0.431	0.193	0.190	0.235	0.255
MER_712	1.520	1.516	1.375	1.498	0.451	0.434	0.520	0.442	0.207	0.225	0.207	0.226
ZVI_34	1.341	1.275	0.973	1.088	0.496	0.528	0.751	0.631	0.249	0.256	0.276	0.288
ZVII_24	1.217	1.241	0.876	1.039	0.578	0.560	0.838	0.621	0.244	0.246	0.304	0.342
ZVII_25	1.266	1.293	0.712	1.125	0.551	0.523	1.064	0.557	0.239	0.251	0.340	0.332
ZVIII_10	1.375	1.366	0.777	1.157	0.479	0.474	0.929	0.541	0.250	0.259	0.358	0.324
ZIX_52	1.469	1.463	1.062	1.250	0.463	0.465	0.679	0.523	0.217	0.218	0.262	0.277
Fossil specimens												
SKX 5017	1.349	1.298	1.191	1.102	0.486	0.522	0.538	0.605	0.256	0.248	0.301	0.303
SK 1813			1.316	1.324			0.503	0.487			0.256	0.268
Homo sapiens												
Inden_131	1.365	1.213	1.149	1.132	0.528	0.647	0.625	0.649	0.205	0.179	0.245	0.236
Inden_164	1.385	0.998	1.245	1.142	0.553	0.841	0.593	0.682	0.169	0.162	0.210	0.194

Inden_342	1.041	0.788	0.967	0.976	0.762	1.094	0.823	0.816	0.198	0.176	0.211	0.209
Inden_438	1.123	0.862	1.044	0.958	0.687	0.971	0.723	0.814	0.203	0.189	0.234	0.230
Campus_8	1.374	1.213	1.111	1.088	0.477	0.597	0.628	0.657	0.252	0.229	0.275	0.263
Campus_43	1.349	1.264	1.078	1.052	0.526	0.598	0.633	0.673	0.216	0.193	0.294	0.277
Campus_45	1.490	1.228	1.250	1.145	0.454	0.623	0.561	0.639	0.217	0.191	0.239	0.234
Campus_57	1.698	1.511	1.381	1.392	0.385	0.483	0.489	0.499	0.204	0.179	0.235	0.220
Campus_62	1.469	1.288	1.325	1.224	0.456	0.572	0.510	0.581	0.225	0.205	0.245	0.236
Campus_64	1.322	1.115	1.026	1.064	0.557	0.708	0.721	0.686	0.200	0.189	0.254	0.254
Campus_65	1.423	1.146	1.018	1.001	0.493	0.681	0.769	0.787	0.210	0.192	0.214	0.213

Table 2. Raw Tb.N., Tb.Sp., and Tb.Th. values for each region of each specimen.